2017

Analysis of Novel Cyanide Antidote Dimethyl Trisulfide for Pharmacokinetic Studies, and Sulfur Mustard Metabolites for Identification of Biomarker of Inhaled Dose

Erica Manandhar
South Dakota State University

ANALYSIS OF NOVEL CYANIDE ANTIDOTE DIMETHYL TRISULFIDE FOR PHARMACOKINETIC STUDIES, AND SULFUR MUSTARD METABOLITES FOR IDENTIFICATION OF BIOMARKER OF INHALED DOSE

BY

ERICA MANANDHAR

A dissertation submitted in partial fulfillment of the requirements for the

Doctor of Philosophy

Major in Chemistry

South Dakota State University

2017

ANALYSIS OF NOVEL CYANIDE ANTIDOTE DIMETHYL TRISULFIDE FOR PHARMACOKINETIC STUDIES, AND SULFUR MUSTARD METABOLITES FOR IDENTIFICATION OF BIOMARKER OF INHALED DOSE

ERICA MANANDHAR

This dissertation is approved as a creditable and independent investigation by a candidate for the Doctor of Philosophy in Chemistry degree and is acceptable for meeting the dissertation requirements for this degree. Acceptance of this dissertation does not imply that the conclusions reached by the candidate are necessarily the conclusions of the major department.

Brian A. Logue, Ph.D
Dissertation Advisor Date

Douglas Raynie, Ph.D
Head, Department of Chemistry & Biochemistry Date

Dean, Graduate School Date

I would like to dedicate this dissertation to my loving parents, Kamal and Ira Manandhar. I am forever grateful for your unconditional love and support.

This dissertation would not have been possible without the love and constant support of my husband, Ranjan Karki. You have helped me stay focused on my goals during the most challenging times. Thank you for not only helping me dream big but also for supporting me throughout my hard work to achieve those dreams. This achievement and many more are dedicated to you.

I would like to thank my brother, my in-laws, family, and friends for the joy you all bring in my life. Each of you have inspired and motivated me, and without you all, I would not be where I am today.

ACKNOWLEDGEMENTS

I would like to express my sincere gratitude and heartfelt appreciation to my advisor, Dr. Brian A. Logue. Your guidance and support has played an instrumental role in shaping my success in graduate school. Thank you for believing in me and constantly reminding me of my potential.

Thank you to the members of LARGE group for the constant inspiration, support, and guidance. I would like to thank my colleague, Adam Pay, for his work in synthesis of compounds needed in this project.

I would like to thank my committee members, the Department of Chemistry and Biochemistry at South Dakota State University, and all the faculty and staff for their assistance and encouragement. My sincere gratitude goes to the institutions and agencies that have funded my research and made the completion of my degree a possibility.

TABLE OF CONTENTS

ABBREVIATIONS

3-MP: 3-mercaptopyruvate

3-MST: 3-MP sulfurtransferase

AALAC: Association for the Assessment and Accreditation of Laboratory Animal Care

ATCA: 2-amino-2-thiazoline-4-carboxylic acid

ATP: Adenosine triphosphate

Cbi: Cobinamide

Cbl: Hydroxocobalamin

CE: Collision energy

CI: Chemical ionization

CIS: Cooled injection system

CWAs: Chemical warfare agents

CXP: Collision cell exit potential

Cys: Cysteine

Cyt c: Cytochrome c

DMDS: Dimethyl disulfide

DMTS-d6: Dimethyl trisulfide-d6

DMTS: Dimethyl trisulfide

DP: Declustering potential

ECM: Extracellular matrix

EDTA: Ethylenediaminetetraacetic acid

EI: Electron impact

FDA: Food and Drug Administration

FT: Freeze thaw

GC: Gas chromatography

GSH: glutathione

HCN: Hydrogen cyanide

HETE: Hydroxyethylthioethyl

IACUC: Institutional Animal Care and Use Committee

IS: Internal standard

ITCA: 2-iminothiazoline-4-carboxylic acid

K_{ow}: Octanol-water partition coefficient

LLOQ: Lower limit of quantification

LOD: Limit of detection

MRM: Multiple reaction monitoring

MS: Mass spectrometry

MSMTESE: 1-methylsulfinyl-2-[2 (methylthio)ethylsulfonyl]ethane

NAD^+: Nicotinamide adenine dinucleotide

PARP: Poly (ADP-ribose) polymerase

PDMS: Polydimethylsiloxane

Phe: Phenylalanine

Pro: Proline

PTV: Programmable temperature vaporization

QC: Quality control

SBESE: 1,1'-sulfonylbis [2-(ethylsulfinyl) ethane]

SBMSE: 1,1'-sulfonylbis [2-(methylsulfinyl) ethane]

SBMTE: 1,1'-sulfonylbis[2-(methylthio) ethane]

SBSE: Stir bar sorptive extraction

SBSNAE: 1,1'-sulfonylbis[2-S- (N-acetylcysteinyl) ethane]

SCN^-: Thiocyanate

SIM: Selective ion monitoring

SM: Sulfur Mustard

SMO-d_4: Sulfur mustard oxide-d4

SMO: Sulfur mustard oxide

SN1: 1^{st} order nucleophilic substitution

TDG: Thiodigycol

TDGO: Thiodigycol oxide

TDU: Thermal desorption unit

TIC: Total ion chromatogram

ULOQ: Upper limit of quantification

Val: Valine

WMD: Weapons of Mass Destruction

XIC: Extracted ion chromatogram

LIST OF FIGURES

LIST OF TABLES

ABSTRACT

ANALYSIS OF NOVEL CYANIDE ANTIDOTE DIMETHYL TRISULFIDE FOR PHARMACOKINETIC STUDIES, AND ANALYSIS OF SULFUR MUSTARD METABOLITES FOR IDENTIFICATION OF BIOMARKERS OF INHALED DOSE

ERICA MANANDHAR

2017

Cyanide poisoning by accidental or intentional exposure poses a severe health risk. The current FDA approved antidotes for cyanide poisoning can be effective, but each suffers from specific major limitations. Dimethyl trisulfide (DMTS), a sulfur donor that detoxifies cyanide by converting it into thiocyanate, is a promising next generation cyanide antidote. Although a validated analytical method to analyze DMTS is not currently available from any matrix, one will be vital for the approval of DMTS as a therapeutic agent against cyanide poisoning. Hence, a stir bar sorptive extraction (SBSE) gas chromatography – mass spectrometry (GC-MS) method was developed and validated for the analysis of DMTS from rabbit whole blood. The limit of detection (LOD) using this method was 0.06 μM with dynamic range from 0.5 – 100 μM. The method described here allows further investigations of DMTS as a promising antidote for cyanide poisoning.

Sulfur mustard (SM) is the most utilized chemical weapon in modern history. Although its exposure can result in wide range of toxic outcomes, airway injury leading to respiratory failure is the principal cause of mortality in victims. Therefore, current investigations are underway which focus on understanding the inhalation toxicity of SM in order to develop effective therapeutic interventions. A major challenge in inhalation studies is the quantification of actual respiratory dose. In this report, we identified biomarkers that have the potential for correlation to inhalation dose. Preliminary data for correlation of two biomarkers to dose are also presented. To our knowledge, there are no studies done in identifying SM biomarkers in inhalation exposure. Additionally, a rapid, simple, and direct GC-MS analysis technique for an important SM biomarker, sulfur mustard oxide (SMO), was developed and validated in swine plasma. The LOD of the method was 0.1 μM, with a linear range from 0.5 -100 μM. The availability of this method will allow easy and rapid diagnosis (within 15 min of exposure) of SM poisoning especially during the asymptomatic latency period (6-24 h post-exposure).

Chapter 1. Introduction

1.1 Overall Significance

Chemical warfare agents (CWAs), such as cyanide and sulfur mustard, have been weaponized and used for many years, resulting in millions of casualties and deaths [1-3]. Despite the efforts of the Chemical Weapons Convention to prohibit development, production, stockpiling, and use of CWAs, their use on civilians, as recent as 2017 [4], indicate the continuous threat that they pose to mankind [5]. Therefore, research on improved toxicological understanding and the development of effective therapeutics are critical to combat the threats of CWAs [2, 3, 6].

Approved antidotes for cyanide poisoning suffer from serious limitations [7-10], whereas treatments for SM poisoning are currently unavailable. This necessitates the development of novel therapeutics, which require pharmacokinetic and toxicokinetic studies based on validated analytical methods. These studies help allow for FDA (Food and Drug Administration) approval of novel drugs, which can potentially save lives of CWA exposed victims. Moreover, the elucidation of the metabolic behavior of biomarkers is necessary for correlation to "internal dose" and revealing the advantages and disadvantages of each marker for detecting CWA exposure. To date, no biomarker studies have been completed on inhaled SM, one of the most important routes of exposure [11, 12]. Biomarker studies and quantification of actual respiratory dose will improve validity of inhalation studies, which are vital in developing effective therapeutic interventions against SM poisoning. Additionally, methods for rapid detection of early

markers will allow for immediate diagnosis of exposure, especially during the latent period of SM (i.e., 6-12 h post exposure when clinical symptoms are not present).

1.2 Project Objectives

The work is comprised of three main objectives: 1) Develop novel analytical method to determine DMTS, a next generation antidote, in plasma, 2) Identify biomarkers of inhalation exposure of SM for potential use in dose-correlation studies, and 3) Develop a simple and rapid technique for analysis of SMO, a diagnostic SM metabolite, from plasma. Chapter 2 describes the analysis of novel cyanide antidote, DMTS using stir bar sorptive extraction (SBSE)- gas chromatography-mass spectrometry (GC-MS). Chapter 3 addresses the identification of biomarkers for inhalation exposure of SM and preliminary correlation of concentration to dose. Chapter 4 details determination of SMO from plasma using a direct and rapid GC-MS method. Chapter 5 contains conclusions and future work.

1.3 Classifications of CWAs

Chemical warfare (CW) agents are Weapons of Mass Destruction (WMD) [13]. These compounds are extremely toxic synthetic chemicals that have a rapid onset of action after dissemination and cause lethal or incapacitating effects on humans. They are usually dispersed as a gas, liquid, or aerosol, or as agents adsorbed to particles that can be made powder [13, 14].

Based on the physicochemical, physiological, and chemical properties, CW agents can be classified in several different ways. However, the most commonly used classification is based on the physiological effects produced by the CW agents.

According to this classification, CW agents are mainly categorized into four distinct subgroups: nerve agents, vesicants (blistering agents), blood agents, and choking agents [13].

Nerve agents, including sarin, soman, tabun, and VX, are a class of highly toxic organophosphates that affect the functioning of the nervous system [15]. Nerve agents are more toxic than other known CWAs, and are capable of causing death within minutes to hours of exposure, depending on concentration [16]. The highly volatile nature of nerve agents is a key physical property contributing to their effectiveness [15, 16]. Routes of exposure for nerve agents include inhalation, ingestion, and dermal absorption.

Choking agents, which includes a wide array of gases such as chlorine, phosgene, ammonia, organohalides, and nitrous oxides, were among the first CW agents produced in large quantities and were used extensively in World War II [13]. Choking agents, also known as pulmonary agents, attack the nose, throat, and the lung tissues, primarily causing pulmonary edema. In severe cases of exposure, the lungs can fill up with fluid, and result in death from lack of oxygen [13].

Blistering agents, also known as vesicants, are toxic chemicals that produce blisters or vesicles, resembling those caused by burns [13]. The chemicals in this CWA class are toxic to skin, lungs, eyes, and mucous membranes. There are three different subclasses within the vesicants: the mustards, the arsenicals, and the halogenated oximes. Overall, vesicants have low lethality compared to other CW agents, but are generally very effective in inflicting pain and producing casualties. Vesicants, mainly sulfur mustard, is one of the most widely used CWA, because of its ability to degrade the

performance and efficiency of soldiers by incapacitating them [13, 17]. The burns caused by vesicants are comparable to thermal burns, however takes longer time to heal.

Blood agents, which mainly include the cyanides, get transported within the body via distribution of blood, and function by inhibiting the ability of cells to utilize and transfer oxygen [18]. These agents are also known as systemic agents [13, 19].

1.4 History and uses of CWAs

The use of chemical warfare agents dates back to the 19th century [13]. Although, historical evidence shows that the use of poisonous extracts from plants were prevalent throughout the Middle Ages and Renaissance, the practice of deploying chemicals on the battlefield only started in 1915 [1]. CWAs, such as phosgene, sulfur mustard, and lewisites, used in World War I caused 100,000 deaths and 1.2 million casualties. During World War II more than a million deaths were reported due to the use of hydrogen cyanide (Zyklon B) in extermination camps by the Nazis [2].

In recent times, CWAs were used in Iran-Iraq war, and during attacks by a Japanese cult in Motsumoto (1994) and the Tokyo subway system (1995) [20]. More recently, strong evidences suggest the use of CWAs such as mustard and chlorine gas in Syria (2015) by Islamic State (IS) militants [21].

Although a wide variety of CWAs exist and are of public health and safety concern, this work is focused on cyanide, a blood agent, and sulfur mustard, a vesicant. The following sections will elaborate in the exposure, toxicity, treatments, and methods used for analysis of cyanide and sulfur mustard.

1.5 Cyanide: Exposure, Toxicity, Antidotes

1.5.1 Exposure to Cyanide

Exposure to cyanide can be caused from natural and anthropogenic sources, or from illicit use of cyanide as a poison [10, 22-25]. Natural sources include release of cyanide into the environment from volcanoes, fungi, bacteria, and plants [26]. Volcanic eruptions can release hydrogen cyanide gas into the atmosphere, which contaminates air and water for miles [26]. Several species of bacteria, fungus, and algae, can also release cyanide into the environment at low concentrations [27]. However, the major natural source of cyanide is cyanogenic plants, which synthesize compounds called cyanogens that produce cyanide upon hydrolysis [28]. Over 800 species of edible plants and fruits, including cassava, almonds, sweet potatoes, yams, peaches, apples, apricots, pears, lima beans, flax seeds, bamboo shoots, etc., have been identified as cyanogenic [29, 30]. For instance, cassava, a staple food in several parts of Africa, contains enough cyanogens that daily consumption of a cassava-rich diet can be equivalent to about half the lethal dose of cyanide [31].

Exposure to cyanide from anthropogenic sources involve occupational exposures during industrial processes (electroplating, plastic processing, mining) and inhalation of hydrogen cyanide gas from fires/smoke (i.e. burning of acrylonitrile, polyurethane, wool, silk, rubber, and cigarettes produces HCN) [32, 33]. Hydrogen cyanide, which is used to prepare different salts of cyanide, is produced worldwide at an estimated amount of 1.4 million tons annually [22]. Extraction of a desired metal from soil or rocks is one of the major uses of cyanide due to its strong binding capacity to gold, silver, zinc, etc. [34].

Other common uses of cyanide include synthesis of pigments, pesticides, plastics, dyes, and insulation. Although occupational exposure of cyanide is of major concern, the leading cause of exposure from anthropogenic sources can be attributed to inhalation of smoke from cigarettes [35] and household or industrial fires [36]. Incomplete combustion of nitrogen containing compounds (e.g., plastic, wool, silk) produces cyanide-containing smoke during building fires [36]. Cyanide develops when the temperature reaches 315 °C (600 °F), and is released as hydrogen cyanide gas. It is reported that the majority of deaths due to smoke inhalation during fires are caused by cyanide poisoning instead of poisoning from carbon monoxide [37]. In 2015, a deadly explosion in a warehouse containing 700 tons of sodium cyanide, severely contaminated air and water in Tianjin, China. After the explosion, cyanide levels in affected zones soared up to 365 times higher than the safety limit [38]. It is not certain if the death of 115 people during this tragic event was a direct result of cyanide exposure. However, thousands of dead fish found on the shore of a contaminated river stoked fears in citizens regarding the short- and long-term health effects of this exposure [38].

Apart from exposure to cyanide due to natural and anthropogenic sources, humans can also be exposed to it due to its illicit use as suicide, homicide, and chemical warfare agent [39]. Although the use of cyanide as poison dates back to earlier times, cyanide was first used as a large-scale chemical weapon during World War I. In more recent times, cyanide was used during the Iran-Iraq war in the late 1980s and in the Tokyo subway attack in 1995 [40, 41]. Cyanide was also used to poison a lottery winner in 2012 [42, 43] and a Pittsburgh physician in 2013 [44].

1.5.2 Mechanism of toxicity and symptoms

Cyanide (LD_{50} = 1.5 mg/kg via oral exposure, LC_{50} = 524 ppm for a 10 min inhalation exposure to HCN) is a rapidly acting, highly toxic compound [10, 22, 23]. The high toxicity of cyanide can be attributed to its strong affinity for ferric ion (Fe^{3+}), which is a common metallic cofactor in metalloenzymes [10, 22]. The main target during cyanide exposure is cytochrome c oxidase, which is the last mitochondrial enzyme found in complex IV of the electron transport chain (Figure 1.1). Cytochrome c oxidase is responsible for carrying electrons to molecular oxygen, thereby reducing it to water (Equation 1.1) [25]. Additionally, it also maintains an electrochemical gradient of H^+ ions, which is essential in the production of adenosine triphosphate (ATP). However, when cyanide binds to the cytochrome c oxidase, it cannot transfer its electrons, inhibiting the cellular respiration [37, 45]. Furthermore, the gradient of H^+ ions disrupts, halting the ATP synthesis. Therefore, in order to compensate for the loss of ATP, glucose is broken down via the glycolysis pathway, which uses nictotinamide adenine dinucleotide (NAD^+). In order to replenish the lost NAD^+, fermentation of lactic acid occurs under hypoxic conditions, leading to the formation of large amounts of lactic acid. The increase in lactic acid concentration in blood decreases the pH of the body, which impairs several other physiological processes, ultimately leading to cell death [46].

$$4\ \text{Cyt c (reduced)} + 8H^+ + O_2 \leftrightarrow 4\ \text{Cyt c (oxidized)} + 4H^+ + 2H_2O \qquad (1.1)$$

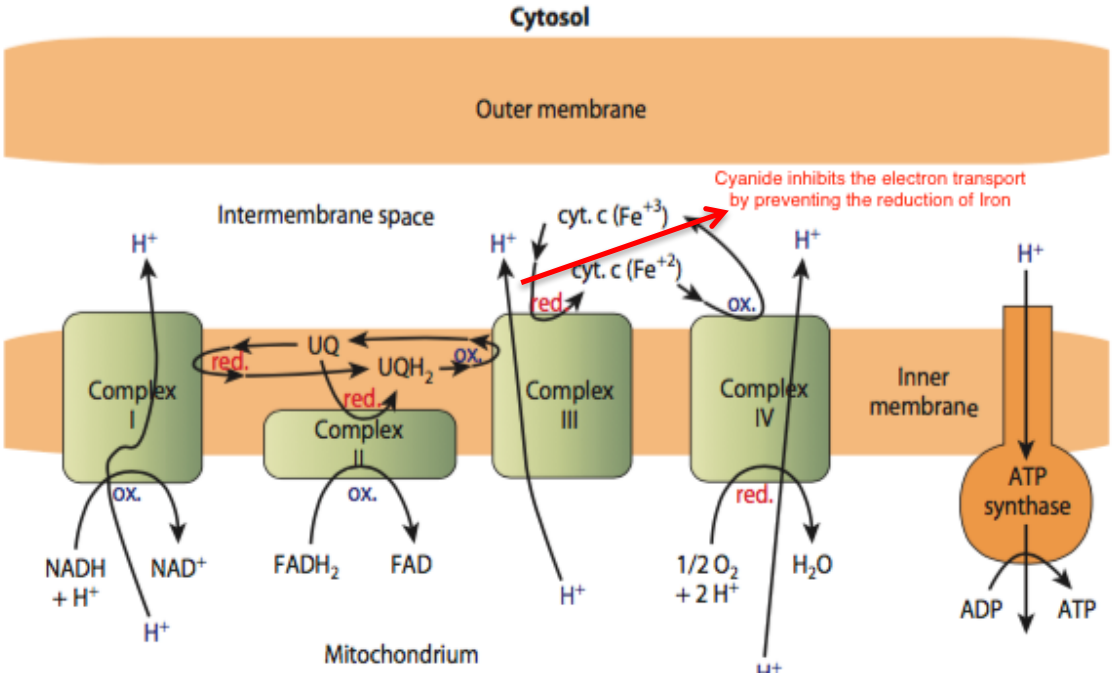

Figure 1.1. Diagram showing the electron transport chain. Cyanide binds to the Fe3+ of the cytochrome c and results in inhibition of cellular respiration [47].

1.5.3 Confirmation of exposure

Determination of cyanide exposure can be accomplished by direct analysis of cyanide or by analysis of its metabolites [22]. Direct analysis of cyanide may be the only way to confirm exposure within the initial minutes following exposure [48, 49]. However, it has several limitations due to high volatility, reactivity, and also short half-life of cyanide in biological fluids, making it difficult to detect once a certain amount of time has elapsed following exposure [50, 51]. Therefore, indirect determination of exposure is performed by analyzing cyanide metabolites that are generally longer-lived *in vivo* and are more stable under normal storage conditions than cyanide [48, 52]. The major metabolites of cyanide that have been detected from urine, saliva, tissue, and blood are thiocyanate (SCN^-) and tautomers 2-amino-2-thiazoline-4-carboxylic acid (ATCA)

and 2-iminothiazolidine-4-carboxylic acid (ITCA) [53-56]. Additionally, cyanocobalamin and cyanide-protein adducts have been evaluated [18].

1.5.4 Current cyanide antidotes

There are currently three U.S. Food and Drug Administration (FDA) approved antidotes for cyanide [10, 57]. The different classes of antidotes differ in their detoxification mechanism. Typically, an ideal antidote is expected to have properties such as rapid onset of action, capability of neutralizing cyanide without interfering with cellular oxygen transport, safe to administer to victims of smoke inhalation, not harmful if given to a non-poisoned patient, and ease of administration without the need of special training or equipment. The detoxification mechanism and properties of the three FDA approved antidotes will be discussed below.

1.5.4.1 Hydroxocobalamin

Hydroxocobalamin (Cbl), also known as vitamin B_{12}, was approved by FDA for treatment of cyanide poisoning in 2006 [10, 57, 58]. Cbl is cobalt-containing compound that detoxifies cyanide by direct sequestration [59, 60]. Due to the high affinity of cobalt towards cyanide, Cbl directly binds with cyanide by replacing its hydroxyl ligand, thereby allowing the cytochrome c oxidase to return to its normal function during cellular respiration [59, 61]. This process leads to the formation of cyanocobalamin, which is excreted from the body in the urine [61]. The properties of Cbl that makes it ideal as an cyanide antidote are: i) it has a rapid onset of action, ii) its detoxification process does not compromise the oxygen carrying capacity of blood, iii) it can be administered to smoke inhalation victims, and iv) it has mild side effects [61]. Despite the advantages of Cbl, its

major limitation is the need for high effective doses [57]. One molecule of Cbl is required to sequester one molecule of cyanide; therefore, due to the 50:1 Cbl:cyanide molecular weight ratio, the recommended dose of Cbl is 5g (administered over 15 min) [8]. Due to the large dosage, Cbl must be administered by IV, which severely limits its applicability in cases of mass casualty situations.

1.5.4.2 Sodium nitrite

Sodium nitrite detoxifies cyanide via two routes i) indirect sequestration and ii) cyanide displacement [62]. Nitrite (classified as a methemoglobin generator) converts hemoglobin, which has low affinity to cyanide, to methemoglobin, which has a relatively high affinity towards cyanide [62]. Methemoglobin serves as a temporary binding site for cyanide, decreasing the presence of free cyanide in the bloodstream. The recently suggested cyanide displacement mechanism of action is postulated to occur as nitrite is converted to nitric oxide, which then displaces cyanide bound to the cytochrome c oxidase [62, 63]. With either of the detoxification mechanism, the major limitation of sodium nitrite is the production of methemoglobin [63]. Excessive methemoglobin is toxic to the body and can lead to headache, cyanosis, fatigue, coma, and even death [10]. Furthermore, administration of sodium nitrite can be fatal for victims of smoke inhalation as it further reduces the oxygen carrying capacity of the blood [62].

1.5.4.3 Sodium thiosulfate

Sodium thiosulfate is the only FDA approved sulfur donor cyanide antidote [10]. It detoxifies cyanide by donating sulfur and converting cyanide into minimally toxic and renally excreted thiocyanate [64]. This detoxification mechanism is dependent on a sulfur

transferase enzyme, rhodanese. Rhodanese has limited availability in the body [9], with very low/no availability in some vital organs such as heart and brain. Therefore, these organs are susceptible to cyanide poisoning even upon administration of thiosulfate [9, 65]. Due to this major drawback, sodium thiosulfate is only useful as combination therapy [23, 66]. Apart from high rhodanese dependency, sodium thiosulfate is also limited due to its short biological half-life and relative low sulfur donor activity [10]. Furthermore, the inorganic thiosulfate has limited lipophilicity as a result of its anionic charge, which results in limited transport across cell membranes in order to reach the endogenous rhodanese within mitochondria.

1.5.5 Novel cyanide antidotes

Considering the serious limitations in each of the available antidotes, several investigations have been in progress for the next generation of cyanide therapeutics. The three major ones that show a good promise in overcoming the current drawbacks are 3-mercaptopyruvate (3-MP), cobinamide (Cbi), and dimethyl trisulfide (DMTS).

1.5.5.1 Cobinamide (Cbi)

Cobinamide is the penultimate precursor during the biological synthesis of hydroxycobalamin, and is seen to have several advantages over hydroxycobalamin as a cyanide antidote [8]. Cbi has a much higher affinity to cyanide, with K_a overall of ~ 10^{22} M^{-1} compared to a K_a of 10^{12} M^{-1} for hydroxocobalamin [67]. The higher affinity can be explained by the difference in structures of the two molecules. Unlike Cbl, Cbi lacks the dimethyl-benzimidazole ribonucleotide tail coordinated to the cobalt atom in the lower axial position (Figure 1.2, blue portion of the structure), which allows it to have two

binding site for ligands: above and below the plane of the corrin ring [68]. Therefore, it is capable of binding two moles of cyanide per mole Cbi. Comparatively, one mole of cyanide is bound per mole of Cbl [8]. Furthermore, in aqueous solution, Cbi exists as aquohydroxocobinamide, which is at least five times more soluble in water than Cbl [8]. The high binding affinity of Cbi means that it can be administered in a smaller dose (1-1.5 g), which makes it more practically feasible than Cbl [8]. Additionally, the relatively high water solubility allows the possibility of intramuscular administration, which makes it a good candidate for mass casualty events [8, 69].

a.

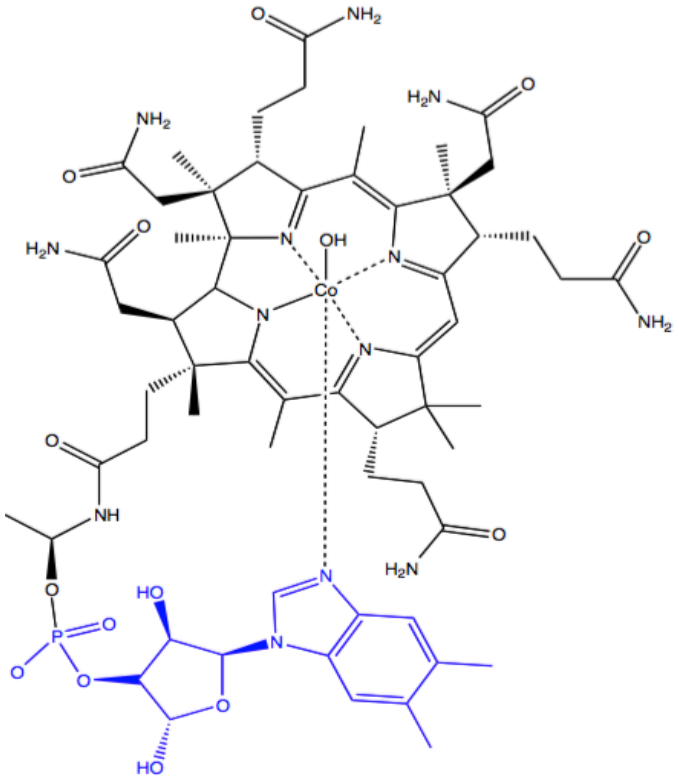

b.

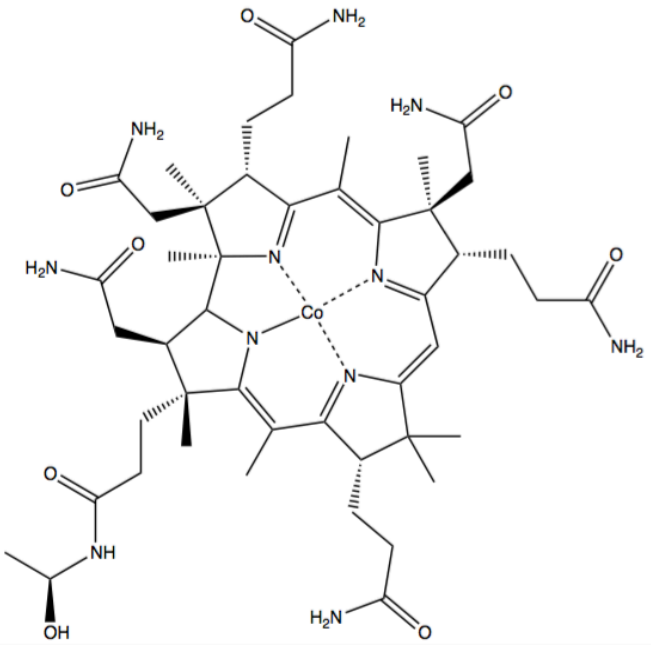

Figure 1.2. Structures of cobalamin (a) and cobinamide (b). The cobalt atom in cobalamin only has one available binding site due to the presence of dimethylbenzimidazole ribonucleotide tail (shown in blue). Cobinamide lacks the dimethylbenzimidazole ribonucleotide tail, which allows its cobalt atom to have two binding sites (upper and lower) for ligands.

1.5.5.2 3-mercaptopyruvate (3-MP)

3-MP is similar to sodium thiosulfate in that it also acts as a sulfur donor and detoxifies cyanide by conversion into thiocyanate [70]. However, instead of being dependent on rhodanese, 3-MP is catalyzed by 3-MP sulfurtransferase (3-MST), which is readily available in liver, kidneys, heart, brain, and lungs. The abundance of 3-MST reduces the vulnerability of these organs to cyanide toxicity upon administration of 3-MP [71]. Additionally, unlike rhodanese, 3-MST is distributed in both cytosol and mitochondria, allowing cyanide detoxification to occur in both. Despite the advantageous properties of 3-MP, its major limitation is that it readily degrades in blood [66, 72]. In order to overcome this drawback, several prodrugs of 3-MP are currently being

investigated, one of which is sulfanegen [71, 72]. Developed in the early 1990s, sulfanegen is a water-soluble prodrug of 3-MP. It is a dimer, which dissociates non-enzymatically into two 3-MP molecules in physiological condition [71]. It also overcomes the drawback of low stability of 3-MP, which makes it an ideal choice as an antidote.

1.5.5.3 Dimethyl trisulfide (DMTS)

DMTS, which detoxifies cyanide by converting it into thiocyanate, is suggested as the most promising next-generation sulfur donor for treatment of cyanide poisoning [10]. Unlike the current sulfur-donor thiosulfate, DMTS can effectively function with or without rhodanese [73]. Additionally, DMTS is highly lipophilic, which permits effective penetration through the cell membrane and the blood brain barrier, allowing better antidotal efficacy than thiosulfate [74]. Recent in-vitro studies have shown that DMTS is 43 times more effective than thiosulfate at detoxifying cyanide in presence of rhodanese [73]. Whereas, in absence of rhodanese, it is 79 times more effective, confirming that DMTS is less dependent on the enzyme [73]. Results from in-vivo studies are consistent with these findings, suggesting that DMTS is superior as a cyanide therapeutic than thiosulfate [74].

Although the mechanism of detoxification in the absence of rhodanese is not fully understood, it is evident that DMTS is effective. The reaction by which DMTS converts cyanide into thiocyanate is shown in Figure 1.3.

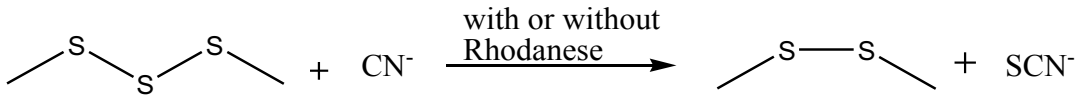

Figure 1.3. Reaction showing the detoxification of cyanide (CN-) to thiocyanate (SCN-) by DMTS. In vitro and in vivo studies suggest that DMTS is capable of metabolizing cyanide even without the presence of a sulfur transferase enzyme like rhodanese.

1.6 Sulfur Mustard: Exposure, Toxicity, Metabolism, and Confirmation of Exposure

1.6.1 Exposure to Sulfur Mustard

Bis(2-chloroethyl)sulfide, commonly known as sulfur mustard (SM), was first synthesized in 1822 by Depretz, by reacting ethane and sulfur dichloride (Equation 1.2) [5]. However, the vesicating properties of SM were not mentioned during or after the synthesis. In 1860, Niemann followed the same procedure and reported that even at trace amounts the synthesized chemical when brought in contact with skin caused pain and blisters after several hours [5]. Later, Clark and Fischer synthesized SM by reacting thiodigycol with hydrochloric acid (Equation 1.3) [5]. Clark suffered burns when a flask broke during the synthesis process, which caused him to be hospitalized for 8 weeks. The mention of this incident allegedly inspired the German Chemical Society to deploy SM for the first time as a chemical weapon in 1917 during the course of the First World War. Upon deployment, 4,000 deaths of British armed forces and over 16,000 nonfatal injuries were reported as a result of SM poisoning during the course of World War I [5, 75].

$$SCl_2 + 2C_2H_4 \rightarrow (Cl - CH_2 - CH_2)_2S \quad (1.2)$$

$$(HO - CH_2CH_2)_2S + 2HCl \rightarrow (Cl - CH_2CH_2)_2S + 2H_2O \quad (1.3)$$

Since the First World War, SM has been deployed in several combat situations, such as United Kingdom against the Red Army (1919), Spain in Morocco (1921-1927), Italy in Libya (1930), Soviet Union against Japan (1930), Italy against Abyssinia (1935-1940), Poland against Germany, Germany against Soviet Union and Poland, Japan against China during Second World War, and Egypt against Yemen (1963-1967) [5]. More recently, evidence suggests the use of SM in Iraq vs. Kurdistan, Iraq vs. Iran, and in Syria (2015) by Islamic State (IS) militants [76].

1.6.2 Mechanism of sulfur mustard toxicity

SM can enter the body through various routes including inhalation, ingestion, and absorption through the skin or eyes. The high lipophilicity of SM allows it to rapidly penetrate through the hair follicles and sweat glands of skin and mucous membranes [77]. SM greatly affects moist body parts such as eyes, mouth, respiratory tract, scrotum, and anus [77, 78]. Inhalation of its aerosol or vapor produces a serious upper respiratory tract irritation [78] and the odor of SM does not provide adequate warning for detection. The LCt50, which is the product of concentration and time that is lethal to 50% of the exposed population via inhalation, is approximately 1500 mg-min/m^3 [5].

The acute effects of SM are usually delayed, with no signs or symptoms in the first hour. Within 2-6 hours post-exposure, typical signs of nausea, headache, fatigue, reddening of the face and neck, soreness of throat, inflammation of eyes, etc. become

severe [5]. Skin inflammation and blistering, accompanied by coughing with pus, becomes marked within the 24 hours after exposure. In severe cases, death may be caused within days or weeks [5]. Whereas in less severe cases, the burns heal slowly with increased vulnerability to infections.

The toxicity of SM can be attributed to its ability to readily alkylate nucleophilic sites (i.e., it is capable of replacing a proton in another molecule by an alkyl cation) [79, 80]. After passing through the cellular membrane, one chloroethyl side chain undergoes a first–order (SN1) intramolecular cyclization, releasing the chloride and forming a positively charged ethylsulfonium ring (Figure 1.4) [80]. This intermediate rapidly reacts with nucleophilic groups (sulfhydryls, phosphates, ring nitrogens, and carboxyls) present in DNA, RNA, and proteins, resulting in irreversible alkylation and cell death [79, 81]. The most important target is the DNA. All bases of DNA are susceptible to alkylation, especially the N7 position of guanine because it is the most negative site within DNA bases [82]. DNA damage can lead directly to cell death or activate poly(ADP-ribose) polymerase (PARP) and other repair enzymes. Over-activation or higher levels of PARP can lead to apoptotic or necrotic cell death, whereas mild levels may be beneficial to cell survival as it triggers DNA repair mechanisms.

The vesicating activity of sulfur mustard can also be attributed to the alkylation of cytoskeletal, extracellular matrix (ECM), and cell anchoring–related matrix proteins. This process can weaken and interfere with the ability of basal keratinocytes to maintain vital connections with the basement membrane, which ultimately leads to epidermal-dermal separation, cell death, and formation of blisters.

Finally, sulfur mustard also targets sulfhydryl-containing proteins, such as glutathione (GSH), which plays a major role in maintaining a redox homeostasis in the tissues. The depletion of GSH initiates oxidative stress, which leads to lipid peroxidation and other oxidative cellular damage.

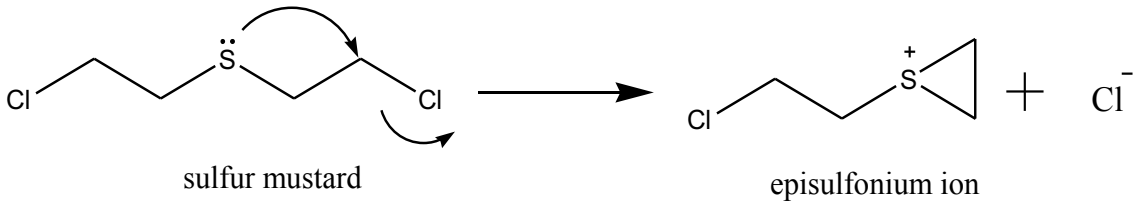

Figure 1.4. Formation of episulfonium ion as a result of first order SN1 intramolecular cyclization.

1.6.3 Metabolism of sulfur mustard

There are four SM metabolic routes identified in animal models [5, 79]. The first route can be considered direct chemical transformations resulting in β-chloroethyl sulfoxide (SMO) from direct oxidation of SM, thiodigycol (TDG) from direct hydrolysis of SM, and thiodiglycol sulfoxide (TDGO) from oxidation of TDG [5, 79]. The second route involves an initial reaction of SM with two molecules of glutathione. The bis-glutathione is metabolized into bis-cysteinyl conjugate followed by β-lyase cleavage of cysteinyl C-S bond and a subsequent methylation and oxidation of the thiol, resulting in 1,1' -sulfonylbis[2-S- (N-acetylcysteinyl) ethane] (SBSNAE), 1,1' -sulfonylbis[2-(methylthio) ethane] (SBMTE), 1-methylsulfinyl-2-[2- (methylthio)ethylsulfonyl]ethane (MSMTESE) and 1,1' - sulfonylbis [2-(methylsulfinyl) ethane] (SBMSE) [5, 83]. The third route involves reaction of SM with DNA at nucleophilic sites resulting in formation of SM-DNA adducts [82]. Finally, the last route involves reaction with amino acid

residues present in proteins, resulting in formation of some major adducts, such as an HETE-valine adduct of hemoglobin and an HETE-cysteine adduct of albumin [5].

1.6.4 Confirmation of exposure

Detection of free sulfur mustard in biological fluids such as urine, plasma, blood, etc. is highly unlikely due to its extensive metabolism via rapid hydrolysis, oxidation, and reactions with glutathione and nucleophilic sites in the body [84]. Therefore, the metabolites as well as alkylated macromolecules are generally exploited to determine exposure to SM. The hydrolysis, oxidation, and β-lyase metabolites appear in biological specimens within 15 min of exposure and are ideal for diagnostic purposes. However, these metabolites undergo relatively rapid elimination (within 5-10 days) [82] and cannot be used as long-term markers. In contrast, adducts to macromolecules (DNA and proteins) are present for relatively long times (30-90 days) post-exposure and can be used for verification of exposure long after the event [82].

The analysis of urinary metabolites in SM-exposed rats were initially reported by Black et al., where they identified oxidative and hydrolysis metabolites SMO, TDG, TDGO, and glutathione-derived metabolites SBSNAE, SBMSE, MSMTESE, and SBMTE [79]. Several analytical methods have been developed over the years for analysis of these metabolites in urine. Quantification of TDG and TDGO has been typically accomplished by derivatization followed by analysis using gas chromatography-tandem mass spectrometry (GC-MS/MS) [85-88]. However, several studies suggested that TDG and TDGO are not unequivocal markers of poisoning, as low concentrations (usually <10ng/mL, but sometimes higher) of TDG and TDGO are observed in urine samples of

animals [89] and humans [90, 91]. In fact, in some studies performed, TDG concentrations in exposed and unexposed individuals had a considerable overlap [92]. Although TDG and TDGO are not definitive markers of SM exposure, their presence in combination of other metabolites can help confirm a potential exposure.

β-lyase metabolites (SBMSE, MSMTSESE, SBMTE), which are unequivocal markers for SM poisoning, were initially analyzed via GC-MS by reducing SBMSE and MSMTESE into a single analyte, SBMTE, using titanium (II) chloride [88, 93]. More recently, methods have been developed to analyze these markers as separate individual entities using LC-MS/MS [83]. The β-lyase and oxidation/hydrolysis products have mainly been studied in urine samples until Li et al. in 2013 developed a simultaneous method for analysis of the seven metabolites (SMO, TDG, TDGO, SBMSE, MSMTESE, SBMTE, and SBSNAE) from plasma [89]. Li et al. showed that all of the seven metabolites were present in the plasma of rats that were exposed to SM. The analysis of metabolites is simpler and involves less time-consuming steps compared to the analysis of SM adducts.

Retrospective and forensic detection for SM poisoning is achieved by analyzing DNA and proteins for SM adducts. Analysis of these macromolecules is typically performed by three different approaches [80]. The first approach involves analysis of the entire alkylated protein or DNA with intact SM adduct(s). In the second approach, macromolecules can be enzymatically or chemically digested to produce a smaller fragment which retain the adduct. Finally, the third approach involves cleaving the adduct from the macromolecule and analyzing the unbound adduct as a free metabolite.

Typically, analysis of protein adducts are chosen over analysis of DNA adducts, as protein adducts are expected to have a much longer half-life, with life spans varying from several weeks to months [94, 95]. Furthermore, the detection of protein adducts is more sensitive and is typically advantageous in determining single, protracted, and intermittent exposure at low concentrations [95]. There are two main protein adduct based methods, which have been significantly improved over the years. Detection of adducts of SM to albumin involves a pronase digestion of SM alkylated albumin, which results in formation of (S-2-hydroxyethylthioethyl)-Cys-Pro-Phe, known as the [(S-HETE)-Cys-Pro-Phe] [96]. This tripeptide product can be analyzed via liquid chromatography-tandem mass spectrometry (LC-MS-MS). SM-adducted hemoglobin is detected as a HETE-Val adduct after Edman degradation, which involves selective cleaving of the N-terminal valine adduct to hemoglobin [97]. It is important to note than albumin adducts undergo faster elimination than hemoglobin adducts (half-life of albumin is 20-25 days, compared to 120 days for hemoglobin), which limits its utility to only a few weeks after exposure [98].

Chapter 2. Determination of Dimethyl trisulfide in rabbit blood using stir bar sorptive extraction – gas chromatography mass spectrometry

2.1 Introduction

Cyanide (LD_{50} = 1.5 mg/kg, oral route, LC_{50} = 524 ppm for a 10 min inhalation exposure to HCN) is a rapidly acting, highly toxic compound that inhibits cytochrome c oxidase and subsequently causes cellular hypoxia, which may eventually result in death [10, 22-25, 33]. It can be introduced into the body by a number of different ways, such as consumption of cyanogenic plants and fruits [28-30] (e.g., cassava roots, yam, sorghum, bitter almonds), inhalation of hydrogen cyanide gas from fire [99] (i.e., burning of acrylonitrile, polyurethane, wool, silk, rubber produces HCN) and cigarette smoke, occupational exposures (e.g., the 2015 warehouse explosion in Tianjin, China [100, 101]) and from use of cyanide as a suicide, homicide, or chemical warfare agent [32, 102, 103] (e.g., in World War I, II, Tokyo subway attack, etc. [22]). The availability of cyanide, due to its versatile use in industrial processes (e.g., electroplating and plastic processing) and its rapidly acting nature, makes it an important and ever-growing threat to mankind [22, 104]. Currently, there are three major classes of cyanide therapeutics that are approved by the U.S. Food and Drug Administration (FDA): methemoglobin generators, direct sequestering agents, and sulfur donors [10, 57, 105, 106].

Sodium nitrite, primarily classified as a methemoglobin generator, is generally agreed to function by indirect sequestration of cyanide [62]. Nitrite oxidizes ferrous (2+) iron to ferric (3+) iron in hemoglobin to form methemoglobin, which strongly binds cyanide to form cyanomethemoglobin. Methemoglobin serves as a temporary binding site

for cyanide ion, and thus transiently decreases free cyanide in the bloodstream. Another recently proposed alternative mechanism of action is the conversion of nitrite to nitric oxide, which can then displace cyanide bound to cytochrome c oxidase [63, 107]. After displacement, cyanide is subsequently converted to less harmful compounds through normal metabolism or neutralized via a combination therapy (e.g., thiosulfate) [107]. With either detoxification mechanism, the major limitation of sodium nitrite is the production of methemoglobin. Excessive methemoglobin production (>30%) is a health risk, especially in children, leading to headaches, cyanosis, fatigue, coma, and even death [57]. Additionally, conversion of hemoglobin to methemoglobin lowers the oxygen carrying capacity of the blood, which can exacerbate carbon monoxide-induced reduction in oxygen carrying capacity in smoke-inhalation victims [10, 62].

While sodium nitrite indirectly binds cyanide, hydroxocobalamin acts by directly sequestering cyanide [10, 59, 108]. The high affinity of cyanide towards the cobalt atom in hydroxocobalamin allows the formation of cyanocobalamin, which is easily excreted from the body in the urine. Although administration of hydroxocobalamin produces only mild side effects, it requires a high dose for optimum therapeutic effect (5 g administered over 15 min) [108]. Therefore, hydroxocobalamin typically needs to be administered intravenously by trained personnel over a long period of time, which severely limits its applicability during mass casualty events [10, 57].

Sodium thiosulfate, the third class of cyanide antidote, is the only currently approved sulfur donor for treatment of cyanide poisoning. It donates a sulfur to cyanide, converting it to minimally toxic and renally excreted thiocyanate [64, 65]. Although

sodium thiosulfate has few adverse effects, its antidotal activity is mainly limited by its short biological half-life, small volume of distribution, and its dependence on rhodanese to aid sulfur transfer [10]. Rhodanese is a sulfur transferase enzyme primarily located in mitochondria of the liver and kidneys, with limited availability in the brain, an organ most susceptible to cyanide-induced histotoxic anoxia. The limited lipophilicity of thiosulfate as a result of its anionic charge, also adversely impacts its ability to penetrate the cell and reach the mitochondrial rhodanese [10].

Considering the serious limitations of the current antidotes, several investigations have been in progress to develop the next generation of cyanide therapeutics [64, 65, 106, 109-111]. One promising approach is the development of a sulfur-donating compound that works effectively with or without rhodanese [64, 65]. Based on this approach, numerous synthetic and naturally occurring sulfur donors have been evaluated for in-vitro and in-vivo efficacy [10], with dimethyl trisulfide (DMTS) suggested as the most promising next generation sulfur donor for treatment of cyanide poisoning. The reaction by which DMTS detoxifies cyanide into thiocyanate is shown in Figure 2.1. The rhodanese sulfur transfer mechanism is well-discussed in the literature [112]. However, the mechanism of direct DMTS sulfur transfer is not well understood, but is known to occur [73]. Moreover, the high lipophilicity of DMTS permits its effective penetration of the cell membrane and the blood brain barrier, allowing better in-vivo antidotal efficacy than thiosulfate [73]. Recent in vitro studies demonstrate that, compared to sodium thiosulfate, DMTS is 43 times more effective at detoxifying cyanide in the presence of rhodanese [73]. Whereas, in absence of rhodanese, the difference in efficacy is even

higher, with DMTS producing 79 times greater efficacy than thiosulfate [73]. These results are consistent with in vivo studies, where the therapeutic antidotal ratio of DMTS was more than triple of what was observed for thiosulfate at the same dose. The *in vivo* and *in vitro* efficacy data confirm that DMTS is a superior cyanide countermeasure compared to the present sulfur donor therapy of thiosulfate.

Despite the potential advantages of DMTS, the lack of a validated analytical method for its analysis may limit vital studies for therapeutic translation of DMTS. The only relevant report in regards to analysis from a biological matrix was published by Shirasu and coworkers, where DMTS was identified as a source of sulfurous malodor in fungating cancer wounds [113]. However, the concentrations of DMTS were not well quantified, and the method was not validated. Besides this single study, DMTS has mainly been identified as a naturally occurring compound contributing to pungent odors in vegetables such as garlic, soy, cabbage, broccoli, and cauliflower [113-117]. In addition, it has also been detected or quantified from fermented and aged food (cheese) and drinks (milk, beer [118], sake, and wine), where it most likely comes from oxidation of methanethiol, a bacterial degradation product of methionine [113, 119-123]. The analysis of DMTS is typically accomplished using headspace analysis or solid-phase microextraction with GC-MS. While these analytical techniques provide direction for the analysis of DMTS from blood, a validated analytical method is not currently available (from any matrix), but is critical for further development of this promising antidote. Therefore, the objective of the current study was to develop a validated method for the analysis of DMTS from whole blood. To accomplish this objective, a stir bar sorptive

extraction (SBSE) GC-MS analysis technique for analysis of DMTS from rabbit whole blood samples was developed.

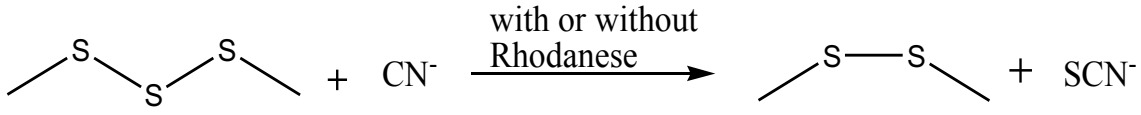

Figure 2.1. Schematic representation of the reaction of DMTS and cyanide to form dimethyl disulfide (DMDS) and thiocyanate.

2.2 Experimental

2.2.1 Reagents and Standards

All reagents were at least reagent grade unless otherwise noted. Methanol (LC-MS grade) and nitric acid were purchased from Fisher Scientific (Fair Lawn, NJ, USA). Reverse-osmosis water was purified to 18.2 MΩ-cm using a polishing unit from Lab Pro, Labconco (Kansas City, KS, USA). Dimethyl trisulfide (DMTS) was obtained from Sigma-Aldrich (St. Louis, MO, USA). Gerstel Twister® stirbars (film thickness 0.5 mm, length 10 mm) were purchased from Gerstel, Inc. (Linthicum, MD, USA). Isotopically labeled internal standard, dimethyl-d6-trisulfide (DMTS-d6), was acquired from US Biological Life Sciences (Salem, MA, USA). DMTS stock solution was prepared fresh for each experiment due to the unstable nature of DMTS. The internal standard solution was prepared from a 10 mM stock solution in methanol stored at -30 °C.

2.2.2 Biological fluids

For method development and validation, rabbit whole blood (EDTA anti-coagulated) was purchased from Pelfreeze Biological (Rogers, AR, USA) and stored at -80 °C until used. Rabbit whole blood was chosen as the method development matrix

because we planned to utilize a rabbit model performed by our collaborators to prove the applicability of the analytical method for the analysis of blood DMTS concentrations. However, at the time we were finalizing the method validation, efficacy studies of DMTS were transitioned to a mouse model. Mouse blood from DMTS efficacy studies was gathered at Sam Houston State University. DMTS was intramuscularly administered at 200 mg/kg. The mice were anesthetized (after 10 and 15 min) and placed on isoflurane. Blood was collected intravenously using a heparinized Pasteur pipette and transferred to heparinized 1.5 mL centrifuge tubes. An aliquot of blood (~150 μL) was then frozen and shipped on dry ice to South Dakota State University. Upon receipt, samples were stored at -80 °C until ready for analysis. Due to the limited volume of mouse blood, the sample (100 μL) was transferred to a clean vial and diluted in DI water to 500 μL before extraction and analysis.

All animals were handled in accordance with the Guide for the Care and Use of Laboratory Animals [124] by an Association for the Assessment and Accreditation of Laboratory Animal Care (AAALAC) International accredited institution. The Institutional Animal Care and Use Committee (IACUC) at Sam Houston State University approved the experiment.

2.2.3 Sample preparation

Blood (450 μL) was added to a 20 mL glass scintillation vial. An aliquot of aqueous nitric acid (1 mL, 90 mM) was added to the blood to lyse the red blood cells and denature the blood proteins. Where appropriate, aqueous DMTS standard (25 μL) was spiked into the denatured blood to achieve the desired final DMTS concentration.

Whenever needed, internal standard (25 μL) was spiked into the prepared blood to produce a final concentration of 5 μM DMTS-d6. A PDMS (poly dimethyl siloxane) coated stir bar was then added to the mixture, the sample was capped, and stir bar sorptive extraction was performed for 1 h at 700 rpm. Following extraction, the stir bar was removed from the solution using a 2-inch Teflon-coated magnet. The stir bar was gently dried by dabbing against a delicate task wipe and then transferred into a Thermal Desorption Unit (TDU) tube. The TDU tube was then placed into an auto-sampler for follow-on thermal desorption and GC-MS analysis. *(Note: Because of the rapid enzymatic degradation of DMTS in blood, for all validation experiments, blood was acid denatured before adding DMTS or IS in order to maintain the reported concentration and minimize error occurring from the rapid decomposition. The reported concentration of all DMTS standards, including QCs and calibrators, excludes the acid dilution volume.)*

2.2.4 GC-MS analysis of DMTS

After SBSE, stir bars were analyzed for DMTS and DMTS-d6 using an Agilent Technologies 7890A gas chromatograph with a 5975C inert XL electron ionization/chemical ionization mass selective detector with a Gerstel MPS 2XL series autosampler. To initiate analysis of the stir bar, the TDU tube with stir bar was transferred to the TDU injector and heated to transfer DMTS to the cooled injection system (CIS). The initial TDU injector temperature was maintained at 60 °C, and increased linearly to 250 °C at a rate of 720 °C/min. The final TDU injector temperature of 250 °C was maintained for 1 min. Desorbed analytes were transferred to the CIS

programmable temperature vaporization (PTV) type inlet in splitless desorption mode with a TDU transfer temperature of 200 °C. To transfer the analyte from the CIS to the GC column, the initial CIS temperature (30 °C) was linearly increased to 200 °C at a rate of 12 °C/s before returning to its initial temperature. Lower CIS temperatures, 10 and 0 °C, were evaluated. However, improvement of the chromatography was not observed, likely due to the relatively high boiling point of DMTS (170 °C).

A DB5-MS bonded-phase column (30 m x 0.25 mm I.D., 0.25 μm film thickness; J&W Scientific, Folsom, CA, USA) was used to separate components of the sample with nitrogen as the carrier gas at a flow rate of 1 mL/min and a column head pressure of 5.565 psi. The GC oven temperature was initially held at 30 °C for 1 min, then elevated at a rate of 120 °C/min to 250 °C, where it was held constant for 1 min, before returning to its initial temperature. The elapsed time from adding the TDU tube to TDU to the end of the analysis was ~ 9 min, which included transfer of the analyte from the PDMS coated stir bar, through the TDU and CIS, and into the column. The actual chromatographic acquisition time was 3.83 min with DMTS and DMTS-d6 eluting at 2.9 min. The GC was interfaced with a mass selective detector using electron ionization with an electron energy of 70 eV. The MS source and quadrupole temperatures were 250 °C and 150 °C, respectively. Selective ion monitoring (SIM) was used to monitor the quantification and identification ions of DMTS (m/z of 126 and 111, respectively) and DMTS-d6 (m/z of 132 and 114, respectively).

2.2.5 Calibration, quantification, and limit of detection

Validation of this method was performed by generally following the Food and

Drug Administration guidelines [125-127]. For calibration and quality-control (QC) standards, a combined DMTS and IS aqueous solution was initially prepared to limit loss of DMTS (i.e., loss from evaporation and degradation). Aqueous DMTS standard (100 μL) was transferred via pipette to a 2 mL glass vial, and a cap with a septum was used to immediately seal the vial. To the closed vial, IS (100 μL of 200 μM) was injected using a 1 mL (0.33 x 12.7 mm) syringe, and subsequently mixed to produce a combined standard of DMTS and IS. This standard solution was refrigerated at 4 °C until it was used for the preparation of calibration or QC standards. *(Note: Mixing of DMTS and IS in a closed vial using a syringe was a crucial step to prevent the rapid and uneven evaporative loss of DMTS and IS when opening and closing vials. Additionally, it was important to introduce IS and DMTS to the blood simultaneously to account for the rapid enzymatic degradation of DMTS.)* Calibration and QC standards were prepared by spiking the combined standard (25 μL) into 1475 μL of denatured blood and extracting as previously described in the sample preparation section. Each calibration standard (0.5, 1, 2, 5, 10, 20, 50, and 100 μM) was prepared in triplicate. To obtain a calibration curve, the average peak-area signal ratios of DMTS to IS were plotted as a function of concentration. Peak areas were calculated by manual integration from baseline to baseline in ChemStation software (Agilent Technologies, Santa Clara, CA). Five preliminary calibration curves were constructed to evaluate the calibration behavior of DMTS. Ultimately, a total of ten calibration curves constructed over the course of preliminary studies and validation experiments confirmed that a non-linear power curve fit ($y=ax^b$) best described the calibration behavior of DMTS.

The limit of detection (LOD) was determined by analyzing multiple concentrations of DMTS in blood below the LLOQ. The LOD was defined as the lowest DMTS concentration that reproducibly produced a signal-to-noise ratio of 3. Noise was measured by averaging the peak-to-peak noise in blank over the retention time of the analyte. The lower limit of quantification (LLOQ) and upper limit of quantification (ULOQ) were defined as the lowest and highest concentrations that satisfied the inclusion criteria of <15% relative standard deviation (as a measure of precision), and a percent deviation within ±15% back-calculated from the nominal concentration (as a measure of accuracy) for all calibration standards within the dynamic range. QC standards were prepared and analyzed in quintuplicate at three concentrations not included in the calibration curve: 1.5 μM (low QC), 7.5 μM (medium QC), and 35 μM (high QC). QCs were prepared fresh daily in order to calculate the intra-assay (within same day) and inter-assay (over three separate days, within six calendar days) accuracy and precision.

2.2.6 Selectivity and sensitivity

The ability to differentiate and quantify DMTS in the presence of other blood components (assay selectivity) was determined by comparing blank blood with DMTS spiked blood. The absence of signals above the baseline in the blank over the elution time of DMTS was indicative of high selectivity.

Short- and long-term stability of DMTS was assessed by analyzing triplicates of low and high QCs in rabbit blood at different storage conditions over multiple time periods. For short-term stability, prepared QCs were evaluated in the autosampler, on the bench-top, and under multiple freeze-thaw (FT) cycles. The autosampler stability was

evaluated by storing PDMS stir bars after SBSE extraction on the autosampler (at ambient temperature), and analyzing them at approximately 0, 1, 5, 10, and 24 h. Internal standard was not used for the autosampler stability experiment, as it would correct for the loss of DMTS during the storage time tested. The bench-top stability was evaluated for two different conditions: non-denatured blood and denatured blood. The low and high QCs for both conditions were allowed to stand at room temperature for 0, 1, 2, 4, 8, 12, and 24 h prior to analysis.

For freeze-thaw stability of DMTS, four sets of QCs (low and high) were prepared. One set of QCs was extracted and analyzed on the same day while the other three sets were stored in a freezer at -80 °C. After 24 h, all three sets of QCs were thawed by running ambient tap water over the base of the sample vial. A single set of thawed QCs was then extracted and analyzed, while the remaining two sets were again stored at -80 °C for 24 h. The procedure was repeated two more times to evaluate three freeze-thaw cycles.

Evaluation of long-term stability in blood was conducted at three storage conditions (-80, -20, and 4 °C). The low and high QCs were analyzed in triplicate on the day they were prepared, and after 1, 2, 5, 10, and 30 days. A simple experiment was also performed to test if loss of DMTS would be minimized by snap freezing of blood samples before storage. Triplicates of high QCs in blood were prepared and snap-frozen using a dry ice–acetone bath before storing them at -80 °C. The recovery of these samples was compared to non-snap frozen samples also stored at -80 °C. For bench-top, freeze-thaw, and long-term stability experiments, internal standard was spiked into the blood

samples after completion of the storage period and prior to SBSE extraction to correct for sample preparation and instrument variability. We also evaluated the long-term stability of DMTS in PDMS-coated stir bars at -80 °C. For this experiment, all stir bars were extracted at the same time from a single denatured solution (50 mL blood, 100 mL 90 mM HNO_3) of appropriate QC concentration (low and high). For each QC solution, fifteen PDMS stir bars (triplicates for 5 storage days) were anchored on a 3-inch cylindrical magnetic stir bar, which was used to stir the denatured blood solution for 1.5 h to perform SBSE. After extraction, the PDMS stir bars were transferred into 2 mL glass vials and capped. The stir bars were analyzed on the day they were prepared, and after 1, 5, 10, and 40 days. Since IS could not be used for this experiment, triplicate of a 5 μM aqueous DMTS solution was prepared, extracted using SBSE, and analyzed on each day the QCs were evaluated for stability in order to correct for instrument variability over different days. For all stability experiments, stability was calculated as a percentage of the initial "time-zero" signal. DMTS was considered stable if the stored sample percentage was within 10% of time zero.

Finally, to verify if the IS corrects for the loss of DMTS during storage and sample preparation, a 5-day stability test was performed. The QCs (low and high) were prepared by spiking the combined standard of DMTS and IS, and were stored at -80 °C for 1, 2, and 5 days. When ready to analyze, the QCs were thawed, denatured with acid, and extracted using SBSE. The DMTS/IS ratio for each day was calculated and compared to Day 0.

2.2.7 Recovery and matrix effects

Recovery of DMTS was evaluated by analyzing triplicates of low, medium, and high aqueous QCs, and comparing them with the equivalent QCs in blood. Recovery was calculated as a percentage by dividing the analyte signal in blood by the aqueous signal. Recovery calculated in this manner will be influenced by blood matrix effects, and therefore, may not reflect a true estimate of recovery. A true recovery from blood cannot be measured discretely, but may be estimated once matrix effects are assessed. Matrix effects were assessed by comparing the aqueous calibration curve with the calibration curve of DMTS in blood. The deviation of b in the power-fit equation ($y=ax^b$) gave a measure of the magnitude of the matrix effects.

2.3 Results and Discussion

2.3.1 GC-MS analysis of DMTS from rabbit blood

The method presented here includes an easy one-pot sample preparation scheme for extraction of DMTS from whole blood. The whole blood is simply treated with acid to lyse RBCs and denature proteins, and then a PDMS stir bar is directly added to the resulting solution. After an hour of SBSE, the stir bar is then analyzed via GC-MS by thermally desorbing the DMTS in the TDU.

SBSE was chosen for sample preparation of DMTS because it has a relatively high phase ratio, SBSE is a single-step solventless process, and it is typically highly reproducible [128]. Specifically, the analysis of DMTS using SBSE takes advantage of the relatively high octanol-water distribution co-efficient of DMTS (log K_{ow} = 1.87). Assuming equilibrium is reached and the K_{ow} of DMTS is a good estimate of the K_{PDMS},

approximately 54% of the DMTS should reside in the PDMS layer of the stir bar (film thickness 0.5 mm, length 10 mm), when the sample volume is 1.5 mL (i.e., the final sample volume used in the current method). The overall sample preparation time is 1 h 10 min, with thermal desorption and chromatographic analysis lasting approximately 15 min (including equilibration time for the following sample). Using this method, roughly 90 individual samples could be processed and analyzed in a 24 h time period.

The total ion chromatogram (TIC) of blank rabbit blood and selected ion chromatograms (m/z = 111, 114, 126 and 132) of spiked (1 μM DMTS and 1 μM IS) blood are plotted in Figure 2.2. The peaks for DMTS and IS eluted at approximately 2.9 min. The method showed excellent selectivity with no interfering or co-eluting peaks in the blank. Quantification ions of DMTS (m/z of 126) and IS (m/z of 132), and identification ions of DMTS (m/z of 111) and IS (m/z of 114) are plotted in Figure 2.2.

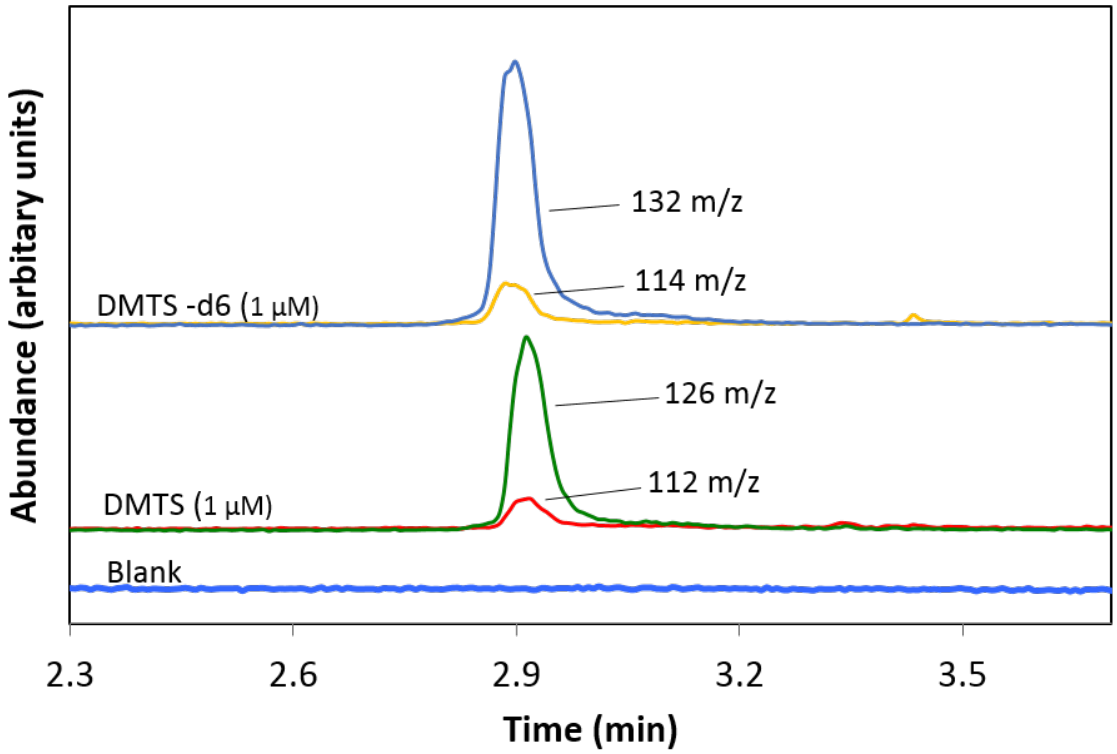

Figure 2.2. Total ion GC-MS chromatograms of non-spiked blood (lower trace, listed as "Blank") and selected ion chromatograms of 1 µM DMTS (middle traces) and 1 µM DMTS-d6 (upper traces). DMTS quantification and identification ions (m/z 126 and 111, respectively) and DMTS-d6 quantification and identification ions (m/z 132 and 114, respectively) are separately plotted.

2.3.2 Dynamic range, limit of detection, and sensitivity

Calibration curves for DMTS were constructed in the range of 0.2 – 200 µM in rabbit blood. Upon analysis of multiple calibration curves using linear (non-weighted and weighted), power, and quadratic fits, we determined that the calibration behavior of DMTS followed a power curve ($y=ax^b$). Using a power fit, 0.2 and 200 µM calibrators did not meet the accuracy and/or precision inclusion criteria, and were excluded. Therefore, the dynamic range for the method was from 0.5 µM (LLOQ) to 100 µM (ULOQ), with a correlation co-efficient (R^2) > 0.998. The b term of the calibration equation ($y=ax^b$) remained consistent over the three calibration curves, producing a

relative standard deviation of within ≤2%, and confirming the uniform calibration behavior of DMTS (Table 2.1).

The dynamic range of the method spanned over two orders of magnitude, which is typically good for analysis from biological samples [129, 130], and should be useful for therapeutic studies where a large range of concentrations is administered. The method achieved an excellent LOD, 60 nM in blood, as compared to other similar methods for therapeutics [70, 106, 130]. The low limit of detection is most likely attributed to the efficient pre-concentration of DMTS in the PDMS layer of the stir bar.

The non-linear behavior of DMTS was verified by over than 10 calibration curves produced with the method presented here from both blood and aqueous samples, and from direction injection of DMTS calibration standards. Non-linear calibration behavior when directly injecting DMTS calibration standards, suggests that the non-linearity did not stem from the extraction process or from the matrix components. This behavior is most likely caused by either higher concentrations of DMTS enhancing the MS ionization process (i.e., more DMTS molecular ions are produced as the concentration of DMTS in the ionization chamber increases) or adsorptive losses at low DMTS concentrations (i.e., a small amount of high affinity sites binding DMTS, with greater amounts of DMTS overwhelming these high affinity sites). Evaluation of the peak shape and calibration behavior of the low and high concentration calibrators indicated no evidence of adsorptive losses. Therefore, it is most likely that the ionization of the DMTS molecular ion, the ion used for quantification, is enhanced at higher concentrations. This may occur

if DMTS molecular ions assist in ionization of more DMTS molecules through energy transfer, similar to chemical ionization.

Table 2.1. Curve equations and R^2 values for separate calibration curves prepared over a three-day period.

Days	Equation	R^2
Day 1	$y = 0.1184x^{1.18}$	0.9984
Day 2	$y= 0.1321x^{1.21}$	0.9992
Day 3	$y= 0.1232x^{1.19}$	0.9984

2.3.3 Accuracy and precision

The accuracy and precision of the method, as determined by quintuplicate analysis of low (1.5 μM), medium (7.5 μM), and high (35 μM) QCs, on three different days (within a 6-day period), are reported in Table 2.2. Considering that DMTS is vulnerable to rapid enzymatic degradation and evaporative loss, the accuracy and precision of the method were remarkable. The intra-assay accuracy (±7-14%) and precision (<2-10% RSD), and inter-assay accuracy (±11%) and precision (<6% RSD) of this method were excellent and well within the FDA method validation guidelines [125-127, 129].

Table 2.2. The accuracy and precision for the analysis of DMTS in spiked rabbit blood by SBSE-GCMS.

Concentration (µM)	Intra-assay						Inter-assay	
	Accuracy (%)[a]			Precision (%RSD)[a]			Accuracy (%)[b]	Precision (%RSD)[b]
	Day 1	Day 2	Day 3	Day 1	Day 2	Day 3		
1.5	100±12.5	100±6.7	100±13.5	9.4	6.3	2.1	100±10.8	5.9
7.5	100±0.1	100±0.2	100±8.3	0.9	0.6	1.1	100±2.8	4.9
35	100±6.5	100±7.6	100±6.5	0.7	1.2	1.3	100±6.9	0.6

[a] QC method validation (N=5)

[b] Mean of three different days of QC method validation (N=15)

2.3.4 Matrix effects and recovery

The assessment of matrix effects provides a measure of ion suppression or enhancement leading to loss or gain of analyte signal. It is typically calculated by comparing the slope of the calibration curve in blood with that of the aqueous calibration curve. For a non-linear power trend, the power (b) in $y = ax^b$ translates to the slope in a linear fit. Hence, matrix effects were evaluated by calculating the ratio of power coefficient of the calibration curve in blood to that in aqueous. This ratio, determined as 0.96, indicated that matrix effects were essentially negligible for the analysis of DMTS in blood. The minimal matrix effect can be attributed to the fact that only hydrophobic analytes ($\log K_{ow} > 2$) are efficiently extracted into the PDMS-coated stir bar. This minimizes the interference from other blood components during DMTS analysis. Note that the power coefficients of IS-corrected aqueous and blood calibration curves, were even closer to each other ($Power_{blood}/Power_{aq} = 0.998$), which gives another indication of

effectiveness of the IS in correcting for any loss of DMTS signal during the analysis process.

Assay recovery of DMTS for low, medium, and high QCs was 66, 63, and 59% respectively. Incomplete recovery can be partly attributed to the rapid enzymatic degradation of DMTS in blood. Although the acid concentration and volume were optimized for the best recovery, the acid-denaturation process may not suffice in completely halting all enzymatic activity. Additionally, lower recovery can also be explained by the hydrophobic nature of DMTS. Since some components of blood provide a more hydrophobic environment than water, these components may interfere with effective partitioning of DMTS into the PDMS layer of the stir bar. Nevertheless, the recovery for all low, medium, and high QCs was very consistent, and sufficient to achieve detection at concentrations as low as 60 nM. It is unlikely that lower recovery is caused from evaporative loss, since both the aqueous and blood samples undergo same sample preparation steps. Therefore, loss of DMTS from evaporation should be comparable.

2.3.5 DMTS storage stability

The bench-top stability of DMTS was evaluated for low and high QCs in both non-denatured and denatured blood for 0, 1, 2, 4, 8, 12 and 24 h. At 1 h, DMTS was undetectable in the non-denatured blood, whereas 65% of the signal was recovered from the denatured blood. This observation confirms that enzyme metabolism and protein binding comprise a key loss mechanism for DMTS. Although DMTS was detectable in

the denatured blood, it is still considered unstable (<90% of the original signal was recovered) at 1h.

Auto-sampler stability, following stir bar extraction of DMTS, was tested for 0, 1, 5, 10, and 24 h, during which, DMTS was stable for the 24 h time period tested (i.e., the DMTS signals at different time periods randomly deviated above and below the time zero signal; the variability was likely caused by differences between stir bars and slight changes in instrument sensitivity over time).

Long-term stability was evaluated for low and high QCs by storing them at -80, -20, and 4°C over a 30-day period. DMTS was rapidly removed from blood when stored at -20 and 4 °C, with less than 10% signal recovered after one day relative to the initial time. However, at -80 °C, although some of the DMTS signal was lost (20-50%), the concentration stayed consistent over the 30 day period with no trend of further loss. The rapid loss at higher temperatures (-20 and 4 °C) likely results from the enzymatic activity of blood proteins. At -80 °C, the rapid initial loss may have resulted from DMTS degradation during the delay times between spiking DMTS and complete freezing, and/or during thawing prior to acid addition. In order to reduce the initial delay time of complete freezing, blood samples were snap frozen using dry ice and acetone bath before transferring to a -80 °C freezer. Results from this experiment showed similar recovery for the snap frozen (79 ± 9.6%) and non-snap frozen (72 ± 12.8%) samples. This suggested that the significant loss mainly takes place during the thawing process, and that snap freezing prior to storage does not provide a definite advantage.

Long-term stability of DMTS in the stir bar was evaluated at -80 °C for 0, 1, 5, 10, and 40 days to determine if the samples could be prepared and the stir bars analyzed at a later date. The signal ratio of DMTS to positive control was determined to compare the stability of DMTS over different days. The high QCs were stable in the stir bar for 5 days (i.e. signal within ±10%), whereas, the low QCs were considered unstable on Day 5. On Day 40, both QCs (high and low) were considered unstable with signal loss of 30-40%.

The freeze-thaw stability test showed that DMTS is lost with each freeze-thaw cycle, which was in agreement with our findings from long-term stability of DMTS in blood at -80 °C. During the freeze-thaw cycle, DMTS is rapidly lost from the blood likely due to the enzymatic activity. Hence, freezing and thawing should be avoided, but if freezing the blood is necessary, then acid should be added immediately after thawing in order to help preserve DMTS.

The 5-day stability study using QCs (low and high) showed that when IS was spiked before the storage, the DMTS to IS ratio remained consistent throughout the storage time, verifying that the IS effectively corrected for any loss of DMTS during storage. Figure 2.3 shows the ability of the IS to correct for signal loss during storage. Figure 2.3A illustrates DMTS stability without IS correction, where DMTS signal is seen to significantly deviate compared to the Day 0 signal. Figure 2.3B shows the DMTS to IS signal ratio for all days. When comparing these two graphs, it is obvious that the IS corrects for the large signal loss due to instability of the DMTS.

Overall, our results from the stability studies suggest that blood samples should be denatured with acid, spiked with IS, extracted and analyzed immediately whenever possible. In any circumstance where immediate analysis is not possible, the blood samples should be spiked with IS, frozen as soon as possible, and stored at -80 °C for future analysis. Once the frozen samples are thawed, they should be prepared and extracted immediately. Once extracted into the PDMS layer, DMTS is stable for at least 24 h on the auto-sampler at ambient temperature. While the DMTS is stable in the stir bar at -80 °C for 24h, it is not recommended to store the stir bar under these conditions unless it is absolutely necessary.

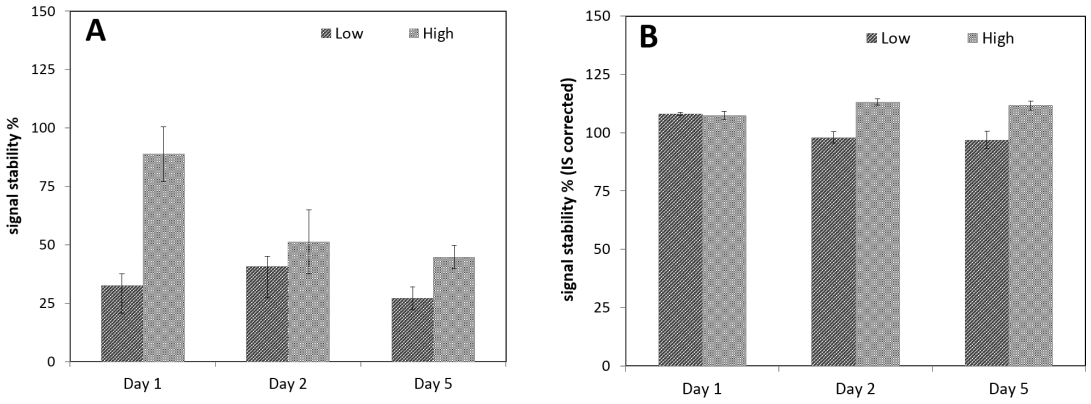

Figure 2.3. Evaluation of the ability of the IS to correct for signal loss during storage at -80 °C. (A) DMTS signal stability plotted without IS correction. (B) IS corrected DMTS signal stability. The uncorrected DMTS signal clearly decreases from Day 0 (due to l loss during storage and freeze-thaw process) and has high variability (due to variation in instrument sensitivity and stir bars). The IS corrected stability remains consistent throughout the time tested, with the IS correcting the DMTS signal for significant loss mechanisms.

2.3.6 Analysis of DMTS exposed animals

The validated SBSE GC-MS method was applied to the analysis of DMTS from blood samples of treated mice. The GC-MS chromatograms of treated and untreated mouse

blood are shown in Figure 2.4. DMTS was detected as a prominent peak at 2.9 min from DMTS- treated mouse blood, whereas no peak was present in the untreated blood. This further verified the selectivity of the method and confirmed its applicability to real-world samples.

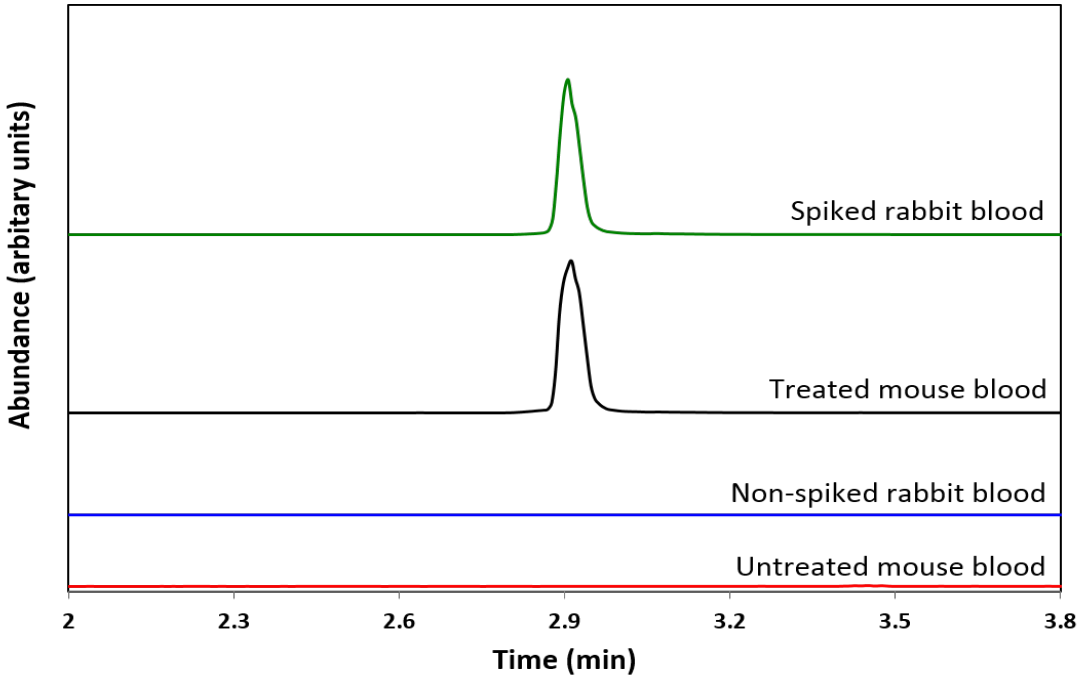

Figure 2.4. GC-MS chromatograms (SIM, m/z 126) for DMTS treated (200 mg/kg) and untreated mice blood, and DMTS spiked and non-spiked rabbit blood.

2.4 Conclusion

A simple and sensitive analytical method for the determination of the DMTS in blood was developed using SBSE-GCMS. The method presented is the first validated method for DMTS analysis from any matrix. The described method is simple, with easy one-pot sample preparation and extraction. The method yielded excellent accuracy and precision, consistent recovery, minimal matrix effects, an excellent detection limit, and a large dynamic range that spanned over 2 orders of magnitude. The ability to store internal

standard spiked samples was also demonstrated. The creation of this method is significant, since there are no analytical methods currently available for analysis of DMTS from blood. The availability of this method will allow further drug development investigations of DMTS as a promising cyanide antidote.

2.5 Acknowledgements

We gratefully acknowledge the support from the CounterACT Program, National Institutes Of Health Office of the Director, and the National Institute of Allergy and Infectious Diseases, Interagency Agreement Numbers Y1-OD-0690-01/AOD14020-001-00000/A120- B.P2014-01. We would also like to acknowledge U.S. Joint Executive Office for Chem Bio Defense, Joint Program Management Protection Contract W911SR-09-0059 for funding the GC-MS instrument. Furthermore, the authors are thankful to Wenhui Zhou, a former graduate student at South Dakota State University for her assistance in preliminary phases of GC-MS method development. The opinions or assertions contained herein are the private views of the authors and are not to be construed as official or as reflecting the views of the National Institutes of Health or the CounterACT Program.

Chapter 3. Identification of sulfur mustard biomarkers for correlation to inhalation studies

3.1 Introduction

Sulfur mustard, bis (2-chloroethyl) sulfide, is a potent vesicant that has been a continued threat as a warfare agent since its first use in World War I [131, 132]. SM has caused more casualties than all other chemical weapons combined [3] and remains the most utilized chemical weapon [131, 133, 134]. For example, during the Iraq-Iran war (1980-1988), over 1,000 tons of SM was used in the battlefields by Iraq resulting in over 100,000 injuries [135, 136]. To this date, more than two decades later, there are still 30,000 of these war victims needing treatment for SM poisoning [137, 138].

SM can enter the body via inhalation, ingestion (of contaminated food), cutaneous, and ocular routes [132]. Exposure can result in short- and long-term health effects, which can include ocular and dermal injury, respiratory tract damage, neurotoxicity, reproductive and developmental toxicity, gastrointestinal effects, hematological effects, cancer, and death [3]. Although SM has a wide range of toxic effects, airway injury is the principal cause of mortality in victims [11].

Injuries from SM inhalation are concentration-dependent. In humans, exposure to low or moderate inhalation dose of SM affects mainly the upper respiratory tract, and can cause nasal mucosal injury, lacrimation, rhinorrhea, loss of smell and taste, and acute edema formation [3, 6, 139]. At high concentrations, injury of greater severity can extend to larynx, sinuses, trachea, bronchi, and other distal regions [3, 6]. Tracheobronchial mucosal sloughing, severe airway edema, ulceration, and formation of fibrin-rich obstructive bronchial casts is seen to occur, which can ultimately lead to fatal outcomes,

including sudden death [3, 6]. Despite its severity, the pathology of airway obstruction is not well understood, and unfortunately, no therapies exist to prevent or alleviate the fatal effects of inhalation exposure. In order to improve the understanding of inhalation toxicity and to properly evaluate and develop effective clinical interventions, animal model studies that accurately replicate the physiological injuries induced by inhalation of SM is desired. Currently, there are only limited number of SM inhalation studies, and a few therapeutic approaches that are under investigation [12].

One of the major challenges of inhalation studies is to accurately deliver a targeted dose [140]. Unlike oral or parenteral routes (i.e. intravenous, cutaneous, sub-cutaneous), the delivered dose in inhalation studies depends on several parameters, such as exposure concentration, breathing frequencies, tidal volume, minute volume, deposition pattern within various regions of respiratory tract [140]. Therefore, in order to confirm/accurately monitor the inhalation dose, a biomarker of exposure (toxin or its byproduct) can be analyzed from a biological specimen of an individual and related to the inhaled dose [141, 142]. The advantage of using a biomarker of exposure to calculate dose is that it estimates the actual "internal" dose of exposure, and also improves reliability of the study by adding internal validity when examining outcome of the exposure [141].

The reaction pathways and breakdown products for SM are presented in Figure 3.1. SM initially undergoes intramolecular cyclization to form a positively charged ethylene episulphonium ion intermediate [3, 132]. This cyclic intermediate can then undergo oxidation or hydrolysis or can react with nucleophiles in the body (e.g.

glutathione, proteins, and DNA). A direct oxidation results in β-chloroethyl sulfoxide (SMO), direct hydrolysis results in thiodigycol (TDG), and oxidation of TDG results in thiodigycol oxide (TDGO). SM can also be detoxified via glutathione pathway, where a molecule of SM reacts with two molecules of glutathione. The bis-glutathione is then metabolized into a bis-cysteinyl conjugate followed by β-lyase cleavage of cysteinyl C-S bond and a subsequent methylation and oxidation of the thiol, resulting in 1,1'-sulfonylbis[2-S-(N-acetylcysteinyl) ethane] (SBSNAE), 1,1'-sulfonylbis[2-(methylthio) ethane] (SBMTE), 1-methylsulfinyl-2-[2-(methylthio)ethylsulfonyl]ethane (MSMTESE) and 1,1' - sulfonylbis [2-(methylsulfinyl) ethane] (SBMSE). Finally, the reactive SM intermediate can also react with nucleophilic sites of DNA and amino acid residues in proteins to form hydroxyethylthioethyl (HETE) adducts.

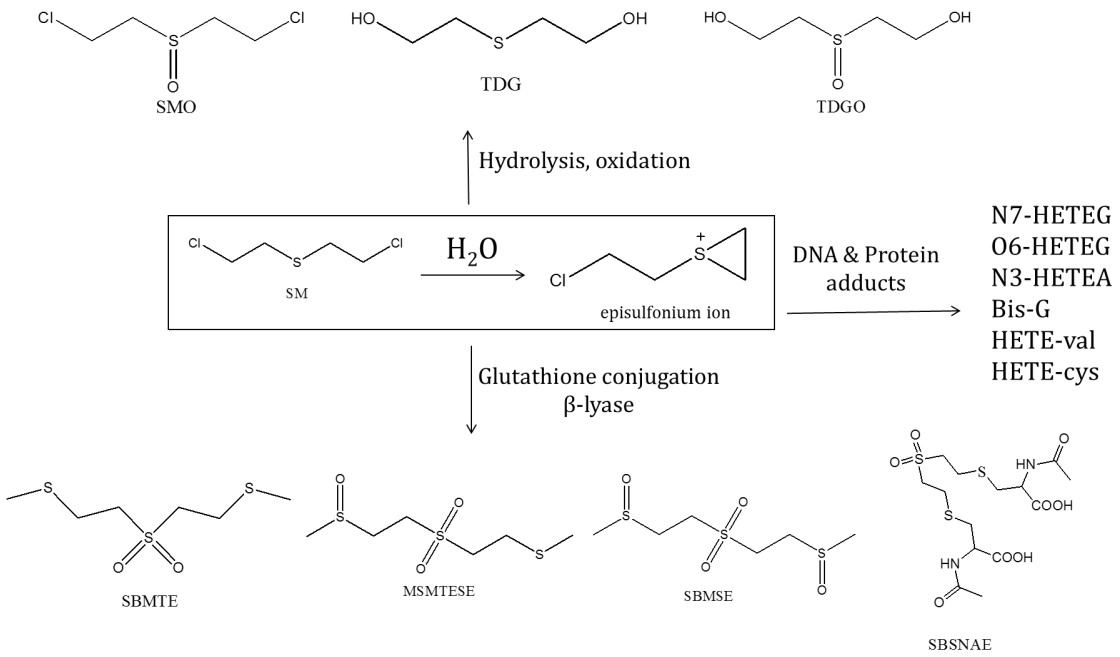

Figure 3.1. Metabolic products of sulfur mustard: hydrolysis, oxidation, β –lyase products, DNA (N7-HETEG, O6-HETEG, N3-HETEA, Bis-G) and protein adducts (HETE-Val and HETE-Cys).

Given the highly reactive nature of SM, its detection as an intact agent is not very likely. Therefore, exposure can be monitored by analyzing its metabolites and/or adducts. The metabolism of SM has been widely studied in animal models, and a number of free metabolites and covalent adducts with macromolecules have been identified. However, all studies on the metabolites and their profiles have only been performed for intravenous, cutaneous, and sub-cutaneous routes [79, 84, 89]. Although the byproducts of SM can be expected to be the same in parenteral and inhalation routes, the relative abundance and toxicokinetic behavior of metabolites will be dependent on factors such as penetration, absorption, and diffusion of SM and metabolites through the different biological barriers. Therefore, it is important that the behavior of biomarkers is known for inhalation exposure.

In this research, we evaluated the potential plasma metabolites of SM, and screened them in the plasma of SM exposed (via inhalation) animals. Biomarkers that were definitive (i.e., not present in plasma of unexposed animals) and had significant concentrations in plasma of exposed specimen were correlated with dose.

3.2 Materials and Methods

3.2.1 Chemicals and reagents

TDG, TDGO, N-acetyl cysteine, ammonium formate, sodium thiomethoxide, sodium thioethoxide, and 18-crown-6 were purchased from Sigma Aldrich (St. Louis, MO, USA). Methanol, methylene chloride, ethanol, chloroform, acetonitrile, potassium permanganate, sodium periodate, hydrogen peroxide, sulfuric acid, nitric acid, sodium bicarbonate, ethanol, hydrochloric acid, and sodium chloride were purchased from Fisher Scientific (Hampton, NH, USA).

For method validation, swine plasma (with EDTA) was purchased from Pelfreeze Biologicals (Rogers, AZ) and rat plasma (Sprague Dawley with sodium citrate was purchased from BioreclamantionIVT (New York, NY, USA)

3.2.2 Synthesis of metabolites

Apart from TDG and TDGO (purchased from Sigma Aldrich), all of the other SM metabolites, and the internal standard (SBESE) were synthesized in house according to previously published methods [143, 144]. The synthesis procedures for all metabolites are briefly explained in the following sections. An overall reaction scheme is presented in Figure 3.2. Note that SM, needed for the synthesis of SMO was only produced *in situ* and immediately oxidized.

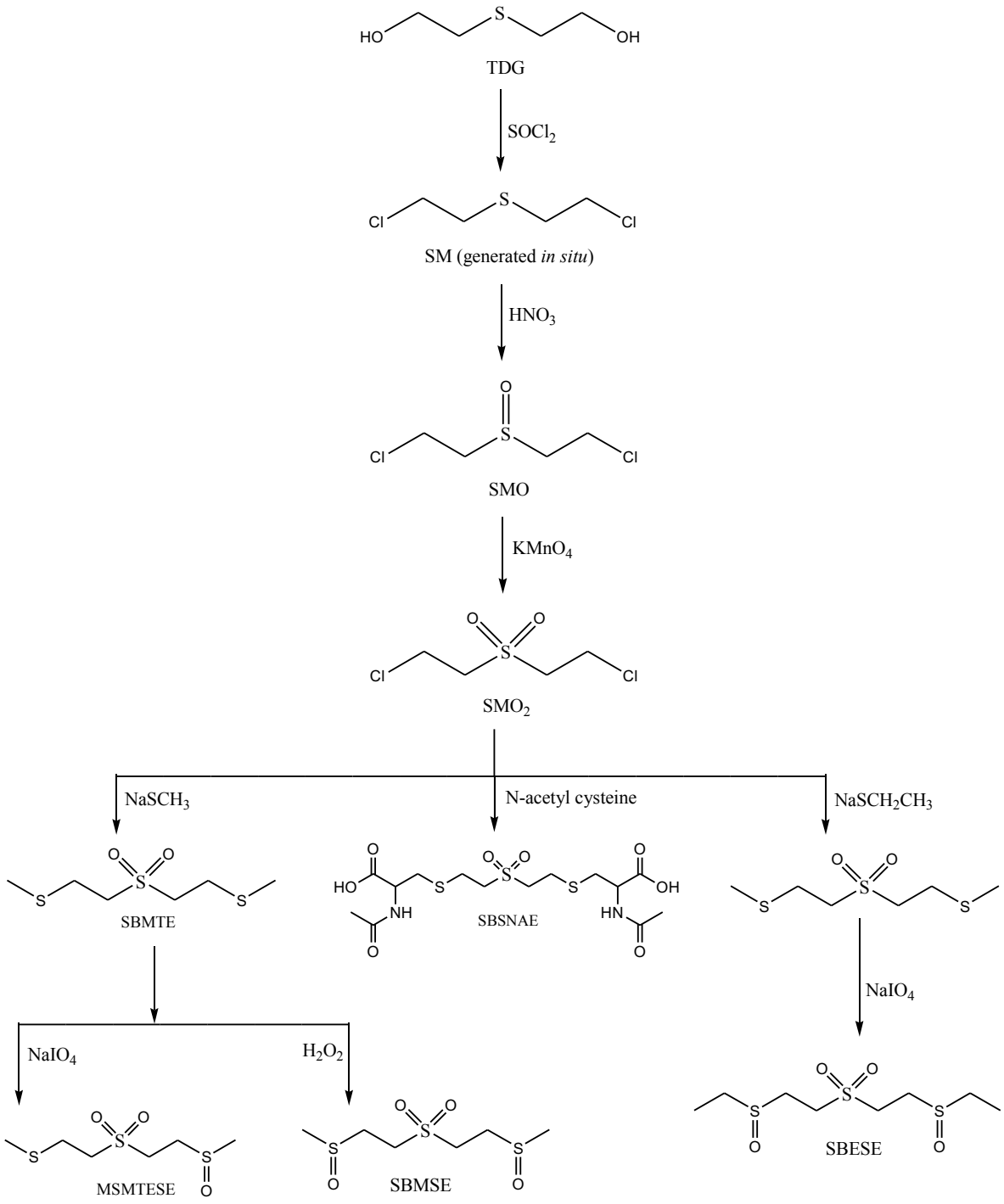

Figure 3.2. Reaction schemes for synthesis of SM metabolites and internal standard (SBESE).

3.2.2.1 Synthesis of 1,1'-sulphinylbis(2-chloroethane) (SMO)

Thiodiglycol (1 g) was dissolved in 15 mL of methylene chloride, to which 2 g (2.1 eq.) of thionyl chloride in 15 mL of methylene chloride was added drop-wise. The reaction was stirred for 30 min at room temperature (rt) to generate sulfur mustard *in situ*. Concentrated nitric acid (0.52 g, 1 eq.) was added drop-wise and the reaction was stirred for 30 min at rt. The final reaction mixture was transferred to a separatory funnel and washed with water. The organic layer was dried under vacuum using a rotary evaporator, which yielded a white solid of SMO (1.3 g, 92%). NMR ^{1}H 400MHz, $CDCl_3$ δ 2.1 (s, 6H) 3.0 (t, 4h) 3.3 (t, 4H).

3.2.2.2 Synthesis of 1,1'-sulfonylbis [2-(methylthio) ethane] (SBMTE)

SMO (1.3 g) was dissolved in 20 mL of water. Concentrated sulfuric acid (1.7 mL, 1.3 eq.) and 1.3 g of potassium permanganate was added to the SMO solution. The reaction mixture was refluxed for 3 h and cooled to rt. The mixture was then diluted with 20 mL of water and extracted with methylene chloride (3x20 mL). The organic layer was washed with aqueous sodium bicarbonate and aqueous sodium chloride. The final organic layer was dried under vacuum using a rotary evaporator. A white solid of sulfur mustard sulfone (SMO_2, 0.94 g, 66%) was obtained as the residue.

Sulfur mustard sulfone (1.1 g) was dissolved in 30 mL of ethanol. Sodium thiomethoxide (1.32 g, 3.3 eq.) and 9 mg (5 mol%) of 18-crown-6 was added to the mixture. The reaction was stirred at rt overnight. Once the starting material disappeared (TLC 1:9 MeOH:$CHCl_3$), 10 mL of 1 M hydrochloric acid was added to quench the base,

and 10 mL of water was added to dilute the mixture. The reaction mixture was allowed to stand for 30 min to allow methanethiol to evaporate. The product was extracted with methylene chloride (4x50 mL). The organic layer was washed with aqueous sodium bicarbonate and aqueous sodium chloride, and was dried under vacuum. SBMTE yielded as a yellow solid (1g, 81%). NMR ^{1}H 400MHz, $CDCl_3$ δ 2.1 (s, 6H) 2.9 (t, 4h) 3.2 (t, 4H).

3.2.2.3 Synthesis of 1-methylsulfinyl-2-[2-(methylthio) ethylsulphonyl] ethane (MSMTESE)

In a 25 mL round bottom flask, 150 mg (1 eq.) of SBMTE was dissolved in 1:1 H_2O: MeOH. Sodium periodate (160 mg, 1.1 eq.) was added and the reaction was stirred at rt for 4 h. The reaction mixture was filtered and the filtrate was evaporated under vacuum, which yielded a white solid of MSMTESE (137 mg, 85%). NMR ^{1}H 400MHz, $CDCl_3$ δ 2.2 (s, 3H) 2.7 (t, 3H), 3.0 (t, 2H), 3.1 (t, 2H), 3.4 (t, 2H), 3.6 (t, 2H).

3.2.2.4 Synthesis of 1,1'-sulfonylbis [2-(methylsulfinyl) ethane] (SBMSE)

In a 100 mL round bottom flask, 200 mg (1 eq.) of SBMTE was suspended in water, and 0.6 mL of 30% peroxide (6 eq.) was added. The reaction was allowed to proceed at room temperature until little starting material remained (TLC chloroform-methanol 9:1). Sodium sulfite (1 g) was dissolved in the mixture to quench the remaining peroxide. The reaction product was extracted in methylene chloride (3x30 mL), and was dried over sodium sulfate and evaporated under vacuum. The product collected, (SBMSE, 162 mg) was a white solid (71%). NMR ^{1}H 400MHz, $CDCl_3$ δ 2.7 (s, 6H), 3.2 (t, 4H), 3.6 (t, 4H).

3.2.2.5 Synthesis of 1,1'-sulfonylbis [2-S-(N-acetylcysteinyl) ethane] (SBSNAE)

In a 100 mL round bottom flask, 400 mg of SMO_2 (1 eq.) and 720 mg of N-acetylcysteine (2.1 eq.) were suspended in 8 mL of water. To the mixture, 0.8 mL of triethylamine (TEA) was added and the reaction was stirred at rt for 2h. The reaction mixture was acidified to pH of 3 using 1 M HCl and placed in the refrigerator overnight. A white colored precipitate formed was vacuum filtered; reaction yield was 70%. NMR ^1H 400MHz, D_2O δ 1.1 (t, 4H). 1.2 (t, 4H), 2 (s, 6H), 3.1 (d, 4H), 3.5 (t, 2H).

3.2.2.6 Synthesis of 1,1'-sulfonylbis [2-(ethylsulfinyl) ethane] (SBESE)

In a 100 mL round bottom flask, 200 mg (1 eq.) of SMO_2 was dissolved in 10 mL of ethanol, and sodium thioethoxide (1.85 g, 2.1 eq.) and 10 mg (5 mol%) of 18-crown-6 was added to the mixture. The reaction was stirred at rt overnight. Water (10 mL) and 470 mg of sodium periodate (2.1 eq.) were added to the mixture. The organic layer was evaporated, leaving a white solid of SBESE. NMR ^1H 400MHz, $CDCl_3$ δ 1.4 (t, 6H) 2.9 (q, 4H), 3.2 (t, 4H), 3.6 (t, 4H).

3.2.3 Characterization of prepared standards

A Bruker Avance 400 MHz NMR was used to characterize the compounds and confirm their purity. The NMR data are presented in the synthesis section for each metabolite. The standards were also analyzed via direct infusion in the mass spectrometer. Based on the information provided by Li et al. [89], the precursor and product ions were identified and verified for each analyte to further confirm the identity of the synthesized standards.

3.2.4 Sample preparation

Sample preparation for the analysis of metabolites was based on Li et al. [89], with a few modifications. Plasma (100 μL, spiked or non-spiked) was added to a 2 mL centrifuge tube. To the plasma, internal standard (400 μL, 0.25 μM) in a mixed solution of acetonitrile-methanol (4:1) was added. The mixture was vortexed and then cold-centrifuged at 8 °C for 15 min at 14,000 rpm. The supernatant was then transferred into a vial and evaporated to dryness under N_2. The residue was reconstituted with 50 μL of water, filtered using 0.22 μm tetrafluoropolyethylene membrane syringe filter into autosampler vials with 200 μL glass inserts for HPLC-MS-MS analysis.

3.2.5 UHPLC-MSMS analysis

Prepared samples were analyzed using a Shimadzu UHPLC (LC-20 AD, Shimadzu Corp., Kyoto, Japan) coupled to a 5500 Qtrap Mass Spectrometer (AB Sciex, Farmingham, MA, USA) with electrospray ion source. The LC parameters were based on Li et al. paper with few modifications in gradient and total chromatographic runtime [89]. Separation of 10 μL of prepared sample was performed using Agilent Zorbax Eclipse C18 column (100 mm x 3 mm x 1.8 μm) protected by a Agilent Zorbax Eclipse Plus C18 guard column (2 mm x 5 mm x 1.8 μm) (both Agilent, Santa Clara, CA, USA). Mobile phase solutions consisted of an aqueous 5 mM ammonium formate with 1% methanol (Mobile Phase A) and 5 mM ammonium formate in 95% methanol (Mobile Phase B). The flow rate was maintained at 0.3 mL/min. The percentage of B was 0, 5, 17, 50, 80, and 0 at 0, 1.5, 2.5, 5, 8, and 10 min, respectively. The total chromatographic run-time was 10 min, with a 3 min equilibration time between runs.

The mass spectrometric detection was performed in positive polarity in multiple reaction monitoring (MRM) mode. The MRM transitions for each analyte was selected based on their scan spectra obtained from infusion analysis of each standard. Collision energy (CE), declustering potential (DP), and collision cell exit potential (CXP) were optimized for each MRM transition. The dwell time for all MRM transitions were 100 ms. Nitrogen gas (30 psi) was used as the curtain and nebulization gas. The ion source was operated at 5000 V and 500 °C. The collision cell was operated at entrance potential of 10 V, with a high collision gas pressure.

3.2.6 Detection of biologically relevant levels from spiked plasma

Prior to analysis of animal samples from an inhalation exposure study, the lowest biologically relevant levels for all plasma metabolites were estimated based on toxicokinetic data from SM sub-cutaneous exposure of rats by Li et al. [89]. Once estimates of the relevant levels were established, plasma samples were spiked with the relevant concentrations of all metabolites and analyzed. During this process, analysis of SBMTE was eliminated because of literature evidence of its low significance in previous studies, and difficulty in analysis.

3.2.7 Screening of metabolites from exposed swine plasma

Inhalation exposure studies were conducted on four (1 control, 3 SM exposed; weights between 46-50 kg) Yorkshire SPF Oak Hill female swine at MRIGlobal, Kansas City, MO. The experiments were conducted in accordance with the Guide for the Care and Use of Laboratory Animals [124] by an Association for the Assessment and

Accreditation of Laboratory Animal Care (AAALAC) International accredited institution. The Institutional Animal Care and Use Committee (IACUC) approved the experiment.

Swine were intubated with an endotracheal tube attached at 90° to a plenum where mustard gas was passed through at positive pressure. Animals were sedated and allowed to breathe spontaneously on the system. The targeted exposure dose was 200 mcg/kg, exposure time was variable depending on respiratory rate and tidal volume. Blood draws were taken through an arterial line placed on femoral artery. Plasma samples were prepared via standard procedures and shipped in dry ice. Upon receipt, samples were stored at -80 °C until analyzed.

After analysis, the concentrations of most promising biomarkers were calculated using external standardization (Note: Internal standard was not available when this study was performed). Toxicokinetic profile was studied by plotting time versus ln (concentration). The kinetic model of the marker was identified and rate constant of elimination (k_{el}) and half-life ($t_{1/2}$) were calculated.

3.2.8 Validation of the method for SMO and SBSNAE in swine plasma

After screening plasma samples from the exposed swine, only those metabolites that showed potential to be used as definitive markers were selected for further analysis. Therefore, validation parameters were only evaluated for SMO and SBSNAE.

Stock solutions (10 mM) of SMO, SBSNAE, and SBESE (IS) were prepared separately in acetonitrile and stored at -30 °C. During the time of analysis, fresh working solutions were prepared from the stock.

The limit-of-detection (LOD) was determined by evaluating triplicates of multiple

low concentrations (0.1 nM – 50 nM) for SMO and SBSNAE in plasma. The lowest concentration that reproducibly produced a signal-to-noise ratio (with noise estimated as peak-to-peak noise) of at least 3 compared to blank plasma samples was confirmed as the LOD.

Matrix-matched calibration curves were produced in swine and rat plasma. The lower and upper limits of quantification were defined with the inclusion criteria of <20% for relative standard deviation (RSD) and accuracy of 100±20% of the nominal calibrator concentration back calculated from the calibration curve. Calibration standards were prepared by serial dilution of a composite stock solution (100 μM; SMO and SBSNAE) in plasma. Calibration standards were prepared from 0.02-10 μM (0.02, 0.05, 0.1, 0.2, 0.5, 1, 2, 5, 10 μM). Refer to Section 2.4 for detailed sample preparation. Calibration curves were generated by plotting concentration versus peak area ratio of analyte (SMO or SBSNAE) to internal standard (SBESE). To determine accuracy and precision of the calibration curve, quintuplicates of low (0.15 μM), medium (0.75 μM), and high (3 μM) QCs were analyzed. Calibration standards and QCs were prepared fresh each day during intra-assay (daily) and inter-assay (over three separate days, within seven calendar days) analyses to calculate intra-assay and inter-assay accuracy and precision.

LODs, linear range, and intra-assay accuracy and precision were also evaluated for rat plasma. Because no differences were observed between the rat and swine plasma, determination of inter-assay accuracy and precision was not pursued for rat plasma. Other validation parameters such as recovery, stability, and matrix effect were already evaluated by Li et al. and hence were not repeated here [89].

3.2.9 Analysis of rat plasma samples for biomarker correlation to inhalation dose

The animal exposure studies were conducted on Sprague Dawley rats at University of Colorado, Denver. Experiments were conducted in accordance with the Guide for the Care and Use of Laboratory Animals [124] by an Association for the Assessment and Accreditation of Laboratory Animal Care (AAALAC) International accredited institution. The Institutional Animal Care and Use Committee (IACUC) approved the experiment.

Rats were anesthetized with a combination of ketamine (100 mg/kg) and xylazine (10 mg/kg), i.m. After induction of anesthesia, a laryngoscope was used to visualize the larynx to facilitate tracheal intubation. A piece of PE 90 tubing was used as a guide for the endotracheal tube. Rats were intubated with a modified glass Pasteur pipette (ca. 5 cm long) to a point in the trachea between the larynx and the bifurcation of the trachea. A glass endotracheal tube was necessary to minimize absorption of SM. The tube was then secured in place by gently wrapping a piece of porous tape around the tube and rostrum of the rat. Sulfur mustard in absolute ethanol (100 µl) or ethanol alone (control) was placed in a water-jacketed (37 °C) glass vapor generator (custom fabricated by Atmar Glass, Kennett Square, PA, USA) and the rats were connected to this device and exposed for 50 min. By the end of the exposure period, the SM in ethanol was completely vaporized and inhaled. This passive exposure system included an inlet one-way respiratory check valve (Hans Rudolph, Inc., Kansas City, MO, USA) to ensure that the only source of air for the animal during the exposure was through the vapor generator. Exhaled air passed out of a 2200 series two-way non-rebreathing Rudolph valve and

through a charcoal-filtered bleach trap to decontaminate any exhaled SM. At the conclusion of the 50-min exposure, the rats were disconnected from the vapor generator, the endotracheal tube was removed and the rats were returned to their cages. The mustard concentration in ethanol was calculated based on average weights of animals in the study and exposure dose groups (1.2, 2.5, and 4.0 mg/kg). Rats were euthanized via anesthesia and blood was drawn from the descending aorta upon death. Plasma was separated from blood and shipped on dry ice. Upon arrival samples were stored at -80 °C until analyzed.

3.3 Results and Discussion

3.3.1 LCMSMS analysis of plasma metabolites

The MRM transitions along with optimized CE, DP, and CXP values for all metabolites of interest and internal standard are listed in Table 3.1. The total chromatographic time for the LCMSMS method was 10 minutes. A representative chromatogram with all metabolites of interest is shown in Figure 3.3. The quantitation ion XICs of the blank and spiked plasma for each analyte are plotted for the duration of their elution time.

Table 3.1. Optimized parameters for MRM transitions for SM metabolites of interest.

Analyte	MRM Transitions	CE (V)	DP (V)	CXP (V)
TDGO	139 → 77[a]	22	50	8
	139 → 63	18	50	10
SBMSE	247 → 183[a]	15	50	16
	247 → 119	29	50	16
SBSNAE	445 → 130	35	55	21
	445 → 357[a]	30	50	29
TDG	123 → 105[a]	9	50	10
	105 → 87	9	50	10
MSMTESE	231 → 75	20	50	10
	231 → 167[a]	15	50	16
SMO	175 → 63	29	103	11
	175 → 59[a]	38	118	11
SBESE (IS)	297 → 141[a]	25	13	9
	297 → 297	10	4	6

[a:] Transition for quantitative ion.

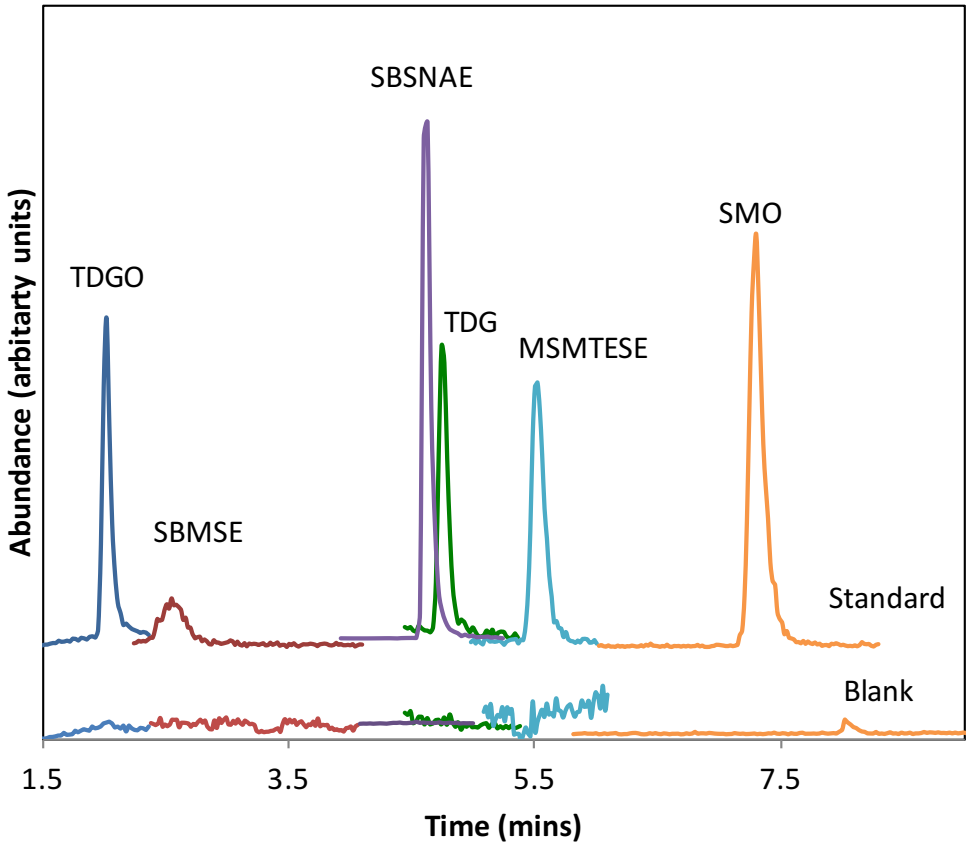

Figure 3.3. Extracted ion chromatograms (XICs) of six plasma metabolites of SM plotted over the time of their elution. Non-spiked swine plasma is shown in the lower trace, whereas the upper trace shows plasma spiked with metabolites.

3.3.2 Detection of metabolites at biologically relevant levels

Metabolites spiked at biologically relevant levels were analyzed to ensure capability of the method for their detection. According to the toxicokinetic plasma profiles from a sub-cutaenous study in rats, the lowest relevant levels for direct metabolites, SMO, TDG, and TDGO were 0.3 µM, 0.4 µM, and 40 nM respectively, and for β-lyase metabolites, SBMTE, SBMSE, MSMTESE, and SBSNAE were 0.09 nM, 0.4 nM, 0.4 nM, and 0.2 nM respectively. TDG, TDGO, SMO, SBMSE, and MSMTESE were detected at the lowest relevant levels from spiked plasma. However, SBMTE and SBSNAE could not be

detected at the lowest biological levels. According to Li et al. SBMTE was a very minor biomarker (lowest c_{max}), with concentrations at or below LLOQ for the most time-points tested. Because of its low importance, SBMTE was eliminated for further analysis. The lowest concentration of SBSNAE was calculated at the time-points before 1h, where the marker has a very low presence in plasma. The profile for SBSNAE increases significantly after 2 h, and has the highest concentration between 2-6 h post-exposure. Therefore, even though SBSNAE couldn't be detected at lowest levels at early time-points, it should be detected quantitatively at greater time-points (2-6 h). Therefore, because SBSNAE is an important β-lyase metabolite and it produces concentrations above the method LOD for most time-points, it was not eliminated.

3.3.3 Identification of metabolites from exposed swine plasma

Plasma samples of swine exposed to SM via inhalation were analyzed for TDGO, SBMSE, SBSNAE, MSMTESE, TDG, and SMO. Among the metabolites of interest, only three (TDGO, SBSNAE, and SMO) were consistently detected from the exposed animals, whereas other metabolites such as TDG, SBMSE, and MSMTESE were not detected.

TDG, which is a direct metabolite, was not detected in any of the samples, even though TDGO was. This is partially attributed to the low sensitivity of TDG in the LCMSMS. Yet, TDG was detected at large concentrations in rat plasma after sub-cutaneous exposure by Li et al. [89] Therefore, the more likely explanation is that the inhalation route provides a different oxidation environment than cutaneous/sub-cutaneous routes. A greater oxidizing environment likely results in facile conversion of TDG into

TDGO, and SM to SMO, lowering the concentration of TDG in plasma to undetectable levels.

SBMSE and MSMTESE may not have been detected because the blood draws for the animal samples spanned only up to 3 hours post-exposure. Unlike, TDGO and SMO, which are direct products of oxidation and hydrolysis of SM, β-lyase metabolites are formed by several steps of biological mechanisms, and hence take longer time to appear in the plasma. Additionally, results from published toxicokinetic studies suggest that β-lyase metabolites like SBMSE and MSMTESE also have very low plasma concentrations (low c_{max}). Therefore, the low concentrations and longer onset of these markers could attribute to the inability in their detection.

SBSNAE, which is also a β-lyase marker, was detected in all swine plasma samples from the inhalation study. This is in agreement with the previously published toxicokinetic studies, because among all the β-lyase metabolites, SBSNAE has the highest c_{max} and faster onset. Unlike SBMSE and MSMTESE that require further cleavage of the cysteinyl residues and subsequent oxidation of terminal sulfides to sulfoxides, SBSNAE is formed in fewer metabolic steps after the glutathione conjugation, and hence, can be detected at earlier time-points than SBMSE and MSMTESE.

Among the three detected metabolites (SMO, TDGO, and SBSNAE), only SMO and SBSNAE can be used as definitive marker. Previous studies have suggested the presence of TDGO at low levels (2-8 ng/mL) in biological specimen of unexposed animals and humans [87, 145]. Because of the endogenous levels that can be dependent

on diet, environment, and other variables, the use of TDGO as a marker for correlation to dose would not be ideal.

The toxicokinetic profiles for SMO and SBSNAE are presented in Figures 3.4 and 3.6 respectively. SMO appeared in the plasma samples immediately and reached the highest level (c_{max}) before 1 h post-exposure. This behavior observed from inhalation exposure in swine mimics the behavior from sub-cutaneous exposure in rats. The plot of time vs. ln (concentration) for SMO for individual swine is shown in Figure 3.5. The slopes for the three animals were similar to each other. SMO followed a one-compartment distribution model which indicates its rapid equilibration throughout the body. The rate constant for the elimination (k_{el}) of SMO was calculated as $0.97 \pm 0.15\ h^{-1}$, and the $t_{1/2}$ was 0.73 ± 0.12 h. The SBSNAE was observed only after 30 min time-point, and its level gradually and continually increased to 4 h, at the final draw. According to toxicokinetics in sub-cutaneous study, SBSNAE should have a c_{max} at 4 h. Unfortunately, the animal samples from inhalation study did not extend over 4 h, and hence the complete profile could not be studied for SBSNAE. However, the results observed for both SMO and SBSNAE are in good agreement with the findings of Li et al. [89].

SMO and SBSNAE can be used as ideal markers for determination of SM exposure. Both metabolites are absent in unexposed samples and can be used as unequivocal confirmation for SM. Moreover, both metabolites have dominant presence in exposed samples, especially during the first 6 h (latency period of SM poisoning). SMO also has a potential to be used as a diagnostic marker immediately (within 15 min) after exposure. Both of these markers should be further evaluated to determine if they can be

used to correlate to inhalation dose.

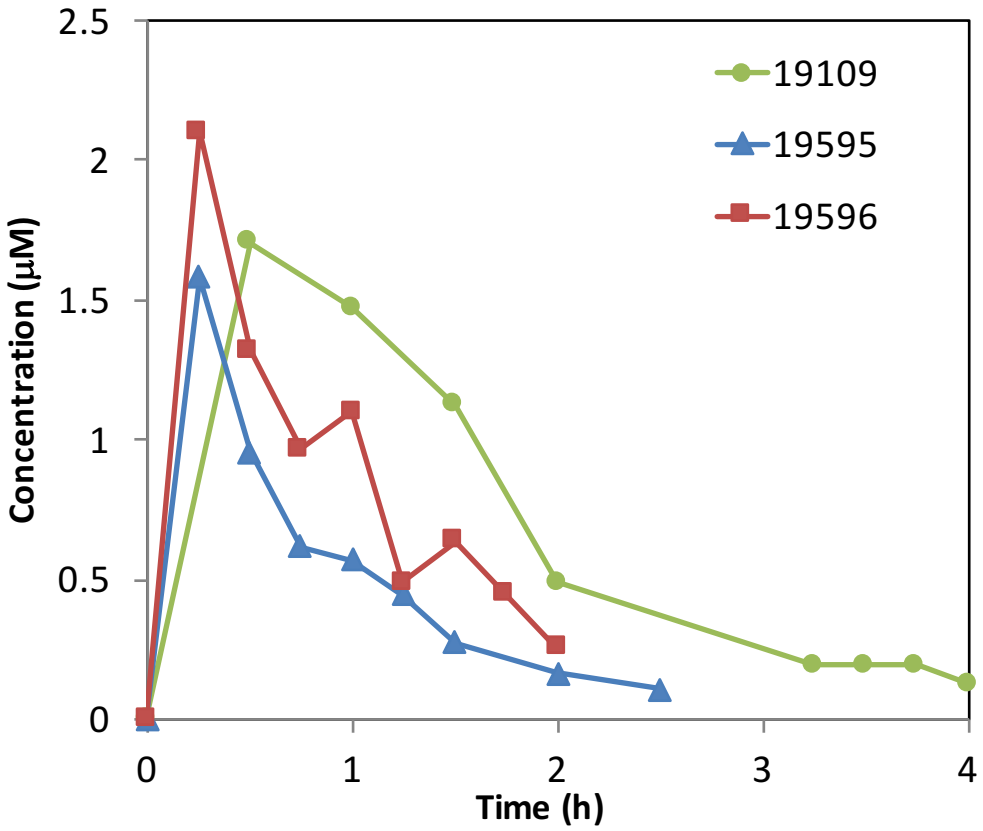

Figure 3.4. Toxicokinetic profile of SMO in swine plasma for inhalation exposure of SM. 19109, 19595, and 19596 designate the three individual animals used for the study.

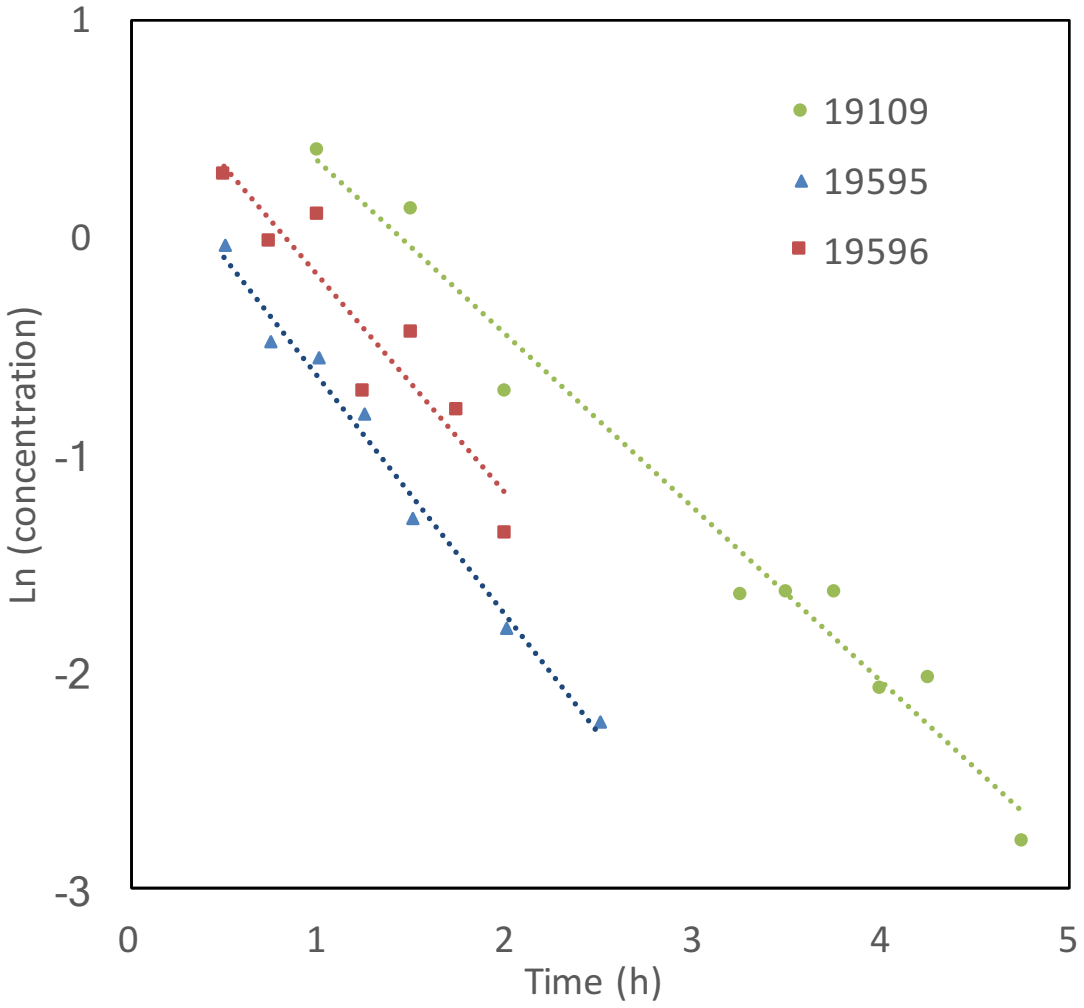

Figure 3.5. Plot of time vs. ln (concentration) for the individual swine (19109, 19595, and 19596). The slopes for each animal were similar to each other. The elimination of SMO followed a one-compartment distribution model.

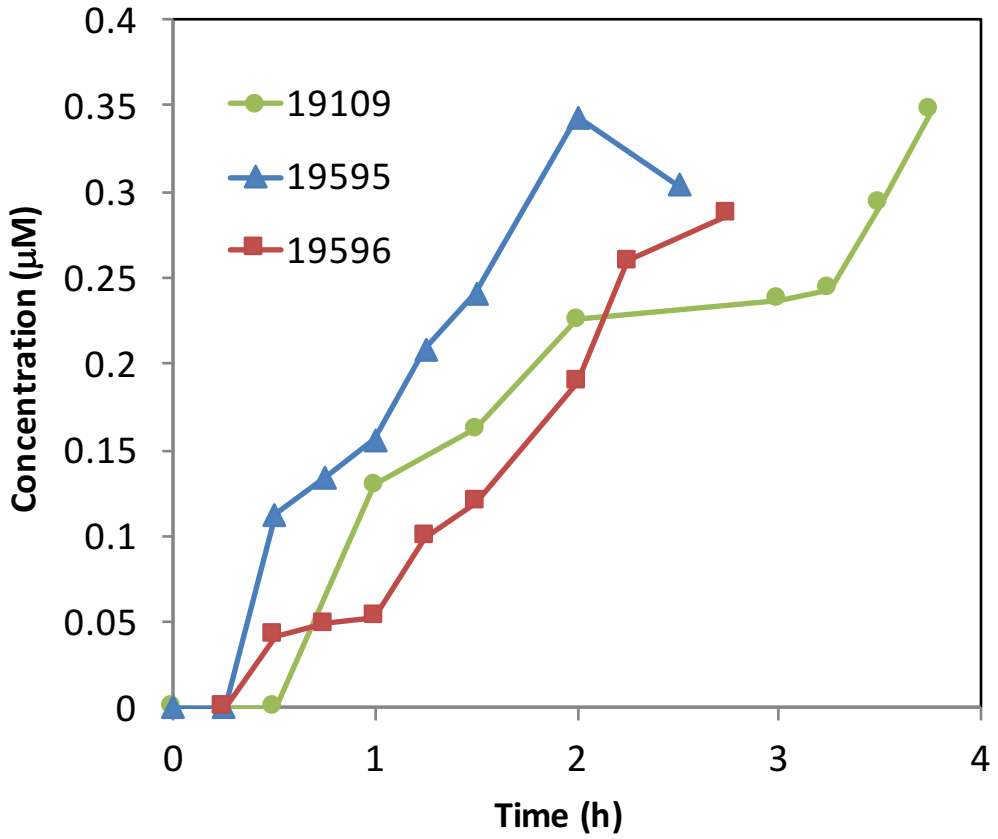

Figure 3.6. Toxicokinetic profile of SBSNAE in swine plasma for inhalation exposure of SM. 19109, 19595, and 19596 designate the three individual animals used for the study.

3.3.4 Validation of the method for SMO and SBSNAE in swine plasma

Validation parameters (LOD, linear range, accuracy and precisions) were only evaluated for SMO and SBSNAE. LOD for SMO was determined as 10 nM in both swine and rat plasma, whereas LOD for SBSNAE was 5 nM and 10 nM for rat and swine plasma respectively. Representative chromatograms for LODs in rat plasma are presented in Figures 3.7 and 3.8.

The linear ranges for SMO (0.05 µM - 5 µM) and SBSNAE (0.05 µM - 10 µM) covered at least two orders of magnitude in both types of plasma (swine and rat).

Calibration curve used $1/x^2$ weighted fitting. Intra-assay accuracies for all QCs were within 100±18% % for SMO and SBSNAE, whereas intra-assay precisions for all QCs were <20 %RSD for both SBSNAE and SMO. Inter-assay accuracies for SMO were within 100 ±17% and within 100±7% for SBSNAE. The inter-assay precision was <13 %RSD for both metabolites. Because the type of plasma did not affect the validation parameters, intra-assay accuracy and precision were evaluated only for one day in rat plasma. Accuracies and precisions for all QCs are listed in Table 3.2 and 3.3 for SBSNAE and SMO respectively.

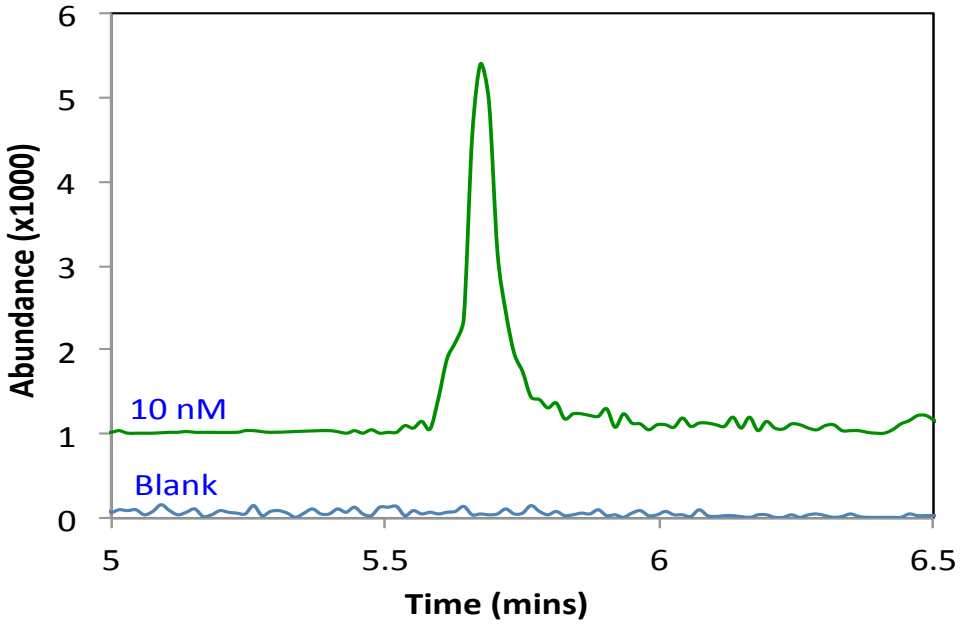

Figure 3.7. LOD for SBSNAE analysis in swine plasma. The lower trace shows non-spiked swine plasma, whereas the upper trace shows 10 nM spiked swine plasma. The LOD concentration (10 nM) reproducibly produced S/N of at least 3.

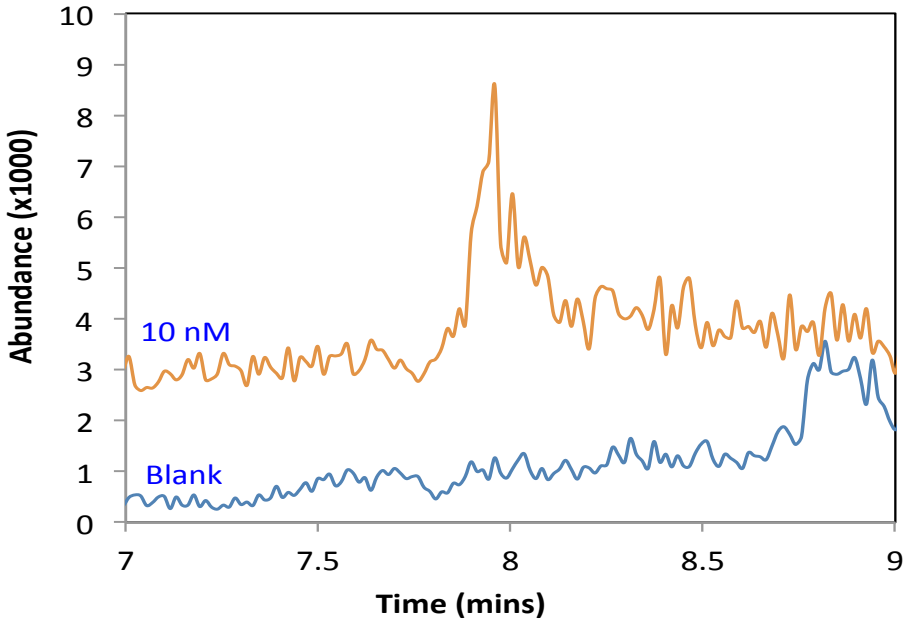

Figure 3.8. LOD for SMO analysis in swine plasma. The lower trace shows non-spiked swine plasma, whereas the upper trace shows 10 nM spiked swine plasma. The LOD concentration (10 nM) reproducibly produced S/N of at least 3.

Table 3.2. Intra- and inter- assay accuracies and precisions for analysis of SBSNAE in spiked swine plasma.

Concentration (μM)	Intra-assay						Inter-assay	
	Accuracy (%)[a]			Precision (%RSD)[a]			Accuracy (%)[b]	Precision (%RSD)[b]
	Day1	Day2	Day3	Day1	Day2	Day3		
0.15	100±4.8	100±8.1	100±13.5	14.2	5.0	2.1	100±1.2	11.5
0.75	100±16.8	100±1.5	100±8.3	3.1	5.0	1.1	100±6.2	9.6
3	100±4.3	100±2.1	100±6.5	2.2	4.2	1.3	100±3.4	4.0

[a] QC method validation (N=5)

[b] Mean of three different days of QC method validation (N=15)

Table 3.3. Intra- and inter- assay accuracies and precisions for analysis of SMO in spiked swine plasma.

Concentration (μM)	Intra-assay						Inter-assay	
	Accuracy (%)[a]			Precision (%RSD)[a]			Accuracy (%)[b]	Precision (%RSD)[b]
	Day1	Day2	Day3	Day1	Day2	Day3		
0.15	100±17.1	100±16.7	100±9.3	19.1	6.8	3.5	100±16.4	12.6
0.75	100±13.6	100±6.7	100±0.4	12.2	6.5	6.8	100±13.2	9.3
3	100±9.3	100±10.5	100±0.9	6.2	6.1	1.6	100±5.8	12.8

[a] QC method validation (N=5)

[b] Mean of three different days of QC method validation (N=15)

3.3.5 Correlation of biomarker concentration to inhalation dose in rats

Rat plasma samples collected at 1, 2, 3, and 7 h from inhalation exposure in three different dose groups (1.2, 2.5, and 4.0 mg/kg) were analyzed. Dose versus peak area ratio (SMO/IS) for SMO at 1 h time-point is plotted in Figure 3.9; error bars represent standard error of the mean (n=3). The SMO concentration showed a linear increase with the dose ($R^2 = 0.98$). Similarly, the dose versus peak area ratio (SBSNAE/IS) for SBSNAE at 7 h time-point is plotted in Figure 3.10. SBSNAE concentration also showed a linear increase with dose, with R^2 value of 0.99. Although these preliminary data indicate linear correlation of exposure dose with metabolite concentration, more detailed study with larger sample size ($n > 5$) at each dose would be required to verify the correlation. Additionally, more time-points (before, at, and after C_{max}) should be investigated for both markers in order to determine the optimal time-point that can be used for dose correlation. Here, the plotted data are for time-points where C_{max} of the analyte should already be achieved. Note that the C_{max} time-point for SMO and SBSNAE is estimated as 0.6 and 4 h respectively; the plotted data (Figures 3.9 and 3.10) are at 1 h for SMO and 7 h for SBSNAE.

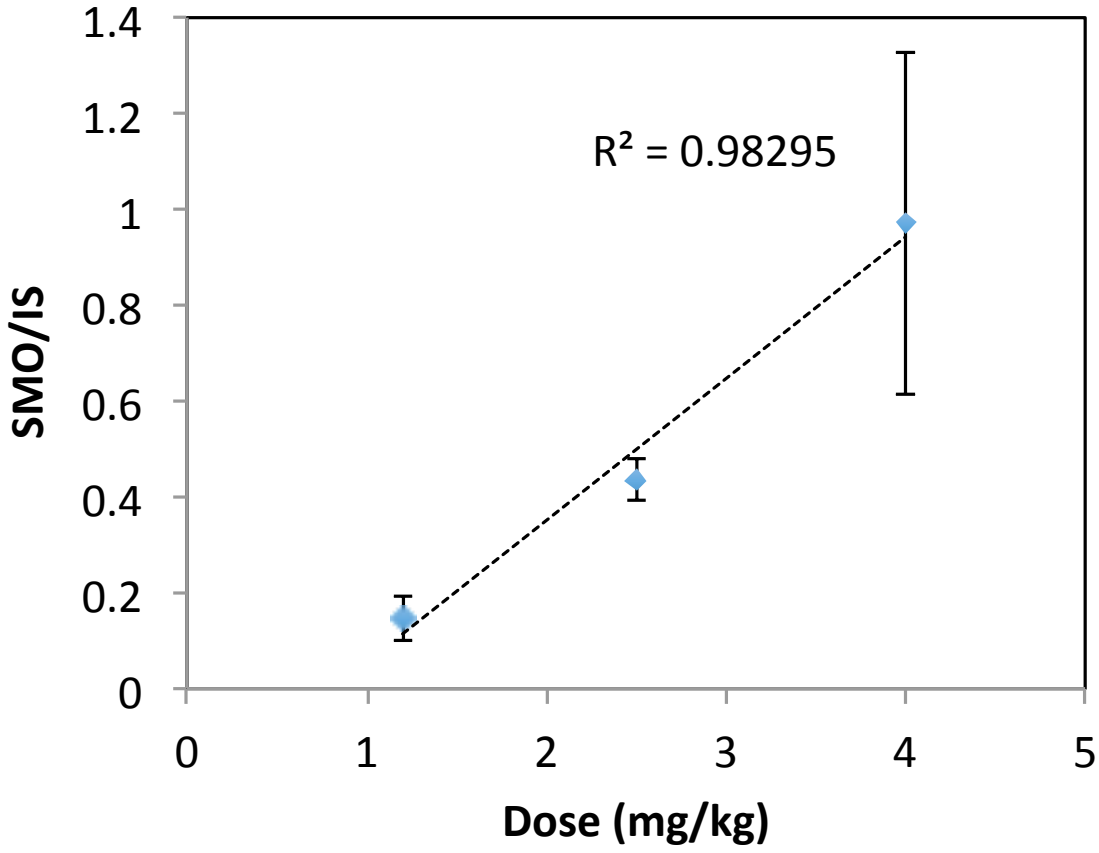

Figure 3.9. Linearity of peak area ratio (SMO/IS) to exposed SM concentrations at 1 h time-point.

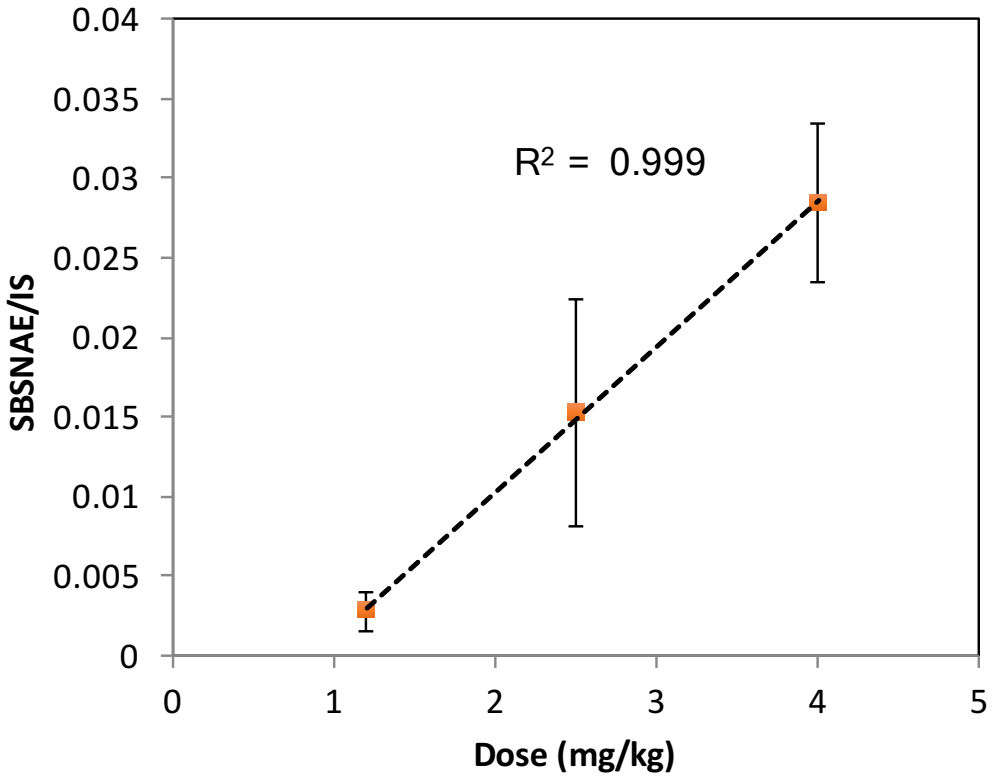

Figure 3.10. Linearity of peak area ratio (SBSNAE/IS) to exposed SM concentrations at 7 h time-point.

3.4 Conclusion

Six plasma metabolites (TDG, TDGO, SBMSE, MSMTESE, SBSNAE, and SMO) of SM were investigated for their potential as biomarkers in inhalation studies. Exposed swine plasma samples from an inhalation study were screened for determination of ideal metabolites for correlation to inhalation dose. Only three metabolites, TDGO, SBSNAE, and SMO, were consistently detected, and only two (SMO and SBSNAE) could be used as unequivocal markers of exposure. Toxicokinetic behavior for SMO and SBSNAE were found to be in good agreement in inhalation and sub-cutaneous exposure. Preliminary data from inhalation studies showed a linear correlation of SMO and SBSNAE with SM

concentration. However, detailed studies with greater number of animals will be important to confirm the correlation. A good correlation will allow use of these biomarkers to calculate the "actual internal dose" in inhalation studies. This is the first reported investigation of SM biomarkers from an inhalation study.

3.5 Acknowledgements

We gratefully acknowledge the support from the CounterACT Program, National Institutes of Health Office of the Director, and the National Institute of Environmental Health Sciences (NIEHS), Grant number U54 ES027698 (CWW). We also want to thank Biomedical Advanced Research and Development Authority (BARDA), Office of the Assistant Secretary for Preparedness and Response, Office of the Secretary, Department of Health and Human Services, under contract No. HHS0100201500020C. We thank the National Science Foundation Major Research Instrumentation Program (Grant Number CHE-0922816), the state of South Dakota, and South Dakota State University for funding the AB SCIEX QTRAP 5500 LC-MS-MS. The LC-MS-MS instrumentation was housed in the South Dakota State University Campus Mass Spectrometry Facility which was supported by the National Science Foundation/EPSCoR grant no. 0091948 and the State of South Dakota. Furthermore, we are thankful to Adam Pay, a graduate student at South Dakota State University for his work on synthesizing the SM metabolites and IS needed for this project. The opinions or assertions contained herein are the private views of the authors and are not to be construed as official or as reflecting the views of the National Institutes of Health, the CounterACT Program, BARDA, the Department of Health and Human Services, the State of South Dakota, or South Dakota State University.

Chapter 4. Analysis of sulfur mustard oxide in plasma using chemical ionization – gas chromatography mass spectrometry

4.1 Introduction

Conflicts around the world have made chemical warfare agents (CWAs), such as 2,2'-dichloro diethyl sulfide (sulfur mustard), a significant threat to mankind. Technological advancement, globalization, easy access to raw materials and technical information, and increased government-sponsored terrorism have proliferated the prospects of chemical terrorism in the modern world [13]. Although joint international efforts have led to destruction of many declared chemical stockpiles, these efforts have not been fully effective in preventing the use of CWAs such as mustards, sarin, cyanide, etc. by terrorist organizations or countries such as Iraq and Syria [1, 5, 146, 147].

After World War II, some of the most catastrophic uses of CWAs occurred during Iran-Iraq conflict. Within the time frame of late 1980s to early 1990s, Iraq allegedly used a combination of CWAs, including sulfur mustard, against Iranian soldiers and its own Kurdish people, resulting in an estimated 50,000 fatalities [5]. More recently, between 2013-2017, over 1400 deaths occurred from use of CWAs by Assad regime on Syrian people [4]. These tragic developments in recent times have established an increasing need to develop and improve analytical methodologies to confirm exposure in concerned individuals.

Sulfur Mustard (SM) is a potent vesicant that produces blisters upon exposure and also causes injury to the respiratory system, eyes, and bone marrow [5, 148, 149]. Additionally, it is a strong alkylating agent that can have long-term mutagenic and

carcinogenic effects. At high doses, SM can cause fatality within days or weeks primarily due to severe airway obstruction caused by formation of pseudomembranes in respiratory tract [6, 132, 148-152]. However, death can also occur from second-degree burns and multi-organ failure [6, 152, 153]. At medium and low doses, the toxicity depends on concentration and duration of exposure, and can result in short- and long-term injury [147]. The clinical effects of both high and low dose SM exposure are characterized by an initial asymptomatic latent period of 6-24 h before the development of pain and lesions [147, 154, 155]. This delayed onset results in delay for clinical diagnosis and treatments. Therefore, a method to rapidly and reliably diagnose SM poisoning from potential victims during this latent period is critical [156].

Although analysis of the intact agent is the most direct diagnostic marker, the rapid conversion of sulfur mustard in biological system limits the window-of-opportunity to detect the intact agent [5]. Therefore, verification of exposure is more reliably achieved by screening plasma or urine for free metabolites that are derived from direct oxidation and hydrolysis of SM, or conjugation with glutathione followed by metabolic conversion (β-lyase metabolites). The oxidation and hydrolysis products, namely, sulfur mustard oxide (SMO), thiodiglycol (TDG), and thiodiglycol oxide (TDGO), appear in plasma and urine within 15 min post-exposure [89]. While several methods have been produced to determine TDG and TDGO using gas chromatography-mass spectrometry (GC-MS) or gas chromatography-tandem mass spectrometry (GC-MS/MS) [84, 88], TDG and TDGO cannot be used as unequivocal markers for SM exposure because of

their presence at low concentrations (0-1 ng/mL for TDG and 2-8 ng/mL for TDGO) in samples from unexposed animals [87, 145].

Furthermore, although β-lyase metabolites can be used for definite confirmation of exposure, and several analytical methods using GC-MS or liquid chromatography-tandem mass spectrometry (LC-MS-MS) are available [83, 89, 157], these metabolites appear in plasma and urine only after 1-2 h post-exposure. Moreover, the β-lyase metabolites are also present at very low concentrations. In a toxicokinetic study performed by Li et al. for subcutaneous injection in rats, the T_{max} for β-lyase metabolites in plasma occurred between 4-8 hours post-exposure. The C_{max} for most β-lyase metabolites ranged between (1-9 μg/L), whereas one of the β-lyase metabolites was below the quantification range of the method (5 μg/L) [89]. In a separate study with cutaneous application of SM in rats, similar results were obtained, with peak levels of hydrolysis and β-lyase products found at 15 min and >1 h respectively [84]. Notably, the concentrations of the β-lyase metabolites (2.5-5.3%) accounted for lower percentage of the applied dose compared to hydrolysis products (3.7-13.6%). The slow rise in β-lyase metabolite concentration and their low C_{max} makes them not ideal for early diagnostic purposes. [84]. The drawbacks of the hydrolysis and β-lyase metabolites for diagnostic analysis indicate the need for a marker that is definitive, has early onset, and has a significant presence in biological specimen of exposed victim.

The oxidative metabolite of SM, sulfur mustard oxide (SMO) has received less attention as a potential SM diagnostic marker. This is likely because most toxicokinetic studies were performed using urine, and SMO is only present as a minor urinary

metabolite [79, 82]. However, recent toxicokinetics data reported by Li et al. shows that SMO is an important metabolite in plasma. It is an early marker with T_{max} of 0.8 h post-exposure [89]. SMO is also present at higher concentrations (C_{max} of > 430 μg/L) compared to β-lyase metabolites (1-9 μg/L) [89]. Additionally, unlike TDG and TDGO, SMO is not an endogenous substance, and hence, its existence is a definite evidence of SM poisoning [82]. Since SMO has been minimally studied, there are limited analytical methods for its determination, especially from plasma. There are only two reported methods for analysis of SMO from plasma, both using LC-MS-MS for detection [89, 158]. Both methods require over 1-1.5 hours for overall analysis (sample preparation and detection). Additionally, one of the reported methods also requires chemical conversion of SMO with 2-(3,5-bis(mercaptomethyl)phenoxy) acetic acid into a stable derivatized product [158]. There are currently no GCMS methods for SMO analysis in the literature. Therefore, in this paper, we present a rapid and simple sample preparation and direct analysis scheme for SMO using chemical ionization (CI)-GCMS for diagnosis of SM poisoning during the latent period between SM exposure and the appearance of clinical symptoms. The availability of this method will allow rapid diagnosis of SM exposure in victims.

4.2 Materials and Methods

Caution: SMO and SMO-d4 are reactive agents. These agents should be handled in well-ventilated hoods. The use of gloves and stringent protective measures should be adopted.

4.2.1 Chemicals and solutions

For method development and validation, swine plasma (EDTA anti-coagulated) was purchased from Pelfreeze Biological (Rogers, AR, USA) and stored at -80 °C until used.

Thiodiglycol, 1,2-dichloroethane-d4, and 2-mercaptoethanol were obtained from Sigma Aldrich (St. Louis, MO, USA). Hydrochloric acid, nitric acid, acetonitrile, methylene chloride were obtained from Fisher Scientific (Fair Lawn, NJ, USA). SMO and SMO-d4 were synthesized in the lab. Reverse-osmosis water was purified to 18.2 MΩ-cm using a Lab Pro polishing unit from Labconco Kansas City, KS, USA.

The structures for SMO and SMO-d4 are provided in Figure 1. For synthesis of SMO, a one-pot reaction scheme was developed. Thiodiglycol (1 eq.) was reacted with concentrated hydrochloric acid (9 eq.) at 90 °C for 90 mins. The upper aqueous layer was removed, and concentrated nitric acid (15 eq.) was added to the reaction flask and stirred at room temperature for 30 mins. The reaction mixture was diluted with 15 mL water and SMO was extracted with 20 mL methylene chloride. The purity was tested with NMR, ^{1}H 400MHz, $CDCl_3$ δ 2.1 (s, 6H) 3.0 (t, 4h) 3.3 (t, 4H).

For synthesis of SMO-d4, sodium metal (0.15 g) was added to dry methanol (5 mL), to which 2-mercaptoethanol (0.45 mL) was added and allowed to react for 30 mins at room temperature with occasional swirling. 1,2-dichloroethane-d4 (3.85 mL) was added to the mixture, and the resulting solution was left in the refrigerator overnight. The solution was filtered, and the filtrate was dried under vacuum using a rotary evaporator. Concentrated hydrochloric acid (4 mL) was added to the residue in the flask and the

remainder of the reaction was carried out as mentioned above. Purity of the product was tested with GCMS (>99% purity).

4.2.2 Sample preparation

An aliquot of 500 μL plasma (spiked or non-spiked) was pipetted into a 2 mL glass vial, to which 50 μL of aqueous 100 μM internal standard (SMO-d4) was added and vortexed for 30 seconds. To the plasma solution, 500 μL of methylene chloride was added for liquid-liquid extraction. The mixture was shaken for 10 s and centrifuged at 6000 rpm for 2 minutes for separation of plasma and organic layers. For centrifugation, the glass sample vial was opened and placed into a 5 mL centrifuge tube. Note that plastic vials and centrifuge tubes must be avoided because components in the plastics leached into the solvent (methylene chloride) and interfered with the analysis of SMO. After centrifugation, vials were removed from the tubes using forceps and the upper plasma layer was carefully removed. A small layer of precipitated proteins formed between the plasma and organic layer, which was also carefully removed without disturbing the lower organic layer. The organic layer was then pipetted into a new 2 mL GC autosampler vial. The organic layer was dried by blowing air, and reconstituted with 25 μL of acetonitrile. The final acetonitrile solution was transferred to a tapered-bottom glass insert (300 μL) in a GC vial and analyzed via CI-GCMS.

4.2.3 GC-MS analysis of SMO

Prepared samples were analyzed for SMO and SMO-d_4 using Agilent Technologies 6890N gas chromatograph and a 5975B inert XL electron ionization (EI)/chemical ionization (CI) mass selective detector (MSD) in CI with a 7683 series

autosampler. A DB5-MS bonded-phase column (30 m x 0.25 mm I.D., 0.25 µm film thickness; J&W Scientific, Folsom, CA, USA) was used with hydrogen as the carrier gas at a flow rate of 1.5 mL/min and a column head pressure of 5.12 psi. The injection was performed in splitless mode (split delay 1min, purge flow 30.1 mL/min), the injection volume was 1 µL, and the injection port was held at 150 °C. Note that it is vital to maintain a relatively low injection temperature in order to prevent degradation of SMO. At higher injection temperatures, significant degradation with loss of most or all of SMO was observed. To prevent in-column degradation, oven temperature greater than 250 °C was not used. The initial GC oven temperature was 80 °C, which was ramped at a rate of 50 °C/min to 250 °C, where it was held constant for 1 min. The chromatographic acquisition time was 4.40 min with SMO and SMO-D_4 eluting at 2.68 min.

The GC-MSD transfer line was heated at 170 °C. The MS source and MS quad temperatures were 250 °C and 150 °C, respectively. Methane was used as a reagent gas for positive ion CI with electron energy of 235 eV. Selective ion monitoring (SIM) was used to monitor the quantification and identification ions of SMO (m/z of 175 and 123, respectively) and SMO-d_4 (m/z of 181 and 127, respectively). For SMO, the major molecular ion, m/z of 175, was selected for quantification. Because SMO has two chlorine atoms, and Chlorine has two major stable isotopes (^{35}Cl 75%, ^{37}Cl 25%), its molecular ions can exist as 175, 177, and 179. Therefore, to prevent overlap of SMO and SMO-d4, an m/z of 181 for SMO-d4 was selected instead of 179. The structures of SMO and SMO-d4 are presented in Figure 4.1.

A

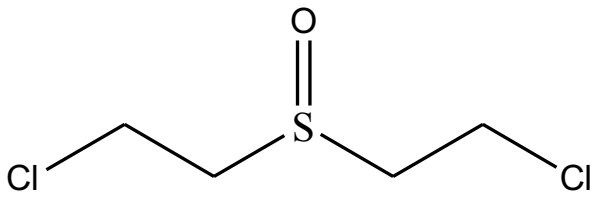

B

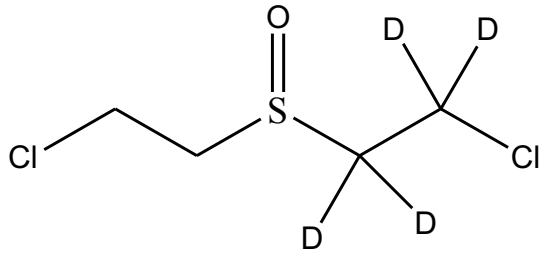

Figure 4.1. Structures of SMO (A) and SMO-d4 (B).

4.2.4 Calibration, quantification, and limit of detection

Bioanalytical method validation was accomplished by generally following the Food and Drug Adminisitration (FDA) guidelines [127, 129]. SMO and SMO-D_4 stock solutions (10 mM) were prepared in acetonitrile and stored at -30 °C. Aqueous solutions of SMO were prepared via serial dilution of the stock; a working solution of 200 µM of SMO-D4 was also prepared in water. An aqueous mix solution of SMO and SMO-D4 for each calibrator was prepared by mixing 50:50 of SMO solution and 200 µM SMO-d4. The mix solution was then spiked (50 µL) into plasma (450 µL) for calibration and quality-control (QC) standards. All calibration standards (0.5, 1, 2, 5, 10, 20, 50, 100 µM) were prepared in triplicates. To obtain a calibration curve, the average peak-area signal

ratios of SMO to SMO-D_4 were plotted as a function of concentration. Peak areas were calculated by manual integration from baseline to baseline in ChemStation software (Agilent Technologies, Santa Clara, CA).

For determining the upper limit of quantification (ULOQ) and lower limit of quantification (LLOQ), a percent relative standard deviation (%RSD) of <20% (as a measure of precision) and a percent deviation within ±20% back-calculated from the nominal concentration of each calibration standard (as a measure of accuracy) were used as inclusion criteria for the calibration standards. Quality control (QC) standards were prepared in swine plasma at three different concentrations: 1.5 μM (low), 7.5 μM (medium) and 35 μM (high). The QC standards were analyzed in quintuplicate each day for 3 days and were run in parallel with the calibration standards. Intra-assay precision and accuracy were calculated from each day's analysis and inter-assay precision and accuracy were calculated from the comparison of the data gathered from three separate days. It should be noted that the inter-assay and intra-assay studies were conducted within 1 week. The limit of detection (LOD) was evaluated by analyzing multiple concentrations of SMO below LLOQ, and determining the lowest concentration which reproducibly produced a signal-to-noise ratio (S/N) (peak-to-peak) of at least 3 compared to the blank at the same retention time.

4.2.5 Selectivity and sensitivity

Selectivity of the method was checked by analyzing blank and and spiked swine plasma samples. A comparison of chromatograms was made among three samples of blank plasma with three samples spiked swine (0.5 μM SMO) to determine if chemical

components of plasma interfered with ability to quantify SMO.

For recovery experiments, detector response obtained from SMO spiked plasma was compared to the detector response obtained for the same moles of SMO prepared in acetonitrile. It is to be noted that in our sample preparation, the analyte is reconstituted in a final volume of 25 µL, which allows for a 20-fold concentration increase before analysis in GCMS. Hence, signals for triplicates of low (1.5 µM), medium (7.5 µM), and high (35 µM) QCs in plasma were compared to the signal produced by 30, 150, and 700 µM of SMO solution in acetonitrile respectively.

4.2.6 Matrix effects

An attempt to assess the effect of matrix components to enhance or suppress the signal of the analyte was accomplished by creating calibration curve from plasma and aqueous solution. A ratio of less than 1 indicates suppression effect, whereas greater than 1 indicates an enhancement effect. The ratio of slopes of non-corrected curves were then compared with the internal standard corrected curves to evaluate the effectiveness of internal standard to minimize the matrix effect.

4.3 Results and Discussion

4.3.1 GC-MS analysis of SMO

The method presented here includes a short, simple, and direct (i.e. no chemical modification) analysis of SMO. Using this method, a plasma sample can be prepared and analyzed within a total analysis time of 15 min. SMO is simply extracted from plasma via liquid-liquid extraction into methylene chloride. Different solvents were investigated to improve extraction of SMO, such as toluene, hexane, and cyclohexane. The test solvents

were selected with the criteria of high K_{ow} (low miscibility with water) and low boiling point. Among the tested solvents, methylene chloride provided the highest extraction efficiency. The high vapor pressure of methylene chloride also allowed for extremely rapid drying (~3 mins for 500 µL of the DCM extract) under just ambient airflow (flow rate of ~40 mL/min). Hence, methylene chloride was chosen as the solvent of choice for extraction from plasma samples.

Following sample preparation, the GCMS analysis was very short with a total chromatographic runtime of less than 5 min, and SMO eluting at 2.68 min. Even with extremely rapid and simple sample preparation and analysis, the SMO was completely resolved from other components in the matrix, with adequate peak shape, although some tailing is present. Representative selected ion chromatograms (SIM), m/z = 175 for SMO and m/z = 181 for SMO-d_4, of both non-spiked and spiked swine plasma is shown in Figure 4.2. However, it is to be noted that the internal standard synthesized in-house, SMO-d4, could attribute to some SMO ions because of its 99% purity. Therefore, for sample analysis, blank samples spiked with only SMO-d4 should be assessed first to calculate the level of SMO produced from the internal standard. A blank-subtraction could potentially be performed for quantification of SMO from real samples. This could be eliminated if a higher purity dichloroethane was used to synthesize the internal standard. Note that in Figure 4.2, no blank subtraction was performed.

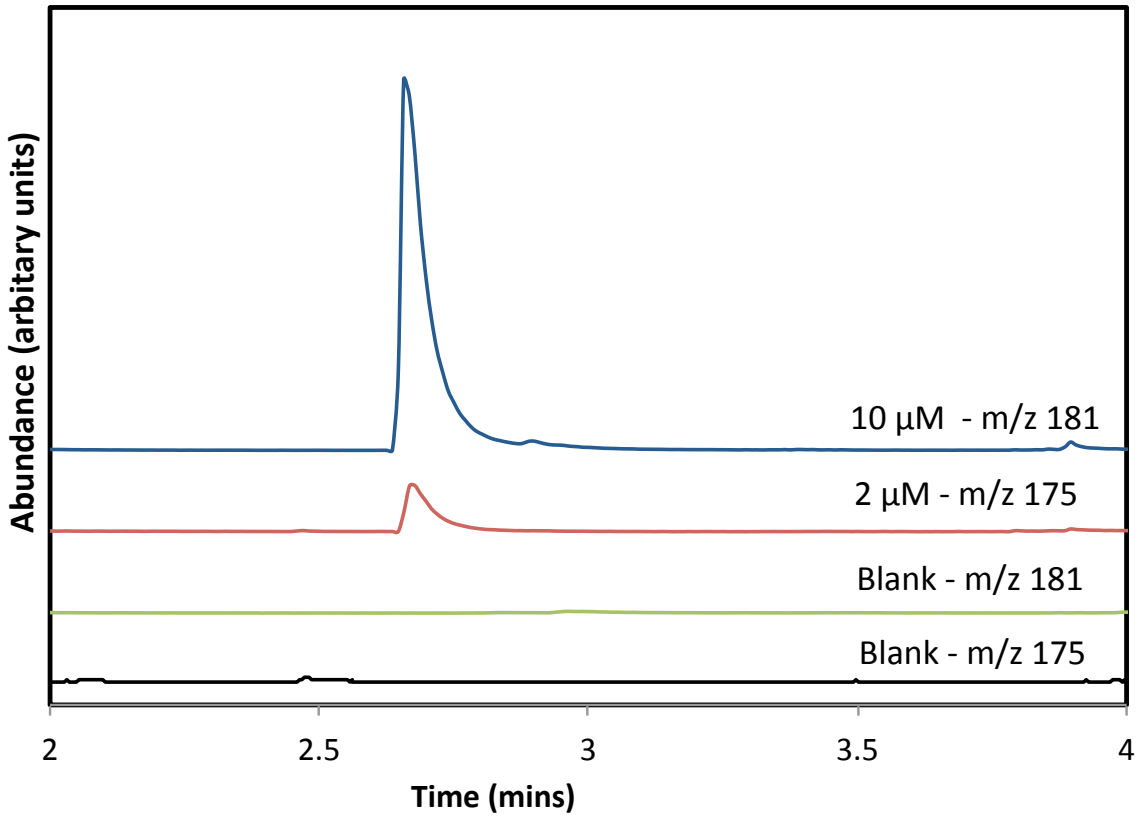

Figure 4.2. Overlay of extracted ion chromatograms (XICs) of m/z 175 (SMO) and m/z 181 (SMO-d4) for non-spiked and spiked swine plasma samples. The two lower traces (black and green) show that there are no components in the plasma matrix that interfere with analysis of either SMO or SMO-d4. The two upper traces (red and blue) show that SMO and SMO-d4 elute at 2.68 min.

4.3.2 Limit-of-detection and linear range

The linearity of the method was evaluated within the concentration range of 0.2 to 500 µM. A calibration curve was constructed by plotting concentration versus corrected signal (peak area of SMO divided by the peak area of corresponding SMO-d4). Upon analysis of calibration standards using non-weighted and weighted ($1/x$ and $1/x^2$) calibration curves, 0.2, 200, and 500 µM standards were excluded based upon the accuracy and/or precision criteria. The linear range of the method spanned over two orders of magnitude, from 0.5-100 µM when using $1/x^2$ weighted linear regression, with

correlation coefficient (R^2) >0.998. The LOD for SMO was 0.1 µM (Figure 4.3).

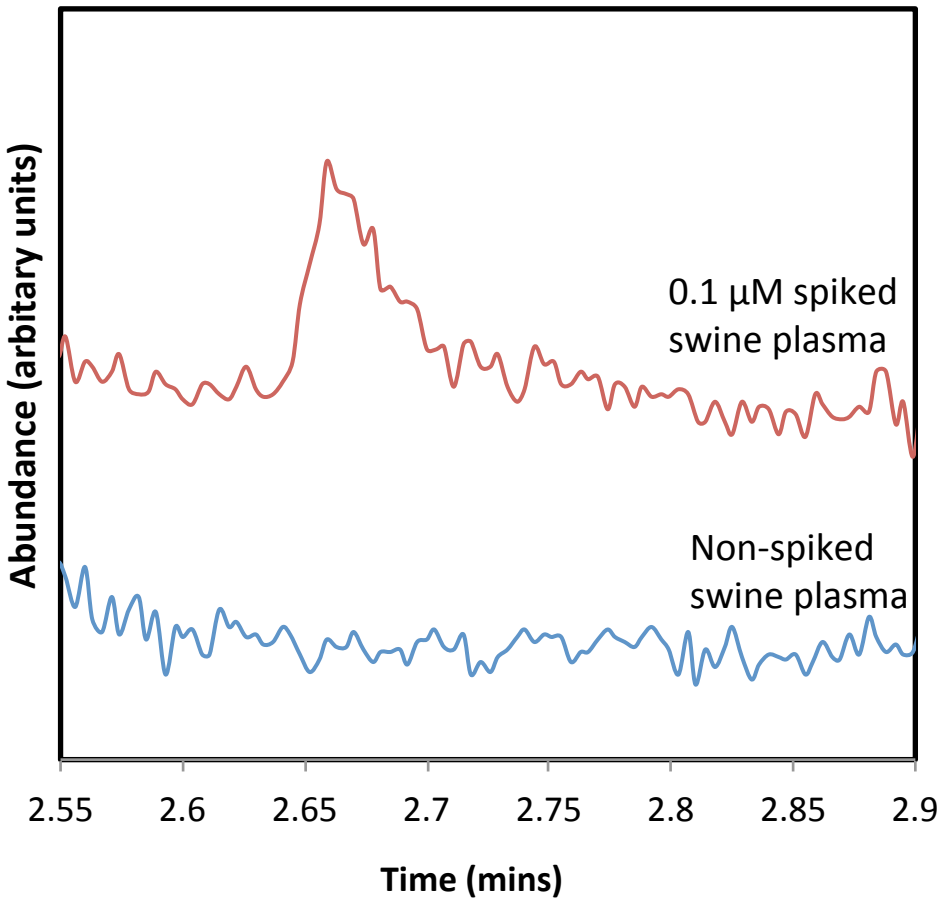

Figure 4.3. LOD of SMO analysis using CI-GCMS; lower trace (blue) shows non-spiked swine plasma, whereas upper trace (red) shows 0.1 µM spiked swine plasma. The LOD concentration (0.1 µM) reproducibly produced a S/N of 3.

4.3.3 Accuracy and precision

Accuracy and precision were determined by quintuplicate analysis of low (1.5 µM), medium (7.5 µM), and high (35 µM) QCs on three different days within 7-day period. The intra-assay accuracy (100± 20%) and precision (<15% RSD) for all QCs were within the acceptable range outlined by FDA for method validation from biological matrix [127, 129]. The inter-assay accuracy (100 ± 13%) and precision (<

16% RSD) were also within the acceptable criteria. The intra- and inter- assay accuracy for low, medium, and high QCs are presented in Table 4.1.

Table 4.1. Intra- and inter- assay accuracies and precisions for analysis of SMO in spiked swine plasma.

Concentration (μM)	Intra-assay						Inter-assay	
	Accuracy (%)[a]			Precision (%RSD)[a]			Accuracy (%)[b]	Precision (%RSD)[b]
	Day 1	Day 2	Day 3	Day 1	Day 2	Day 3		
1.5	100±16.9	100±15.4	100±2.7	7.5	14.3	1.3	100±1.4	15.7
7.5	100±16.7	100±1.8	100±3.9	3.1	0.9	1.3	100±6.3	7.8
35	100±19.7	100±3.9	100±13.5	12.3	2.5	3.6	100±12.1	9.5

[a] QC method validation (N=5)

[b] Mean of three different days of QC method validation (N=15)

4.3.4 Matrix effects

An attempt was made to assess matrix effects by evaluating the slope of calibration curve (non-corrected) in swine plasma compared to in aqueous samples. Both the aqueous and plasma calibrators showed a highly non-linear behavior. Therefore, the matrix effect could not be determined. However, the matrix effect and non-linear behavior was corrected with internal standard; the slopes of internal standard corrected curves in plasma and aqueous were very close (ratio of 0.97). The non-corrected and corrected calibration curves in plasma and aqueous are presented in Figure 4.4.

4.3.5 Recovery

Recovery for low, medium, and high QCs were 19%, 22%, and 23% respectively. The low recovery can be explained by loss during liquid-liquid extraction from plasma and also some possible loss during the drying process. The loss during extraction can be attributed to incomplete extraction and incomplete transfer of organic layer based on

solvent loss when removing plasma layer and loss to the vessel. However, any loss of SMO during this process is corrected by the internal standard, with raw signals resulting in high standard deviations (>28% RSD), whereas internal standard corrected signals resulting in low standard deviation (<6% RSD).

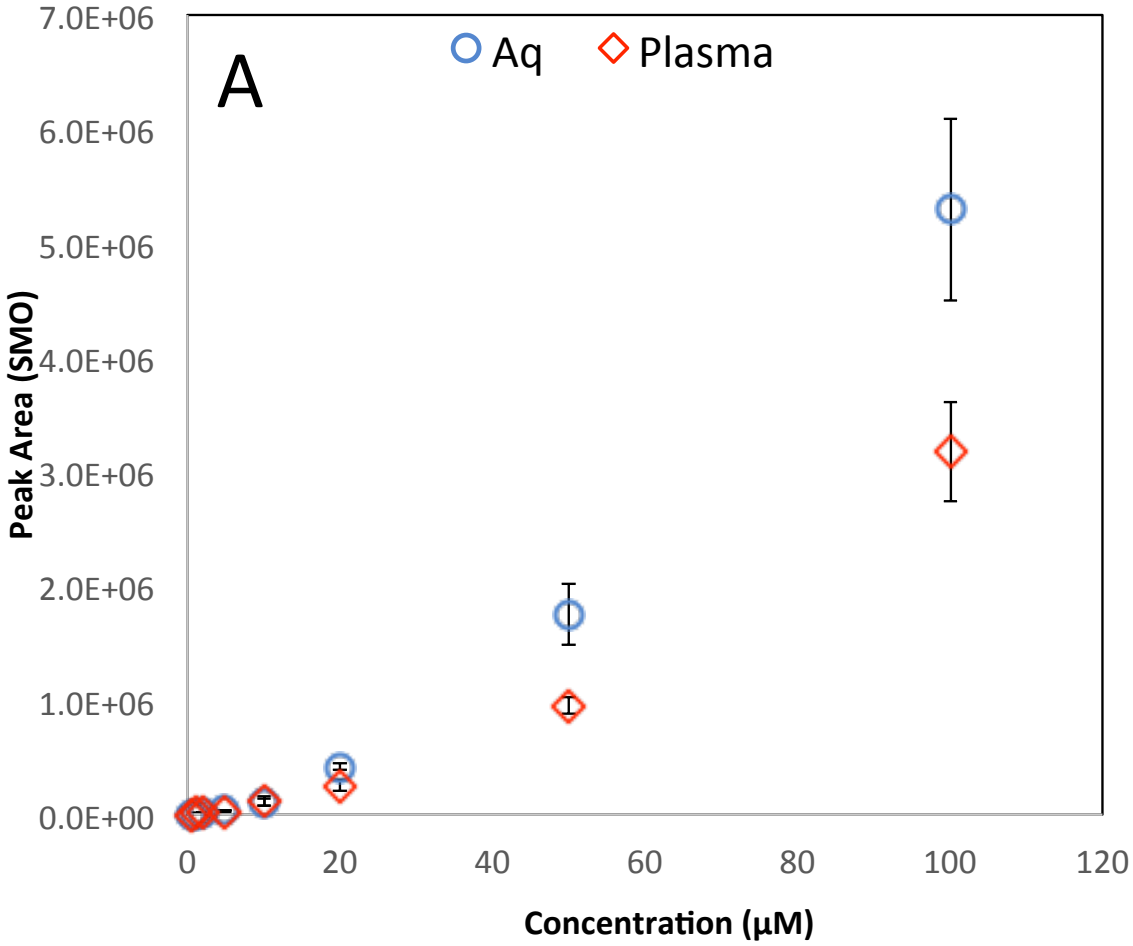

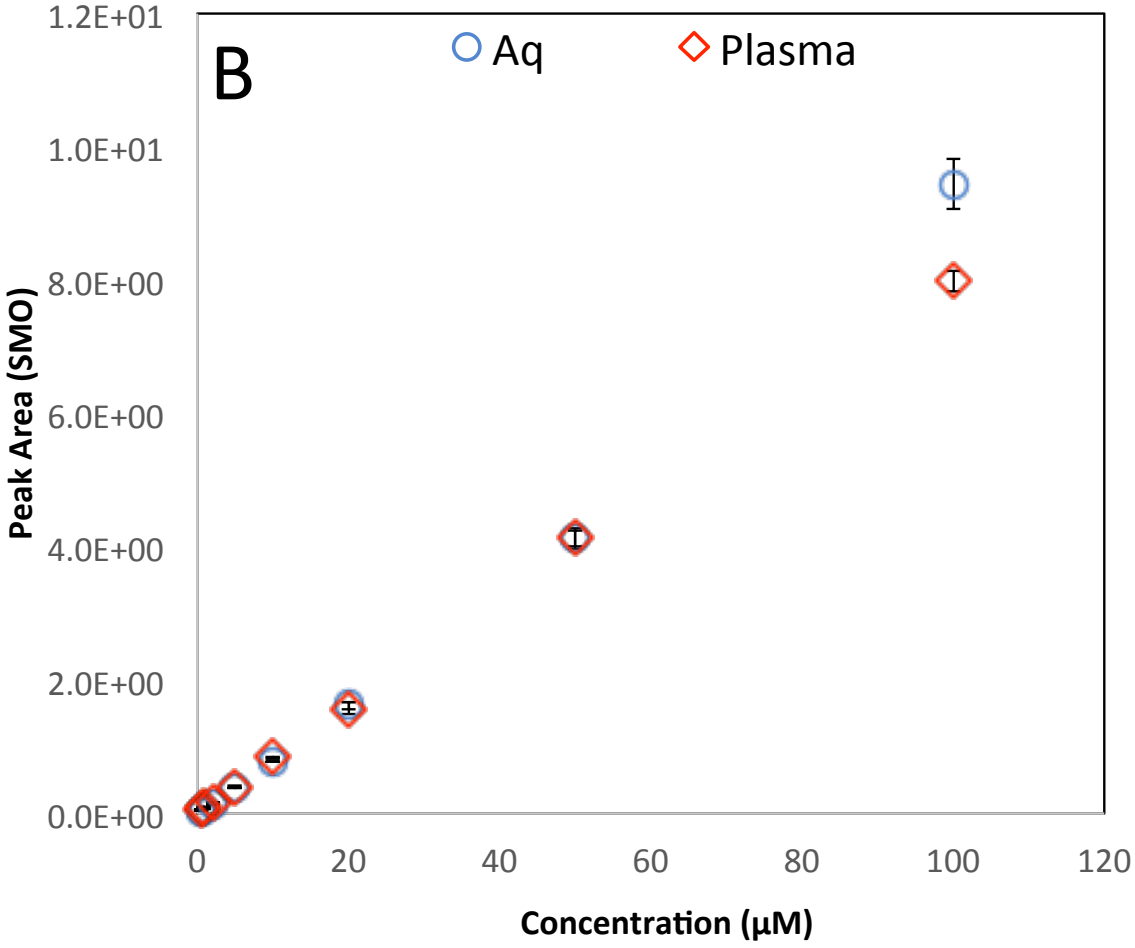

Figure 4.4. Figure showing non-corrected (A) and internal standard corrected (B) calibration curves. Both aqueous and plasma non-corrected curves showed non-linear behavior, and could not be compared to determine matrix effect. The ratio for slopes of corrected plasma and aqueous curve was close to 1(slope plasma/aqueous = 0.97), indicating that the internal standard is effective in correcting any matrix effects.

4.4 Conclusion

A GC-MS method for analysis of SMO from plasma was developed which features very simple sample preparation, rapid analysis, wide linear range of over two orders of magnitude, and requires no chemical modification. To our knowledge, this is the first GC-MS method for analysis of SMO, which is an important early biomarker for sulfur

mustard poisoning. The availability of this method should allow easy and rapid diagnosis of sulfur mustard poisoning for potential victims.

4.5 Acknowledgements

We gratefully acknowledge the support from the CounterACT Program, National Institutes of Health Office of the Director, and the National Institute of Environmental Health Sciences (NIEHS), Grant number U54 ES027698 (CWW). We also want to thank Biomedical Advanced Research and Development Authority (BARDA), Office of the Assistant Secretary for Preparedness and Response, Office of the Secretary, Department of Health and Human Services, under contract No. HHS0100201500020C. Furthermore, we are thankful to Adam Pay, a graduate student at South Dakota State University for his work on synthesizing the SMO needed for this project. The opinions or assertions contained herein are the private views of the authors and are not to be construed as official or as reflecting the views of the National Institutes of Health or the CounterACT Program.

Chapter 5. Broader Impacts, Conclusions, and Future Work

5.1 Broader Impacts

Cyanide and SM are CWAs that pose significant global threat to mankind. Research on improved toxicological understanding and development of effective therapeutic interventions are crucial to defend against these CWA threats. The novel method presented here for DMTS will allow pharmacokinetic and drug development studies on this promising therapeutic, potentially leading to a live-saving antidote. Additionally, metabolite studies for inhalation route of SM exposure will help identify potential markers for calculation of "actual respiratory dose". This would allow for standardization of dose over different inhalation studies, improving the accuracy and reliability of the studies. Furthermore, an easy and rapid method was developed for SMO, an early marker of SM exposure. The availability of this method can allow for immediate diagnosis of SM exposure in victims. The work presented here will contribute towards development and approval of life-saving treatments for CN and SM poisoning.

5.2 Conclusions

A novel SBSE-GCMS method was developed for analysis of DMTS from blood. The method was effective in analyzing DMTS from blood of treated animals. A simple, direct, and rapid method was developed for analysis of SMO from plasma. The method will allow rapid diagnosis of SM poisoning within 15 post-exposure. Plasma metabolites for SM exposure via inhalation were identified, and correlation of metabolite concentration with dose was investigated.

5.3 Future Work

Future work should include pharmacokinetic studies of DMTS in various animal models before leading to human studies. Comprehensive inhalation studies should be done in animals for SM exposure in order to establish a correlation of biomarker concentration to dose. Eventually, the ideal biomarker should be used to calculate "actual dose" for inhalation studies of SM. Animal studies should be performed to confirm the effectiveness of SMO as a diagnostic marker.

References

[1] J. K. Smart, "History of chemical and biological warfare: an American perspective," *Medical Aspects of Chemical and Biological Warfare. Washington, DC: Office of the Surgeon General,* pp. 9-86, 1997.

[2] B. Riley, "The toxicology and treatment of injuries from chemical warfare agents," *Current Anaesthesia & Critical Care,* vol. 14, no. 3, pp. 149-154, 2003.

[3] C. W. White, R. C. Rancourt, and L. A. Veress, "Sulfur mustard inhalation: mechanisms of injury, alteration of coagulation, and fibrinolytic therapy," *Annals of the New York Academy of Sciences,* vol. 1378, no. 1, pp. 87-95, 2016.

[4] "Assad kills at least 85 with chemical weapons; A dictator defies the world," (in English), *The Economist,* Online material April 8th, 2017 2017.

[5] K. Ghabili, P. S. Agutter, M. Ghanei, K. Ansarin, Y. Panahi, and M. M. Shoja, "Sulfur mustard toxicity: history, chemistry, pharmacokinetics, and pharmacodynamics," *Critical reviews in toxicology,* vol. 41, no. 5, pp. 384-403, 2011.

[6] L. A. Veress, H. C. O'neill, T. B. Hendry-Hofer, J. E. Loader, R. C. Rancourt, and C. W. White, "Airway obstruction due to bronchial vascular injury after sulfur mustard analog inhalation," *American journal of respiratory and critical care medicine,* vol. 182, no. 11, pp. 1352-1361, 2010.

[7] A. H. Hall, R. Dart, and G. Bogdan, "Sodium thiosulfate or hydroxocobalamin for the empiric treatment of cyanide poisoning?," *Annals of emergency medicine,* vol. 49, no. 6, pp. 806-813, 2007.

[8] M. Brenner *et al.*, "Comparison of cobinamide to hydroxocobalamin in reversing cyanide physiologic effects in rabbits using diffuse optical spectroscopy monitoring," *Journal of biomedical optics,* vol. 15, no. 1, pp. 017001-017001-8, 2010.

[9] M. Brenner *et al.*, "Sulfanegen sodium treatment in a rabbit model of sub-lethal cyanide toxicity," *Toxicology and applied pharmacology,* vol. 248, no. 3, pp. 269-276, 2010.

[10] I. Petrikovics, M. Budai, K. Kovacs, and D. E. Thompson, "Past, present and future of cyanide antagonism research: From the early remedies to the current therapies," *World J Methodol,* vol. 5, no. 2, p. 88, 2015.

[11] M. D. McGraw, J. S. Rioux, R. B. Garlick, R. C. Rancourt, C. W. White, and L. A. Veress, "From the Cover: ImpairedProliferation and Differentiation of the Conducting Airway Epithelium Associated With Bronchiolitis Obliterans After Sulfur Mustard Inhalation Injury in Rats," *Toxicological Sciences,* vol. 157, no. 2, pp. 399-409, 2017.

[12] M. R. Perry *et al.*, "A novel sulfur mustard (HD) vapor inhalation exposure system for accurate inhaled dose delivery," *Journal of pharmacological and toxicological methods,* vol. 71, pp. 120-128, 2015.

[13] K. Ganesan, S. Raza, and R. Vijayaraghavan, "Chemical warfare agents," *Journal of pharmacy and bioallied sciences,* vol. 2, no. 3, p. 166, 2010.
[14] T. T. Marrs, R. L. Maynard, and F. Sidell, *Chemical warfare agents: toxicology and treatment*. John Wiley & Sons, 2007.
[15] C. P. Holstege, M. Kirk, and F. R. Sidell, "Chemical warfare: nerve agent poisoning," *Critical care clinics,* vol. 13, no. 4, pp. 923-942, 1997.
[16] L. K. Wright, R. B. Lee, N. M. Vincelli, C. E. Whalley, and L. A. Lumley, "Comparison of the lethal effects of chemical warfare nerve agents across multiple ages," *Toxicology letters,* vol. 241, pp. 167-174, 2016.
[17] R. Bhattacharya, S. Flora, and R. Gupta, "Handbook of Toxicology of Chemical Warfare Agents," *Academic Press, Boston,* pp. 255-270, 2009.
[18] M. J. Fasco, C. R. Hauer, R. F. Stack, C. O'Hehir, J. R. Barr, and G. A. Eadon, "Cyanide adducts with human plasma proteins: albumin as a potential exposure surrogate," *Chemical research in toxicology,* vol. 20, no. 4, pp. 677-684, 2007.
[19] H. B. Leavesley, L. Li, K. Prabhakaran, J. L. Borowitz, and G. E. Isom, "Interaction of cyanide and nitric oxide with cytochrome c oxidase: implications for acute cyanide toxicity," *Toxicological Sciences,* vol. 101, no. 1, pp. 101-111, 2008.
[20] T. Okumura *et al.*, "The Tokyo subway sarin attack: disaster management, part 2: hospital response," *Academic Emergency Medicine,* vol. 5, no. 6, pp. 618-624, 1998.
[21] E. Schmitt, "ISIS Used Chemical Arms at Least 52 Times in Syria and Iraq, Report Says," *The New Your Times,* 2016.
[22] B. A. Logue, D. M. Hinkens, S. I. Baskin, and G. A. Rockwood, "The analysis of cyanide and its breakdown products in biological samples," *Crit. Rev. Anal. Chem.,* vol. 40, no. 2, pp. 122-147, 2010.
[23] M. C. Reade, S. R. Davies, P. T. Morley, J. Dennett, and I. C. Jacobs, "Review article: management of cyanide poisoning," *Emerg Med Australas,* vol. 24, no. 3, pp. 225-238, 2012.
[24] R. K. Bhandari *et al.*, "Simultaneous determination of cyanide and thiocyanate in plasma by chemical ionization gas chromatography mass-spectrometry (CI-GC-MS)," *Anal. Bioanal. Chem.,* vol. 404, no. 8, pp. 2287-2294, 2012.
[25] A. H. Hall, G. E. Isom, and G. A. Rockwood, *Toxicology of Cyanides and Cyanogens: Experimental, Applied and Clinical Aspects*. John Wiley & Sons, 2015.
[26] W. H. Organization, "Hydrogen cyanide and cyanides: Human health aspects," *Concise international chemical assessment document,* vol. 61, 2004.
[27] C. J. Knowles, "Microorganisms and cyanide," *Bacteriological Reviews,* vol. 40, no. 3, p. 652, 1976.
[28] A. Knight and R. Walter, "Plants causing sudden death," *A guide to plant poisoning of animals in North America,* pp. 1-56, 2002.

[29] F. Nartey, R. Smith, and E. Bababumni, "Toxicological aspects of cyanogenesis in tropical foodstuffs," *Toxicol. Trop., Taylor & Francis, London,* pp. 53-73, 1980.
[30] E. Conn, "Cyanogenic glycosides," *Int. Rev. Biochem.,* vol. 27, pp. 21-43, 1979.
[31] M. C. Reade, S. R. Davies, P. T. Morley, J. Dennett, and I. C. Jacobs, "Review article: management of cyanide poisoning," *Emergency Medicine Australasia,* vol. 24, no. 3, pp. 225-238, 2012.
[32] R. Schnepp, "Cyanide: sources, perceptions, and risks," *Journal of Emergency Nursing,* vol. 32, no. 4, pp. S3-S7, 2006.
[33] R. K. Bhandari, E. Manandhar, R. P. Oda, G. A. Rockwood, and B. A. Logue, "Simultaneous high-performance liquid chromatography-tandem mass spectrometry (HPLC-MS-MS) analysis of cyanide and thiocyanate from swine plasma," *Anal. Bioanal. Chem.,* vol. 406, no. 3, pp. 727-734, 2014.
[34] M. Webster, "definitions-Cyanide report a problem," *catalyst,* vol. 16, p. 17.
[35] P. Darby and J. Wilson, "Cyanide, smoking, and tobacco amblyopia," *The British journal of ophthalmology,* vol. 51, no. 5, p. 336, 1967.
[36] T. Cummings, "The treatment of cyanide poisoning," *Occupational Medicine,* vol. 54, no. 2, pp. 82-85, 2004.
[37] P. Lawson-Smith, E. C. Jansen, and O. Hyldegaard, "Cyanide intoxication as part of smoke inhalation-a review on diagnosis and treatment from the emergency perspective," *Scandinavian journal of trauma, resuscitation and emergency medicine,* vol. 19, no. 1, p. 1, 2011.
[38] K. H. Jason Hanna, "China: Sodium cyanide levels well past limit at Tianjin explosion site," (in English), News article August 20, 2015 2015
[39] K. A. Wolnik, F. L. Fricke, E. Bonnin, C. M. Gaston, and R. D. Satzger, "The Tylenol tampering incident-tracing the source," *Analytical chemistry,* vol. 56, no. 3, pp. 466A-474A, 1984.
[40] R. Suskind, "The Untold Story of al-Qaeda's Plot to Attack the Subways," *Time Magazine,* vol. 26, 2006.
[41] J. L. Way, "Cyanide intoxication and its mechanism of antagonism," *Annual Review of Pharmacology and Toxicology,* vol. 24, no. 1, pp. 451-481, 1984.
[42] A. DOSTER. (2013, Jan 13). *The Poisoned Lottery Winner's Mysterious Death and the Insane Details from the Investigation*. Available: http://www.chicagomag.com/Chicago-Magazine/The-312/April-2013/Poison-Lotto/
[43] J. Gorner, "Lottery winner's cyanide poisoning death remains unsolved five years later," (in English), website July 25, 2017 2017.
[44] G. Botelho, "Pittsburgh professor convicted for fatally poisoning wife with cyanide," (in English), electronic in website November 8, 2014 2014.

[45] R. Gracia and G. Shepherd, "Cyanide poisoning and its treatment," *Pharmacotherapy: The Journal of Human Pharmacology and Drug Therapy,* vol. 24, no. 10, pp. 1358-1365, 2004.
[46] S. I. Baskin, J. B. Kelly, B. I. Maliner, G. A. Rockwood, and C. Zoltani, "Cyanide poisoning," *Medical aspects of chemical warfare,* vol. 11, pp. 372-410, 2008.
[47] M. Vos, P. Verstreken, and C. Klein, "Stimulation of electron transport as potential novel therapy in Parkinson's disease with mitochondrial dysfunction," ed: Portland Press Limited, 2015.
[48] A. B. Sousa, H. Manzano, B. Soto-Blanco, and S. L. Górniak, "Toxicokinetics of cyanide in rats, pigs and goats after oral dosing with potassium cyanide," *Archives of toxicology,* vol. 77, no. 6, pp. 330-334, 2003.
[49] A. M. Calafat and S. B. Stanfill, "Rapid quantitation of cyanide in whole blood by automated headspace gas chromatography," *Journal of chromatography B,* vol. 772, no. 1, pp. 131-137, 2002.
[50] F. Moriya and Y. Hashimoto, "Potential for error when assessing blood cyanide concentrations in fire victims," *Journal of forensic science,* vol. 46, no. 6, pp. 1421-1425, 2001.
[51] F. L. Rodkey and R. F. Robertson, "Analytical precautions in measurement of blood cyanide," *Clinical chemistry,* vol. 24, no. 12, pp. 2184-2185, 1978.
[52] A. Pettigrew and G. Fell, "Simplified colorimetric determination of thiocyanate in biological fluids, and its application to investigation of the toxic amblyopias," *Clinical Chemistry,* vol. 18, no. 9, pp. 996-1000, 1972.
[53] K. Tsuge, M. Kataoka, and Y. Seto, "Cyanide and Thiocyanate Levels in Blood and Saliva of Healthy Adult Volunteers," *Journal of Health Science,* vol. 46, no. 5, pp. 343-350, 2000.
[54] B. A. Logue, W. K. Maserek, G. A. Rockwood, M. W. Keebaugh, and S. I. Baskin, "The analysis of 2-amino-2-thiazoline-4-carboxylic acid in the plasma of smokers and non-smokers," *Toxicology Mechanisms and Methods,* vol. 19, no. 3, pp. 202-208, 2009.
[55] S. Ershad, L.-A. Sagathforoush, and G. Karim-Nezhad, "A selective optical chemosensor based on a thia-containing Schiff-base iron (III) complex for thiocyanate ion," *Analytical Sciences,* vol. 25, no. 5, pp. 665-668, 2009.
[56] B. A. Logue, N. P. Kirschten, I. Petrikovics, M. A. Moser, G. A. Rockwood, and S. I. Baskin, "Determination of the cyanide metabolite 2-aminothiazoline-4-carboxylic acid in urine and plasma by gas chromatography–mass spectrometry," *Journal of Chromatography B,* vol. 819, no. 2, pp. 237-244, 2005.
[57] C. A. DesLauriers, A. M. Burda, and M. Wahl, "Hydroxocobalamin as a cyanide antidote," *American journal of therapeutics,* vol. 13, no. 2, pp. 161-165, 2006.

[58] D. J. O'Brien, D. W. Walsh, C. M. Terriff, and A. H. Hall, "Empiric management of cyanide toxicity associated with smoke inhalation," *Prehospital and disaster medicine,* vol. 26, no. 05, pp. 374-382, 2011.

[59] C. Brunel, C. Widmer, M. Augsburger, F. Dussy, and T. Fracasso, "Antidote treatment for cyanide poisoning with hydroxocobalamin causes bright pink discolouration and chemical–analytical interferences," *Forensic Sci. Int.,* vol. 223, no. 1, pp. e10-e12, 2012.

[60] L. Randaccio, S. Geremia, N. Demitri, and J. Wuerges, "Vitamin B12: unique metalorganic compounds and the most complex vitamins," *Molecules,* vol. 15, no. 5, pp. 3228-3259, 2010.

[61] A. H. Hall and B. H. Rumack, "Hydroxycobalamin/sodium thiosulfate as a cyanide antidote," *The Journal of emergency medicine,* vol. 5, no. 2, pp. 115-121, 1987.

[62] S. I. Baskin, A. M. Horowitz, and E. W. Nealley, "The antidotal action of sodium nitrite and sodium thiosulfate against cyanide poisoning," *J. Clin. Pharmacol.,* vol. 32, no. 4, pp. 368-375, 1992.

[63] L. K. Cambal *et al.*, "Acute, sublethal cyanide poisoning in mice is ameliorated by nitrite alone: complications arising from concomitant administration of nitrite and thiosulfate as an antidotal combination," *Chem. Res. Toxicol.,* vol. 24, no. 7, pp. 1104-1112, 2011.

[64] I. Petrikovics *et al.*, "Cyanide antagonism with carrier erythrocytes and organic thiosulfonates," *Toxicol. Sci.,* vol. 24, no. 1, pp. 86-93, 1995.

[65] I. Petrikovics *et al.*, "Optimization of liposomal lipid composition for a new, reactive sulfur donor, and in vivo efficacy studies on mice to antagonize cyanide intoxication," *J. Drug Delivery,* vol. 2011, 2011.

[66] S. E. Patterson, A. R. Monteil, J. F. Cohen, D. L. Crankshaw, R. Vince, and H. T. Nagasawa, "Cyanide antidotes for mass casualties: water-soluble salts of the dithiane (sulfanegen) from 3-mercaptopyruvate for intramuscular administration," *Journal of medicinal chemistry,* vol. 56, no. 3, pp. 1346-1349, 2013.

[67] G. Hayward, H. Hill, J. Pratt, N. Vanston, and R. Williams, "1196. The chemistry of vitamin B 12. Part IV. The thermodynamic trans-effect," *Journal of the Chemical Society (Resumed),* pp. 6485-6493, 1965.

[68] V. S. Sharma, R. B. Pilz, G. R. Boss, and D. Magde, "Reactions of nitric oxide with vitamin B12 and its precursor, cobinamide," *Biochemistry,* vol. 42, no. 29, pp. 8900-8908, 2003.

[69] J. Lee, J. Armstrong, K. Kreuter, B. J. Tromberg, and M. Brenner, "Non-invasive in vivo diffuse optical spectroscopy monitoring of cyanide poisoning in a rabbit modelPresented in part in Chest 128 (4) 301S (October 2005) and Journal of Investigative Medicine 53 (1) S113 (January 2005) as abstracts," *Physiological measurement,* vol. 28, no. 9, p. 1057, 2007.

[70] M. W. Stutelberg, C. V. Vinnakota, B. L. Mitchell, A. R. Monteil, S. E. Patterson, and B. A. Logue, "Determination of 3-mercaptopyruvate in

rabbit plasma by high performance liquid chromatography tandem mass spectrometry," *J. Chromatogr. B: Biomed. Sci. Appl.,* vol. 949, pp. 94-98, 2014.

[71] H. T. Nagasawa, D. J. Goon, D. L. Crankshaw, R. Vince, and S. E. Patterson, "Novel, orally effective cyanide antidotes," *Journal of medicinal chemistry,* vol. 50, no. 26, pp. 6462-6464, 2007.

[72] A. Spallarossa *et al.*, "The “rhodanese” fold and catalytic mechanism of 3-mercaptopyruvate sulfurtransferases: crystal structure of SseA from Escherichia coli," *Journal of molecular biology,* vol. 335, no. 2, pp. 583-593, 2004.

[73] G. A. Rockwood, D. E. Thompson, and I. Petrikovics, "Dimethyl trisulfide A novel cyanide countermeasure," *Toxicol. Ind. Health,* p. 0748233715622713, 2016.

[74] E. Manandhar, N. Maslamani, I. Petrikovics, G. A. Rockwood, and B. A. Logue, "Determination of dimethyl trisulfide in rabbit blood using stir bar sorptive extraction gas chromatography-mass spectrometry," *Journal of Chromatography A,* vol. 1461, pp. 10-17, 2016.

[75] H. L. Gilchrist, *A comparative study of world war casualties from gas and other weapons*. US Government Printing Office, 1928.

[76] S. Ebnesajjad, "Chemical Warfare Agents Syria: poisonous fruits of chemistry," (in English), electronic, website 2017.

[77] K. J. Smith, C. G. Hurst, R. B. Moeller, H. G. Skelton, and F. R. Sidell, "Sulfur mustard: its continuing threat as a chemical warfare agent, the cutaneous lesions induced, progress in understanding its mechanism of action, its long-term health effects, and new developments for protection and therapy," *Journal of the American Academy of Dermatology,* vol. 32, no. 5, pp. 765-776, 1995.

[78] A. J. Feister, *Medical defense against mustard gas: toxic mechanisms and pharmacological implications*. CRC press, 1991.

[79] R. Black, K. Brewster, R. Clarke, J. Hambrook, J. Harrison, and D. Howells, "Biological fate of sulphur mustard, 1, 1'-thiobis (2-chloroethane): isolation and identification of urinary metabolites following intraperitoneal administration to rat," *Xenobiotica,* vol. 22, no. 4, pp. 405-418, 1992.

[80] J. R. Smith, B. R. Capacio, W. D. Korte, A. R. Woolfitt, and J. R. Barr, "Analysis for plasma protein biomarkers following an accidental human exposure to sulfur mustard," *Journal of analytical toxicology,* vol. 32, no. 1, pp. 17-24, 2008.

[81] A. R. Haake and R. R. Polakowska, "Cell death by apoptosis in epidermal biology," *Journal of Investigative Dermatology,* vol. 101, no. 2, pp. 107-112, 1993.

[82] H. Xu *et al.*, "Four sulfur mustard exposure cases: Overall analysis of four types of biomarkers in clinical samples provides positive implication for early diagnosis and treatment monitoring," *Toxicology Reports,* vol. 1, pp. 533-543, 2014.

[83] R. W. Read and R. M. Black, "Analysis of β-lyase metabolites of sulfur mustard in urine by electrospray liquid chromatography-tandem mass spectrometry," *Journal of analytical toxicology,* vol. 28, no. 5, pp. 346-351, 2004.

[84] R. Black, J. Hambrook, D. Howells, and R. Read, "Biological fate of sulfur mustard, 1, 1′-thiobis (2-chloroethane). Urinary excretion profiles of hydrolysis products and β-lyase metabolites of sulfur mustard after cutaneous application in rats," *Journal of analytical toxicology,* vol. 16, no. 2, pp. 79-84, 1992.

[85] C. L. Young *et al.*, "A rapid, sensitive method for the quantitation of specific metabolites of sulfur mustard in human urine using isotope-dilution gas chromatography-tandem mass spectrometry," *Journal of analytical toxicology,* vol. 28, no. 5, pp. 339-345, 2004.

[86] E. Jakubowski *et al.*, "Quantification of thiodiglycol in human urine after an accidental sulfur mustard exposure," *Toxicology Methods,* vol. 10, no. 2, pp. 143-150, 2000.

[87] J. Riches, R. W. Read, and R. M. Black, "Analysis of the sulphur mustard metabolites thiodiglycol and thiodiglycol sulphoxide in urine using isotope-dilution gas chromatography–ion trap tandem mass spectrometry," *Journal of Chromatography B,* vol. 845, no. 1, pp. 114-120, 2007.

[88] R. M. Black and R. W. Read, "Improved methodology for the detection and quantitation of urinary metabolites of sulphur mustard using gas chromatography-tandem mass spectrometry," *Journal of Chromatography B: Biomedical Sciences and Applications,* vol. 665, no. 1, pp. 97-105, 1995.

[89] C. Li, J. Chen, Q. Liu, J. Xie, and H. Li, "Simultaneous quantification of seven plasma metabolites of sulfur mustard by ultra high performance liquid chromatography–tandem mass spectrometry," *Journal of Chromatography B,* vol. 917, pp. 100-107, 2013.

[90] E. Wils, A. Hulst, A. De Jong, A. Verweij, and H. Borer, "Analysis of thiodiglycol in urine of victims of an alleged attack with mustard gas," *Journal of analytical toxicology,* vol. 9, no. 6, pp. 254-257, 1985.

[91] E. Wils, A. Hulst, and J. Van Laar, "Analysis of thiodiglycol in urine of victims of an alleged attack with mustard gas, part II," *Journal of analytical toxicology,* vol. 12, no. 1, pp. 15-19, 1988.

[92] A. E. Boyer *et al.*, "Quantitation of the sulfur mustard metabolites 1, 1′-sulfonylbis [2-(methylthio) ethane] and thiodiglycol in urine using isotope-dilution gas chromatography-tandem mass spectrometry," *Journal of analytical toxicology,* vol. 28, no. 5, pp. 327-332, 2004.

[93] R. M. Black, R. J. Clarke, and R. W. Read, "Analysis of 1, 1′-sulphonylbis [2-(methylsulphinyl) ethane] and 1-methylsulphinyl-2-[2-(methylthio) ethylsulphonyllethane, metabolites of sulphur mustard, in urine using gas chromatography-mass spectrometry," *Journal of Chromatography A,* vol. 558, no. 2, pp. 405-414, 1991.

[94] P. L. Skipper and S. R. Tannenbaum, "Protein adducts in the molecular dosimetry of chemical carcinogens," *Carcinogenesis,* vol. 11, no. 4, pp. 507-518, 1990.
[95] D. Noort, H. Benschop, and R. Black, "Biomonitoring of exposure to chemical warfare agents: a review," *Toxicology and applied pharmacology,* vol. 184, no. 2, pp. 116-126, 2002.
[96] J. Hambrook, D. Howells, and C. Schock, "Biological fate of sulphur mustard (1, 1′-thiobis (2-chloroethane)): uptake, distribution and retention of 35S in skin and in blood after cutaneous application of 35S-sulphur mustard in rat and comparison with human blood in vitro," *Xenobiotica,* vol. 23, no. 5, pp. 537-561, 1993.
[97] D. Noort, A. Fidder, C. Degenhardt-Langelaan, and A. Hulst, "Retrospective detection of sulfur mustard exposure by mass spectrometric analysis of adducts to albumin and hemoglobin: an in vivo study," *Journal of analytical toxicology,* vol. 32, no. 1, pp. 25-30, 2008.
[98] D. Noort, A. G. Hulst, L. P. de Jong, and H. P. Benschop, "Alkylation of human serum albumin by sulfur mustard in vitro and in vivo: mass spectrometric analysis of a cysteine adduct as a sensitive biomarker of exposure," *Chemical research in toxicology,* vol. 12, no. 8, pp. 715-721, 1999.
[99] J. L. Way, "Pharmacologic aspects of cyanide and its antagonism," *Cyanide Biol. Academic Press, New York,* pp. 29-40, 1981.
[100] E. Y. Chan, Z. Wang, C. K. Mark, and S. Da Liu, "Industrial accidents in China: risk reduction and response," *The Lancet,* vol. 386, no. 10002, pp. 1421-1422, 2015.
[101] F. Xu and J. P. Webb, "Tianjin chemical clean-up after explosion," *Can. Med. Assoc. J.,* vol. 187, no. 13, pp. E404-E404, 2015.
[102] K. A. Wolnik, F. L. Fricke, E. Bonnin, C. M. Gaston, and R. D. Satzger, "The Tylenol tampering incident-tracing the source," *Anal. Chem.,* vol. 56, no. 3, pp. 466A-474A, 1984.
[103] M. Eckstein, "Cyanide as a chemical terrorism weapon," *JEMS: a journal of emergency medical services,* vol. 29, no. 8, p. suppl 22, 2004.
[104] R. Jackson *et al.*, "Development of a fluorescence-based sensor for rapid diagnosis of cyanide exposure," *Anal. Chem.,* vol. 86, no. 3, pp. 1845-1852, 2014.
[105] M. Brenner *et al.*, "Sulfanegen sodium treatment in a rabbit model of sub-lethal cyanide toxicity," *Toxicol. Appl. Pharmacol.,* vol. 248, no. 3, pp. 269-276, 2010.
[106] M. W. Stutelberg *et al.*, "Simultaneous determination of 3-mercaptopyruvate and cobinamide in plasma by liquid chromatography–tandem mass spectrometry," *J. Chromatogr. B: Biomed. Sci. Appl.,* vol. 1008, pp. 181-188, 2016.
[107] L. L. Pearce, E. L. Bominaar, B. C. Hill, and J. Peterson, "Reversal of Cyanide Inhibition of Cytochrome c Oxidase by the Auxiliary Substrate

Nitric Oxide AN ENDOGENOUS ANTIDOTE TO CYANIDE POISONING?," *J. Biol. Chem.,* vol. 278, no. 52, pp. 52139-52145, 2003.
[108] V. S. Bebarta *et al.*, "Intravenous cobinamide versus hydroxocobalamin for acute treatment of severe cyanide poisoning in a swine (Sus scrofa) model," *Annals of emergency medicine,* vol. 64, no. 6, pp. 612-619, 2014.
[109] I. Petrikovics *et al.*, "Encapsulated rhodanese with two new sulfur donors in cyanide antagonism," *Toxicol. Lett.,* vol. 196, p. S144, 2010.
[110] I. Petrikovics, L. Pei, W. McGuinn, E. Cannon, and J. Way, "Encapsulation of rhodanese and organic thiosulfonates by mouse erythrocytes," *Fundam. Appl. Toxicol.,* vol. 23, no. 1, pp. 70-75, 1994.
[111] A. Chan *et al.*, "Cobinamide is superior to other treatments in a mouse model of cyanide poisoning," *Clin. Toxicol.,* vol. 48, no. 7, pp. 709-717, 2010.
[112] B. Sorbo, "CRYSTALLINE RHODANESE. 2. THE ENZYME CATALYZED REACTION," *ACTA CHEMICA SCANDINAVICA,* vol. 7, no. 8, pp. 1137-1145, 1953.
[113] M. Shirasu, S. Nagai, R. Hayashi, A. Ochiai, and K. Touhara, "Dimethyl trisulfide as a characteristic odor associated with fungating cancer wounds," *Biosci., Biotechnol., Biochem.,* vol. 73, no. 9, pp. 2117-2120, 2009.
[114] W. Boatright and Q. Lei, "Headspace Evaluation of Methanethiol and Dimethyl Trisulfide in Aqueous Solutions of Soy-protein Isolates," *J. Food Sci.,* vol. 65, no. 5, pp. 819-821, 2000.
[115] R. G. Buttery, D. G. Guadagni, L. C. Ling, R. M. Seifert, and W. Lipton, "Additional volatile components of cabbage, broccoli, and cauliflower," *J. Agric. Food Chem.,* vol. 24, no. 4, pp. 829-832, 1976.
[116] H. W. CHIN and R. Lindsay, "Volatile sulfur compounds formed in disrupted tissues of different cabbage cultivars," *J. Food Sci.,* vol. 58, no. 4, pp. 835-839, 1993.
[117] N. K. Sinha, D. E. Guyer, D. A. Gage, and C. T. Lira, "Supercritical carbon dioxide extraction of onion flavors and their analysis by gas chromatography-mass spectrometry," *J. Agric. Food Chem.,* vol. 40, no. 5, pp. 842-845, 1992.
[118] R. T. Marsili, L. Laskonis, and C. Kenaan, "Evaluation of PDMS-based extraction techniques and GC-TOFMS for the analysis of off-flavor chemicals in beer," *Journal-American Society of Brewing Chemists,* vol. 65, no. 3, p. 129, 2007.
[119] A. Isogai, R. Kanda, Y. Hiraga, T. Nishimura, H. Iwata, and N. Goto-Yamamoto, "Screening and identification of precursor compounds of dimethyl trisulfide (DMTS) in Japanese sake," *J. Agric. Food Chem.,* vol. 57, no. 1, pp. 189-195, 2008.
[120] L. Gijs, P. Perpete, A. Timmermans, and S. Collin, "3-Methylthiopropionaldehyde as precursor of dimethyl trisulfide in aged beers," *J. Agric. Food Chem.,* vol. 48, no. 12, pp. 6196-6199, 2000.

[121] F. Pelusio *et al.*, "Headspace solid-phase microextraction analysis of volatile organic sulfur compounds in black and white truffle aroma," *J. Agric. Food Chem.,* vol. 43, no. 8, pp. 2138-2143, 1995.
[122] H. M. Burbank and M. C. Qian, "Volatile sulfur compounds in Cheddar cheese determined by headspace solid-phase microextraction and gas chromatograph-pulsed flame photometric detection," *J. Chromatogr. A,* vol. 1066, no. 1, pp. 149-157, 2005.
[123] P. A. Vazquez-Landaverde, J. Torres, and M. Qian, "Quantification of trace volatile sulfur compounds in milk by solid-phase microextraction and gas chromatography–pulsed flame photometric detection," *J. Dairy Sci.,* vol. 89, no. 8, pp. 2919-2927, 2006.
[124] I. o. L. A. R. C. o. Care, U. o. L. Animals, and N. I. o. H. D. o. R. Resources, *Guide for the care and use of laboratory animals*. National Academies, 1985.
[125] R. Guidance, "Validation of chromatographic methods," *Center for Drug Evaluation and Research (CDER), Washington,* vol. 2, 1994.
[126] V. P. Shah *et al.*, "Bioanalytical method validation—a revisit with a decade of progress," *Pharm. Res.,* vol. 17, no. 12, pp. 1551-1557, 2000.
[127] G. A. Shabir, "Validation of high-performance liquid chromatography methods for pharmaceutical analysis: Understanding the differences and similarities between validation requirements of the US Food and Drug Administration, the US Pharmacopeia and the International Conference on Harmonization," *J. Chromatogr. A,* vol. 987, no. 1, pp. 57-66, 2003.
[128] H. A. Soini, K. E. Bruce, D. Wiesler, F. David, P. Sandra, and M. V. Novotny, "Stir bar sorptive extraction: a new quantitative and comprehensive sampling technique for determination of chemical signal profiles from biological media," *Journal of chemical ecology,* vol. 31, no. 2, pp. 377-392, 2005.
[129] R. R. Kalakuntla and K. S. Kumar, "Bioanalytical method validation: A quality assurance auditor view point," *J. Pharm. Sci. Res.,* vol. 1, no. 3, pp. 1-10, 2009.
[130] H. A. Schwertner, S. Valtier, and V. S. Bebarta, "Liquid chromatographic mass spectrometric (LC/MS/MS) determination of plasma hydroxocobalamin and cyanocobalamin concentrations after hydroxocobalamin antidote treatment for cyanide poisoning," *J. Chromatogr. B: Biomed. Sci. Appl.,* vol. 905, pp. 10-16, 2012.
[131] J. C. Dacre and M. Goldman, "Toxicology and pharmacology of the chemical warfare agent sulfur mustard," *Pharmacological reviews,* vol. 48, no. 2, pp. 289-326, 1996.
[132] K. Kehe and L. Szinicz, "Medical aspects of sulphur mustard poisoning," *Toxicology,* vol. 214, no. 3, pp. 198-209, 2005.
[133] M. Etezad-Razavi, M. Mahmoudi, M. Hefazi, and M. Balali-Mood, "Delayed ocular complications of mustard gas poisoning and the relationship with

respiratory and cutaneous complications," *Clinical & experimental ophthalmology,* vol. 34, no. 4, pp. 342-346, 2006.
[134] K. Manning, D. Skegg, P. Stell, and R. DOLL, "Cancer of the larynx and other occupational hazards of mustard gas workers," *Clinical Otolaryngology,* vol. 6, no. 3, pp. 165-170, 1981.
[135] K. Agin, "Comparison of serum magnesium values among sulfur mustard induced asthma with non-chemical asthmatic in Iranian war victims," 2005.
[136] M. Wattana and T. Bey, "Mustard gas or sulfur mustard: an old chemical agent as a new terrorist threat," *Prehospital and disaster medicine,* vol. 24, no. 1, pp. 19-29, 2009.
[137] K. Kehe, H. Thiermann, F. Balszuweit, F. Eyer, D. Steinritz, and T. Zilker, "Acute effects of sulfur mustard injury—Munich experiences," *Toxicology,* vol. 263, no. 1, pp. 3-8, 2009.
[138] S. mansour Razavi, P. Salamati, M. Saghafinia, and M. Abdollahi, "A review on delayed toxic effects of sulfur mustard in Iranian veterans," *DARU Journal of Pharmaceutical Sciences,* vol. 20, no. 1, p. 51, 2012.
[139] H. Rahmani, I. Javadi, and S. Shirali, "Respiratory complications due to sulfur mustard exposure," *International journal of current research and academic review,* vol. 4, no. 6, p. 143, 2016.
[140] J. Pauluhn and U. Mohr, "Inhalation studies in laboratory animals—current concepts and alternatives," *Toxicologic pathology,* vol. 28, no. 5, pp. 734-753, 2000.
[141] R. Mayeux, "Biomarkers: potential uses and limitations," *NeuroRx,* vol. 1, no. 2, pp. 182-188, 2004.
[142] B. S. Hulka, "Biological markers in epidemiology," 1990.
[143] R. Black, K. Brewster, J. Harrison, and N. Stansfield, "The chemistry of 1, 1′-thiobis-(2-chloroethane)(sulphur mustard) part i. Some simple derivatives," *Phosphorus, Sulfur, and Silicon and the Related Elements,* vol. 71, no. 1-4, pp. 31-47, 1992.
[144] R. Black, K. Brewster, R. Clarke, and J. Harrison, "The chemistry of 1, 1′-thiobis (2-chloroethane)(sulphur mustard) part II. 1 The synthesis of some conjugates with cysteine, N-acetylcysteine and N-acetylcysteine methyl ester," *Phosphorus, Sulfur, and Silicon and the Related Elements,* vol. 71, no. 1-4, pp. 49-58, 1992.
[145] M. Pesonen *et al.*, "Capsaicinoids, chloropicrin and sulfur mustard: possibilities for exposure biomarkers," *Frontiers in pharmacology,* vol. 1, 2010.
[146] B. G. Pantazides *et al.*, "Simplified method for quantifying sulfur mustard adducts to blood proteins by ultrahigh pressure liquid chromatography–isotope dilution tandem mass spectrometry," *Chemical research in toxicology,* vol. 28, no. 2, pp. 256-261, 2015.
[147] K. Ghabili, P. S. Agutter, M. Ghanei, K. Ansarin, and M. M. Shoja, "Mustard gas toxicity: the acute and chronic pathological effects," *Journal of applied toxicology,* vol. 30, no. 7, pp. 627-643, 2010.

[148] S. Somani and S. Babu, "Toxicodynamics of sulfur mustard," *International journal of clinical pharmacology, therapy, and toxicology,* vol. 27, no. 9, pp. 419-435, 1989.
[149] D. Sinclair, "Mustard-gas Poisoning in Man," *British medical journal,* vol. 2, no. 4570, p. 290, 1948.
[150] K. Kehe, F. Balszuweit, J. Emmler, H. Kreppel, M. Jochum, and H. Thiermann, "Sulfur mustard research—strategies for the development of improved medical therapy," *Eplasty,* vol. 8, 2008.
[151] Z. M. Hassan, M. Ebtekar, M. Ghanei, M. Taghikhani, M. R. N. Daloii, and T. Ghazanfari, "Immunobiological consequences of sulfur mustard contamination," *Iranian Journal of Allergy, Asthma and Immunology,* vol. 5, no. 3, pp. 101-108, 2006.
[152] T. Zilker and N. Felgenhauer, "S-mustard gas poisoning–experience with 12 victims," *Clin. Toxicol,* vol. 40, no. 3, p. 251, 2002.
[153] M. Balali-Mood and M. Hefazi, "Comparison of early and late toxic effects of sulfur mustard in Iranian veterans," *Basic & clinical pharmacology & toxicology,* vol. 99, no. 4, pp. 273-282, 2006.
[154] A. L. Ruff and J. F. Dillman, "Signaling molecules in sulfur mustard-induced cutaneous injury," *Eplasty,* vol. 8, 2008.
[155] S. Mellor, P. Rice, and G. Cooper, "Vesicant burns," *British journal of plastic surgery,* vol. 44, no. 6, pp. 434-437, 1991.
[156] J. R. Barr *et al.*, "Analysis of urinary metabolites of sulfur mustard in two individuals after accidental exposure," *Journal of analytical toxicology,* vol. 32, no. 1, pp. 10-16, 2008.
[157] I. A. Rodin, A. V. Braun, E. I. Savelieva, I. V. Rybalchenko, I. A. Ananieva, and O. A. Shpigun, "Rapid method for the detection of metabolite of sulfur mustard 1, 1′-sulfonylbis [2-S-(N-acetylcysteinyl) ethane] in plasma and urine by liquid chromatography-negative electrospray-tandem mass spectrometry," *Journal of Liquid Chromatography & Related Technologies,* vol. 34, no. 16, pp. 1676-1685, 2011.
[158] M. Qi *et al.*, "Simultaneous determination of sulfur mustard and related oxidation products by isotope-dilution LC–MS/MS method coupled with a chemical conversion," *Journal of Chromatography B,* vol. 1028, pp. 42-50, 2016.